NMR RELAXATION IN SURFACTANT SYSTEMS, A STUDY OF MOLECULAR DYNAMICS AND ORGANIZATION

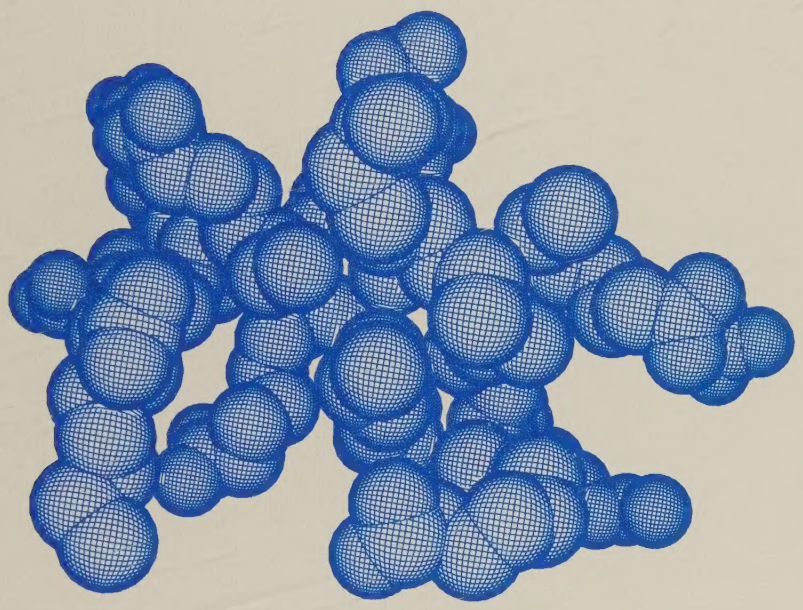

HARALD WALDERHAUG

Diss. Kemi

1985

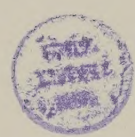

NMR RELAXATION IN SURFACTANT SYSTEMS, A STUDY OF MOLECULAR DYNAMICS AND ORGANIZATION

HARALD WALDERHAUG

1985

NMR RELAXATION IN SURFACTANT SYSTEMS. A STUDY OF MOLECULAR DYNAMICS AND ORGANIZATION.

HARALD WALDERHAUG

CAND. MAG.

AVHANDLING FÖR FILOSOFIE DOKTORSEXAMEN

AVHANDLINGEN KOMMER ATT FÖRSVARAS VID EN OFFENTLIG DISPUTATION I SAL G, KEMICENTRUM, LUND LÖRDAGEN DEN 1 JUNI 1985, KL. 10.15.

Walderhaug, H., (1985)

Thesis, University of Lund

Division of Physical Chemistry I

Chemical Center, P.O.B. 124

S-221 00 LUND

Sweden

Organization
LUND UNIVERSITY

Department of Physical Chemistry 1
Chemical Center, P.O.B. 124
S-220 07 LUND 7 Sweden

Document name
DOCTORAL DISSERTATION

Date of issue
April 9, 1985

CODEN:

Author(s)
Harald Walderhaug

Sponsoring organization

Title and subtitle

NMR RELAXATION IN SURFACTANT SYSTEMS. A STUDY OF MOLECULAR DYNAMICS AND ORGANIZATION.

Abstract

The method of Nuclear Magnetic Resonance (NMR) is used to extract information on surfactant hydrocarbon chain order and dynamics in surfactant systems. NMR spin relaxation of the nuclei 13-C, 2-H and 14-N in micellar systems is interpreted by means of a two-step model, providing one organizational and two dynamic parameters, viz. an order parameter, a correlation time for a fast (10^{-11} s) local reorientation of the chain segments and a correlation time for a slower process (10^{-9} s) involving micellar tumbling and monomer lateral diffusion over the curved surface of the micelle. For other isotropic systems like microemulsions and a cubic liquid crystalline phase it is shown that the spin relaxation can be interpreted by means of a three-step model to account for certain line broadening effects in the NMR spectra. Order parameters are also extracted by means of quadrupole splittings in 2-H NMR signals from lamellar liquid crystalline phases. When compared with isotropic surfactant systems consisting of the same surfactant it is found that the geometry of the aggregates only weakly influences the local properties of the surfactant alkyl chains.

A method for probing fluidity of micellar interiors is also presented. The rates of the diffusive anisotropic reorientation of a solubilizate are determined by means of 2-H spin relaxation and compared with the rates of reorientation for the same molecules when dissolved in liquid hydrocarbons with known viscosities. The reorientation for the micellar case is found to be hydrodynamic in nature. The micellar viscosities so determined closely resemble those of simple hydrocarbon liquids with the same length of the alkyl chains as that of the surfactant molecules and at the same temperature, thus supporting the picture of micelles with a very liquid-like interior.

Key words

Classification system and/or index terms (if any)

Supplementary bibliographical information

Language
English

ISSN and key title

ISBN

Recipient's notes

Number of pages

Price

Security classification

Distribution by (name and address) Harald Walderhaug, Department of Physical Chemistry 1, Chemical Center, P.O.B. 124, S-220 07 LUND 7, Sweden.

I, the undersigned, being the copyright owner of the abstract of the above-mentioned dissertation, hereby grant to all reference sources permission to publish and disseminate the abstract of the above-mentioned dissertation.

Signature Harald Walderhaug **Date** April 9, 1985

DOKUMENTDATABLAD
enl SIS 61 41 21

CONTENTS

LIST OF PAPERS 1

1. INTRODUCTION. 3

1.1 Surfactants. 4

1.2 The NMR Method. 6

2. SPIN-LATTICE RELAXATION MEASURING THE ANISOTROPIC REORIENTATION OF A SOLUBILIZATE. A METHOD FOR PROBING FLUIDITY OF A MICELLAR INTERIOR. 8

3. NMR RELAXATION IN THE SURFACTANT HYDROCARBON CHAIN OF ISOTROPIC TWO-COMPONENT SURFACTANT/WATER SYSTEMS. 12

3.1 General Considerations. 12

3.2 ^{13}C Spin-Lattice Relaxation in Micellar Systems. 14

3.3 ^{2}H and ^{14}N Spin-Lattice and Spin-Spin Relaxation in a Micellar and a Cubic Liquid Crystalline System. 18

3.3.1 The Micellar Solution Phase. 20

3.3.2 The Cubic Liquid Crystalline Phase. 22

4. SURFACTANT HYDROCARBON CHAIN ORDER IN TWO LAMELLAR LIQUID CRYSTALLINE PHASES. 25

5. ^{13}C SPIN RELAXATION IN MICROEMULSIONS. 28

5.1 ^{13}C Spin-Lattice Relaxation in a Four-Component Microemulsion. 28

5.2 ^{13}C Spin-Lattice Relaxation in a Three-Component Microemulsion. 30

6. CONCLUDING REMARKS. 33

REFERENCES 34

ACKNOWLEDGMENTS 37

LIST OF PAPERS

The thesis consists of a summary and the following papers:

I. MICELLAR FLUIDITY. A DEUTERIUM NUCLEAR MAGNETIC RESONANCE STUDY OF THE ANISOTROPIC REORIENTATION OF SOLUBILIZED TRANS-DECALIN-d_{18}.
P. Stilbs, H. Walderhaug and B. Lindman
J. Phys. Chem., 87, 4762 (1983).

II. MICELLAR DYNAMICS AND ORGANIZATION. A MULTIFIELD ^{13}C NMR SPIN-LATTICE AND $\{^{1}H\}$-^{13}C NUCLEAR OVERHAUSER EFFECT STUDY.
H. Walderhaug, O. Söderman and P. Stilbs
J. Phys. Chem., 88, 1655 (1984).

III. NMR RELAXATION IN ISOTROPIC SURFACTANT SYSTEMS. A ^{2}H, ^{13}C AND ^{14}N NMR STUDY OF THE MICELLAR (L_1) AND CUBIC (I_1) PHASES IN THE DODECYLTRIMETHYLAMMONIUM CHLORIDE/WATER SYSTEM.
O. Söderman, H. Walderhaug, U. Henriksson and P. Stilbs
Accepted for publication, J. Phys. Chem.

IV. A ^{13}C AND ^{2}H NUCLEAR MAGNETIC RESONANCE STUDY OF HYDROCARBON CHAIN ORDER IN ISOTROPIC AND ANISOTROPIC PHASES FORMED IN THE SODIUM P-OCTYLBENZENESULFONATE-SHORT CHAIN ALCOHOL- WATER SYSTEM.
O. Söderman, H. Walderhaug and B. Lindman
To appear in J. Phys. Chem.

V. ORDER AND DYNAMICS OF THE HYDROPHOBIC/HYDROPHILIC INTERFACE IN MICROEMULSIONS OF THE COSURFACTANT TYPE. A ^{13}C NMR RELAXATION STUDY.
O. Söderman and H. Walderhaug
Submitted to Langmuir.

VI. A STUDY OF THE ^{13}C NMR RELAXATION OF AOT IN WATER-IN-OIL MICROEMULSIONS.

J. Carnali, B. Lindman, O. Söderman and H. Walderhaug

Submitted to Langmuir.

1. INTRODUCTION

This thesis deals with the problem of determining the physical state of the hydrocarbon chains of various organized surfactant systems by means of Nuclear Magnetic Resonance (NMR) relaxation methods.

Surfactants are chemical compounds which consist of a polar group and a non-polar group and which therefore are amphiphilic in nature. They have been known for a long time because of their detergent properties; fats and oils are solubilized in water solutions of soaps. Amphiphiles are also important in living systems where biological amphiphiles play an important role in the digestion process of fats in the body, for instance.

Surfactants are also important in technical applications. Because of this growing technical importance of surfactant systems questions of fundamental character are raised. An example here are so-called "microemulsions" [1-3] studied by NMR relaxation in papers V and VI. These may contain at the same time large amounts of oil and water but are thermodynamically stable, isotropic and highly fluid. Microemulsions are important in e.g. tertiary oil recovery processes. For this reason they have been studied extensively but still there exist uncertainties as regards the molecular organization in such systems.

In what follows I will first briefly describe surfactant systems and then proceed to describe the NMR method. Thereafter, special applications of the NMR method to the problems alluded to above will be presented.

1.1 Surfactants.

Surfactant molecules consist of a polar and a non-polar part. The non-polar part consists of one or more hydrocarbon chains. The polar group may be either ionic, zwitterionic or nonionic. Figure 1 shows representative surfactant molecules.

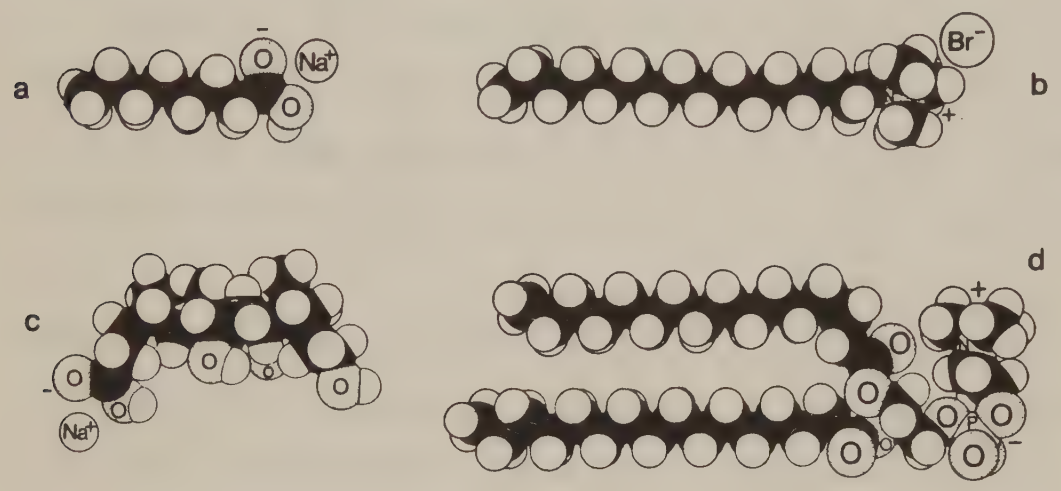

Figure 1. Space filling molecular models of a: sodium octanoate, b: hexadecyltrimethylammonium bromide, c: sodium cholate, d: dipalmitoylphosphatidylcholine.

When immersed in water the amphiphilic molecules usually start to form roughly spherical aggregates above a certain concentration called the critical micelle concentration (c.m.c.). These aggregates are termed micelles and in the case of ionic surfactants consist of some 30 - 80 monomers. For nonionic surfactants they are generally larger. This aggregation happens because of the unfavourable water-hydrocarbon contact which is avoided when the aggregation takes place; the surfactant molecules turn their polar head groups towards

the water while the hydrocarbon chains make up a micellar liquid-like hydrocarbon interior. Upon increasing the surfactant concentration the micelles often start to grow into rods and eventually certain liquid crystalline phases are formed. For ionic surfactants addition of a third component like a long-chain alcohol or a hydrocarbon increases the number of phases that can be formed. Figure 2 shows a phase diagram for a typical three-component system of an ionic surfactant. Also indicated is the molecular organization in the various phases of this system.

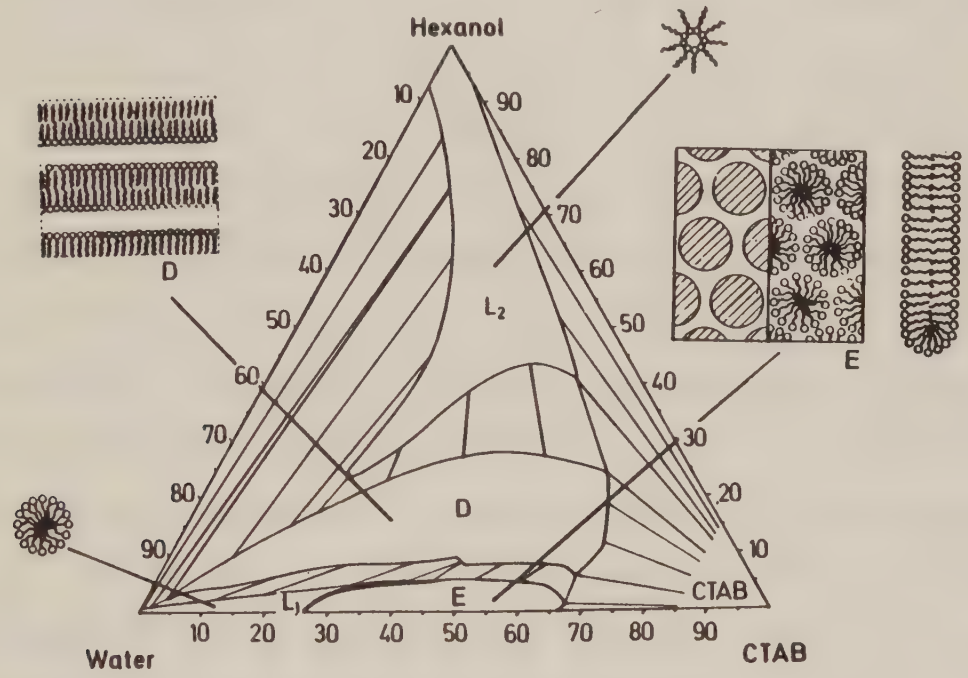

Figure 2. Phase diagram for the ternary system hexadecyltrimethylammonium bromide (CTAB)/hexanol/water. L_1 and L_2 denote isotropic micellar solutions with normal and reversed aggregates, respectively. E and D denote the normal hexagonal and lamellar liquid crystalline phases.

This phase behaviour occurs only above a certain temperature specific for each surfactant and termed the Krafft point. This is the temperature where the monomer solubility has reached c.m.c.

In this thesis particular concern is devoted to the physical state of the hydrocarbon chains of aggregated surfactant molecules. Several methods exist for such investigations[4-6] and in this thesis the method of NMR is used to extract information on structure and dynamics of these chains in various amphiphilic systems.

1.2 The NMR Method.

Many nuclei have a spin and a thereby associated magnetic moment. Examples of such nuclei are proton, ^{1}H, deuterium, ^{2}H, ^{13}C and ^{14}N to mention but a few. When placed in a strong magnetic field the magnetic moments of the nuclei line up with the field. Only certain directions of the magnetic moment vector relative to the magnetic field are allowed according to quantum physics. These directions correspond to different energies of the magnetic moments. Transitions between the energy levels can be induced by irradiation of electromagnetic energy and the response versus frequency of irradiation constitutes the NMR spectrum. For commersially available NMR magnetic field strengths, ranging today from 1 to 12 Tesla, the frequencies of the irradiation are in the range of 40 - 500 MHz for ^{1}H.

The technique of pulsed radiofrequency radiation followed by Fourier transformation of the (time domain) response is generally needed to study most nuclei due to their low sensitivity. For instance, the natural abundance of the ^{13}C isotope is only 1%. The most abundant carbon isotope, ^{12}C (99%), has zero spin and is therefore not detectable by NMR.

The return of the magnetization (the resultant of the individual nuclear magnetic moments in a macroscopic sample) from a non-equilibrium situation to equilibrium after a radiofrequency pulse, is a relaxation process. The study of such relaxation gives a very detailed picture of the dynamics on a molecular level of the system under investigation. In NMR there are two kinds of relaxation in the absence of a radiofrequency field; one process involves energy exchange with the surroundings - the "lattice". This is the process whereby the magnetization returns to equilibrium along the magnetic field direction. Often it can be described as a first order process with a time constant T_1, which is called the spin-lattice or longitudinal relaxation time.

The other process is the one occuring in the plane perpendicular to the magnetic field. This process does not involve any energy exchange with the surroundings but causes an irreversible loss of the component of the magnetization in this plane. It is termed transverse or spin-spin relaxation and is also often describable as a first order process with a time constant T_2, called the transverse (or spin-spin) relaxation time.

It is the motion of the nuclei that gives rise to the relaxation. By means of statistical arguments the nuclear, i.e. the molecular, motion can be described by correlation functions (see later), furnishing the connection between microscopic events and the macroscopic observable spin relaxation.

2. SPIN-LATTICE RELAXATION MEASURING THE ANISOTROPIC REORIENTATION OF A SOLUBILIZATE. A METHOD FOR PROBING FLUIDITY OF A MICELLAR INTERIOR.

In paper I interest is focussed on the problem of quantifying the concept of fluidity of the hydrocarbon core of normal micelles in two-component ionic surfactant/water systems. Fluidity and viscosity are concepts which are defined in macroscopic terms in a hydrodynamic picture. However, efforts have been made[7] to measure the influence that the macroscopic viscosity of simple fluids exerts on the reorientational process of small dissolved molecules. It is found that the reorientation can be described hydrodynamically even for such small molecules as trans-Decalin (see Figure 3) when dissolved in hydrocarbon liquids whose molecules are of comparable size to trans-Decalin.

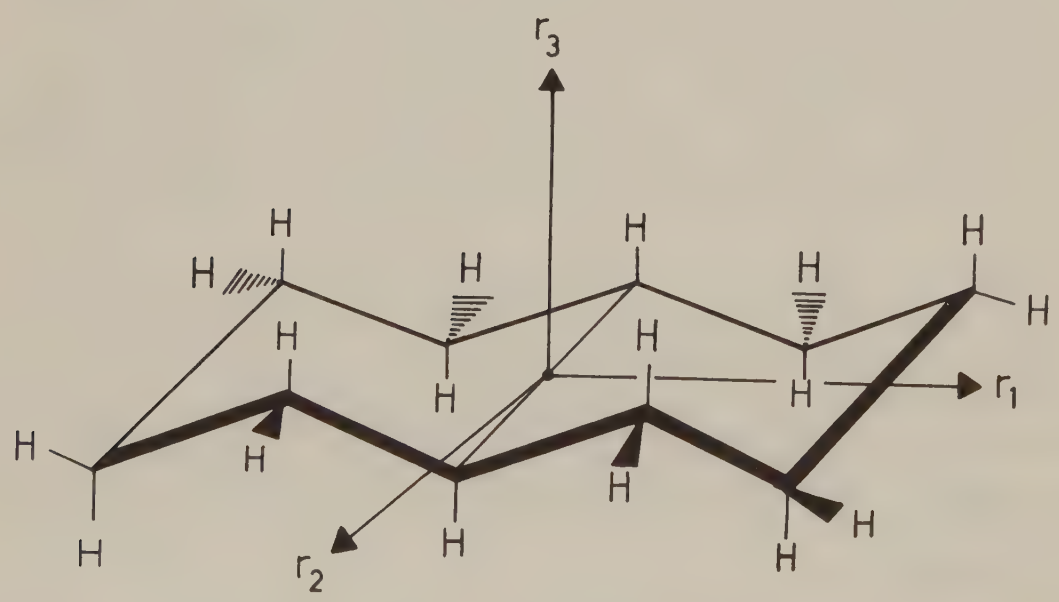

Figure 3. The trans-Decalin molecule. The three principal axes of the diffusion tensor are indicated.

Woessner[8] and Huntress[9] have developed the relation between the

$\{^1H\}$-^{13}C dipolar and ^2H quadrupolar spin-lattice relaxation times (T_1) and the three components of the rotational diffusion tensor in its principal axes system for a rigid ellipsoid undergoing diffusive anisotropic reorientation. This relation is given for ^2H under extreme narrowing conditions by:

$$1/T_1 = (3/16)\cdot X^2\cdot\{C_1/(4R_1 + R_2 + R_3) + C_2/(4R_2 + R_3 + R_1) + C_3/(4R_3 + R_1 + R_2) + C_4/6(R + (R^2-L^2)^{\frac{1}{2}}) + C_5/6(R - (R^2-L^2)^{\frac{1}{2}})\} \quad (1)$$

It is assumed that the electric field gradient asymmetry parameter, $\eta = 0$. R_k is the rotational diffusion coefficient for the reorientation around axis k in the principal axes system of the rotational diffusion tensor (see Figure 3). $R = (R_1 + R_2 + R_3)/3$ and $L^2 = (R_1R_2 + R_2R_3 + R_3R_1)/3$. The C's are expressed in terms of direction cosines for the respective C-H bond vectors in the above mentioned principal axes system and these are known from a molecular mechanics calculation on trans-Decalin. X is the quadrupolar coupling constant which has been set equal to 178 kHz.

To evaluate the R_k's one needs at least three T_1's. In deuteriated trans-Decalin there are three deuterium positions giving rise to three geometrically independent interactional directions, thereby furnishing three (geometrically) independent T_1's. The extracted R_k's are connected to the reorientational correlation times, τ_k, around axis k by the relation:

$$\tau_k = 1/(6R_k) \quad (2)$$

According to hydrodynamic theories the various correlation times for reorientation of an asymmetric top like trans-Decalin should follow

linear relations of the form[7,10]:

$$\tau_k = C_k\eta + \tau_k^o \qquad (3)$$

C_k and τ_k^o are phenomenological constants for axis k in the molecule and η is the viscosity of the medium. Such linear relationships have been found in simple liquids[7] and are shown in Figure 4.

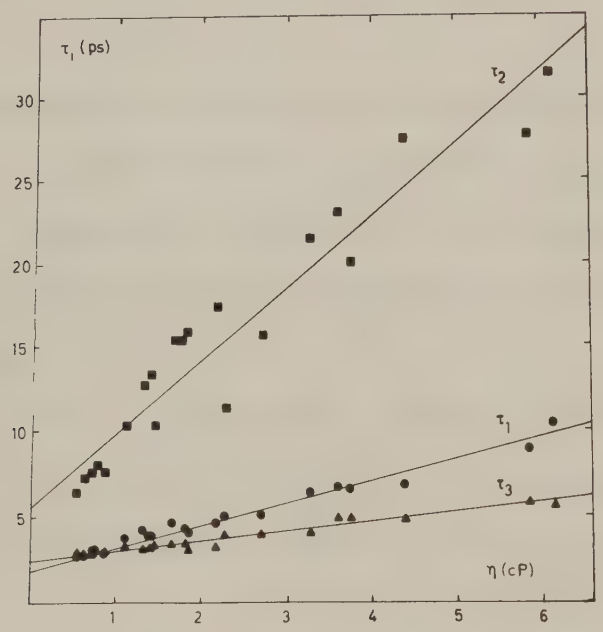

Figure 4. Experimentally determined relation between the respective rotational correlation times for trans-Decalin as a function of viscosity in simple fluids.

When trans-Decalin is solubilized in micelles linear relations between the reorientational correlation times and the length of the hydrocarbon chain of the surfactant molecules are found. Moreover, roughly the same proportions between the various τ_k are observed in micelles and in simple liquids. These findings strongly suggest that the concept of viscosity indeed has a meaning for microheterogeneous systems of this kind.

The micellar viscosities are determined by comparing the reorientational correlation times of the solubilizate with those measured for trans-Decalin when dissolved in simple liquids. It is found that the micellar viscosity is approximately the same as that of simple hydrocarbon fluids with the same length of the hydrocarbon chain. This result is shown in more detail in Figure 5.

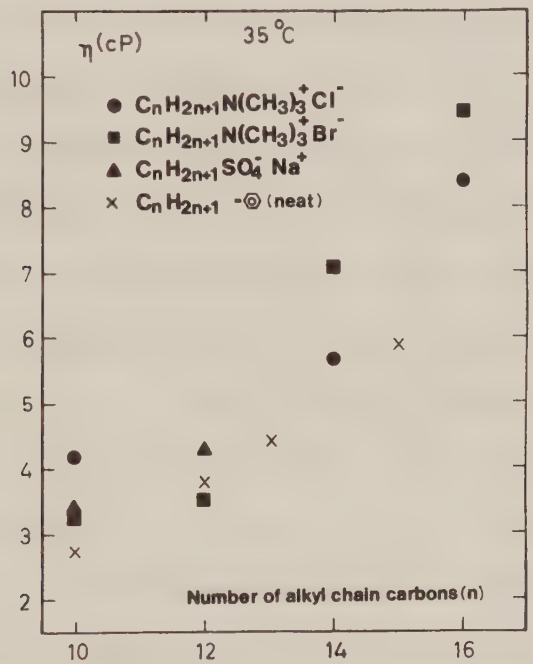

Figure 5. Result of a least-squares fit (see paper I) of the rotational correlation times of trans-Decalin solubilized in micelles to the viscosity concept, when using the linear relations between the τ_k and viscosity, shown in Figure 4.

As shown in papers II and III (see part 3 of the summary) the geometry of the surfactant aggregates only weakly influences the local properties of the hydrocarbon chains. This observation together with our results (Figure 5) could indicate that the viscosity of the hydrocarbon interior of e.g. liquid crystalline systems like normal hexagonal or cubic phases resemble that found for micelles with the same surfactant hydrocarbon chain length.

3. NMR RELAXATION IN THE SURFACTANT HYDROCARBON CHAIN OF ISOTROPIC TWO-COMPONENT SURFACTANT/WATER SYSTEMS.

3.1 General Considerations.

In papers II and III interest is focussed on the organization and dynamics of the hydrocarbon chains in isotropic aggregated binary surfactant / water systems. For anisotropic systems, like liquid crystalline phases, it is rather straight-forward to extract structural information about hydrocarbon chains from observed static effects in the NMR spectra, e.g. quadrupolar splittings in deuterium signals of deuteriated amphiphiles[11-13]. However, isotropic surfactant systems give rise to high resolution NMR spectra. Therefore, this kind of information is not extractable from NMR spectra of such systems.

NMR relaxation contains the sought-after information. ^{13}C spin-lattice relaxation times together with the observation of narrow NMR lines from aggregated surfactant systems imply extreme narrowing conditions if a single exponential correlation function is assumed for the motion of the nuclei. However, there is a marked magnetic field dependence in the spin-lattice relaxation and the nuclear Overhauser effect (n.O.e.) (see below) is for ^{13}C generally markedly reduced. In paper III it is demonstrated that there is a magnetic field dependence also for ^{2}H spin-lattice and spin-spin relaxation in a deuteriated amphiphile. Such effects are also reported for polar head nuclei such as ^{14}N [14] and for the water ^{17}O nucleus[15] in micellar systems.

It is therefore not possible to describe the NMR relaxation for ^{13}C in isotropic aggregated surfactant systems by a single correlation function for the motion for the surfactant alkyl chain segments. This conclusion is also valid for the ^{2}H, ^{14}N and ^{17}O nuclei mentioned above.

We have approached the problem of interpreting NMR relaxation data using a motional model for the surfactant alkyl chains in these systems that is based on previous knowledge about the structure of micelles and related aggregates[16]. It consists of a division of the motion into two parts; one fast motion occuring on the picosecond (10^{-12}s) time-scale and one slower process occuring on a time-scale of nanoseconds (10^{-9}s). The former process consists of local reorientations of the methylene segments and is slightly anisotropic. The anisotropy of the fast local process gives rise to static effects in NMR spectra from liquid crystals. The slow process is ascribed to motions involving the whole aggregate and/or lateral diffusion of the surfactant molecule. These processes are isotropic for micelles and therefore average the residual anisotropy, left over by the fast process, to zero. The total correlation function G(t) can be written[16]:

$$G(t) = (1-S^2)G^f(t) + S^2G^s(t) \qquad (4)$$

$G^f(t)$ and $G^s(t)$ are the correlation functions for the fast and slow motions, respectively. S is defined as:

$$S \equiv (1/2)\langle 3\cos^2\theta_{MD} - 1 \rangle_f \qquad (5)$$

where θ_{MD} is the angle between the C-H bond axis (for ^{13}C) or the electric field gradient axis (for ^2H) and the local director (normal to the micellar surface). The average is over a time long compared to the fast motion but short compared to the slow process. S is termed the "order parameter" and is a measure of the amplitude of the segmental motions. It is zero if the fast motion is isotropic.

Figure 6 shows pictorially the division of the interactional fluctuation into the fast and slow components.

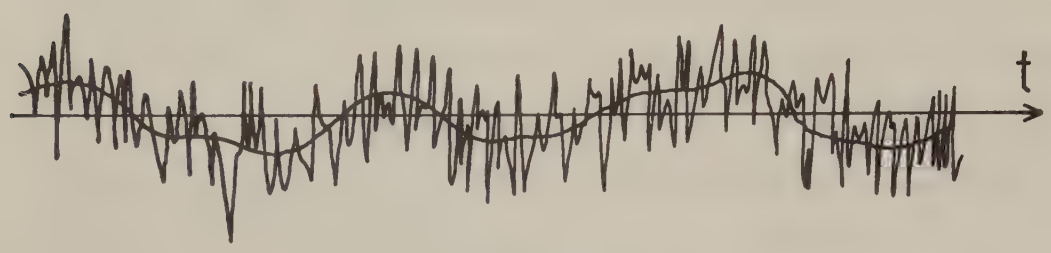

Figure 6. A schematic picture of the fluctuation of the interaction (dipolar or quadrupolar) due to the fast and slow motions.

In paper III it is demonstrated that the slow motion for simple micelles is describable by a single exponential correlation function, leading to the spectral density function for the so-called "two-step model" of Wennerström et al.[16] for NMR relaxation:

$$J(\omega)/G(0) \equiv \tilde{J}(\omega) = (1-S^2)\cdot 2\tau_c^f + S^2\cdot 2\tau_c^s/(1 + (\omega\tau_c^s)^2) \qquad (6)$$

τ_c^f and τ_c^s are the correlation times for the fast and slow motions, respectively. Extreme narrowing conditions apply for the fast motion, i.e. $\omega\tau_c^f \ll 1$, where τ_c^f is an <u>effective</u> correlation time for this motion.

The two-step model is not restricted to surfactant hydrocarbon chains in its application. It has been used to account for the relaxation of polar head group nuclei like ^{14}N [14] (see also paper III) and the ^{17}O nucleus of water[15] in micellar systems.

3.2 ^{13}C Spin-Lattice Relaxation in Micellar Systems.

The expressions for the dipolar spin-lattice relaxation time, T_1, and n.O.e. for a ^{13}C nucleus under complete proton decoupling are given by[17]:

$$1/T_1 = (N_i/20)[\mu_o\gamma_H\gamma_C\hbar/4\pi r^3_{C-H}]^2(\tilde{J}(\omega_H - \omega_C) + 3\tilde{J}(\omega_C) + 6\tilde{J}(\omega_H + \omega_C)) \quad (7)$$

$$\text{n.O.e.} = (1/20)(\gamma_H \cdot \gamma_C)[\mu_o\hbar/4\pi r^3_{C-H}]^2(N_i T_1)(6\tilde{J}(\omega_H + \omega_C) - \tilde{J}(\omega_H - \omega_C)) \quad (8)$$

where the various symbols have their usual meaning. N_i is the number of protons directly bonded to the carbon and ω_H and ω_C are the angular Larmor frequencies of proton and carbon, respectively. By inserting $\tilde{J}(\omega)$ given by eq.(6) into eqs.(7) and (8) it is seen that the NMR spin-lattice relaxation is governed by one organizational and two dynamic parameters, viz. the order parameter, S,and the fast and slow correlation times, τ_c^f and τ_c^s. In Figure 7 is shown the variation of T_1 with magnetic field strength and correlation time for a $^{13}C^1H_2$ group as predicted from a single isotropic motion model and from the two-step model.

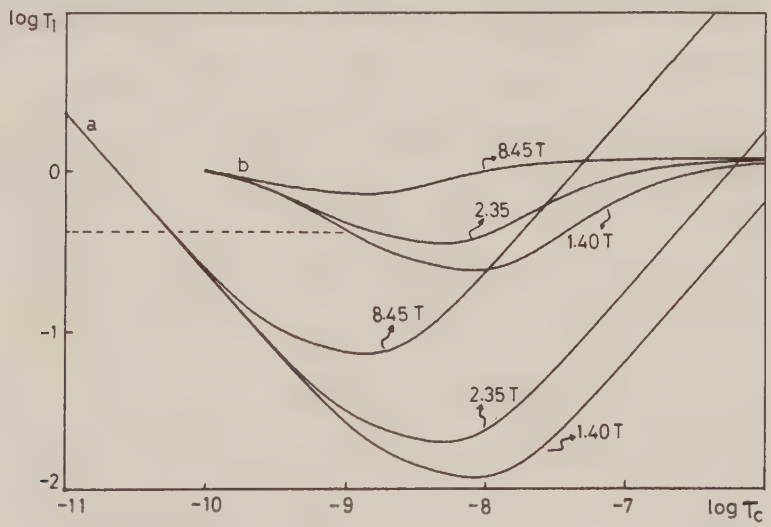

Figure 7. Theoretical predictions of ^{13}C T_1 for a CH_2 group at three magnetic field strengths. The curves under (a) represent the predictions of a single isotropic motion model while those under (b) represent the predictions of the two-step model. In this case, S = 0.2 and τ_c^f = 20 ps. The dashed line indicates a typical micelle T_1.

By performing at least three independent relaxation measurements at different magnetic field strengths it is possible to extract the information on order and dynamics furnished by the two-step model, for all or most carbons along the alkyl chain of aggregated surfactant molecules. Since the slow motion involves the surfactant molecule as a whole the slow correlation time is equal for all carbons in the calculations. The computational procedure for extracting the various parameters is described in paper II and references therein.

In paper II the influence of inter alia different surfactant alkyl chain length and temperature on the organization and dynamics were investigated. In Figure 8 the order parameter and fast correlation time profiles for one of the systems in this study are shown.

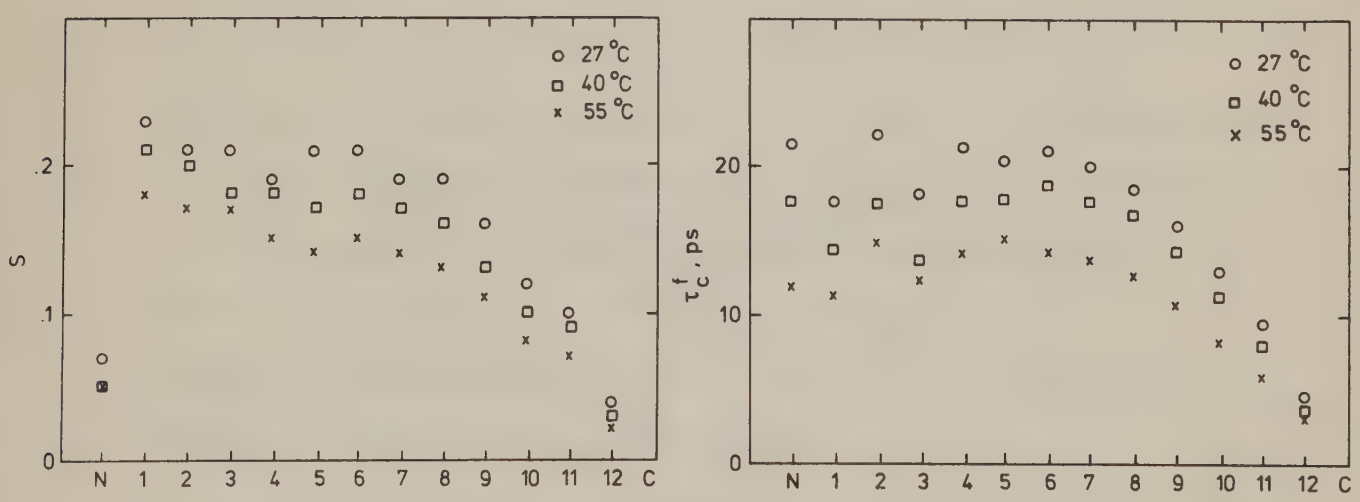

Figure 8. (a) The order parameter as a function of chain position and temperature for one of the micellar systems studied in paper II (30 wt% dodecyltrimethylammonium chloride in water). N denotes head group methyls of the surfactant molecule. (b) The fast correlation times as a function of chain position and temperature for the same system as in (a).

For all systems studied the order parameter is highest at the polar end, and then decreases towards the terminal methyl group. The order parameter profiles show a typical "S"-shape reflecting the packing conditions of the hydrocarbon chains in more or less spherical aggregates (see Figure 8).

The rate of the fast local motions increases towards the terminal methyl group and the fast correlation times are of the order of 10 ps, approximately equal to correlation times extracted from liquid hydrocarbons with comparable chain lengths at the same temperature. This finding stronly supports the picture of micelles with a liquid-like hydrocarbon interior.

When the temperature is raised the order decreases and the mobility increases a little. These effects are seen in Figure 8.

The slow correlation times, τ_c^s, reported in paper II are 1-2 ns, depending on system and temperature. They are too short when compared with theoretical correlation times, assuming contributions from micellar tumbling and monomer lateral diffusion processes. They are also rather insensitive to changes of the micellar radius as the length of the alkyl chains are varied. A reason for this insensitivity is proposed in the study presented in paper III (see below).

Recently, progress has been made in the field of theoretical simulation techniques on simple surfactant systems like ordinary micelles. Gruen[18] has made computer simulations and has calculated inter alia order parameter profiles for spherical micelles of the type investigated in paper II. He finds an almost exact agreement between our experimentally and his theoretically calculated order papameters. From the simulation the signs of the order papameters can be extracted but from relaxation measurements only the absolute values can be found (see eq.(6)).

In Gruens simulations only equilibrium characteristics of the systems are calculated. When compared with Molecular Dynamics (MD) simulations[19] which explicitly take into account the time evolution of a system, the equilibrium properties calculated from these simulations agree at least qualitatively with those of Gruens simulations. Such time resolved simulations also give some further insight into what we measure with the fast correlation time of the two-step model. The MD simulations show that internal trans-gauche isomerizations in the alkyl chains and interchain collisions give rise to reorientational processes for the CH_2 segments occuring on the picosecond time scale at normal temperatures.

3.3 ^2H and ^{14}N Spin-Lattice and Spin-Spin Relaxation in a Micellar and a Cubic Liquid Crystalline System.

In paper III a NMR spin-lattice relaxation study is presented for the micellar solution phase (L_1) and the cubic liquid crystalline phase (I_1) of the system dodecyltrimethylammonium chloride (DOTAC)/water. The investigated relaxation was that of the deuterons of the amphiphile deuteriated at the carbon adjacent to the polar head group (the so-called α-position) and that of the ^{14}N nucleus in the trimethylammonium head group. In addition some ^{13}C relaxation data are presented for the cubic phase.

The cubic liquid crystalline phase (I_1), occuring between the micellar solution phase (L_1) and the hexagonal liquid crystalline phase in the binary system DOTAC/water, is, contrary to other liquid crystalline mesophases, optically isotropic and its NMR spectra show no static effects. Rather, it gives NMR spectra with the same resolution as from micellar

solutions. Therefore, information on order and dynamics of the hydrocarbon chains in this phase can only be obtained from indirect methods like those employed for micellar systems.

In paper II the question of how to describe the slow motion for micelles was raised. The possibility that some types of slow processes not describable by single correlation functions contribute to the ^{13}C spin-lattice relaxation was put forward.

In order to check this possibility we synthesized α-deuteriated DOTAC and made ^{2}H T_1 and T_2 measurements at no less than 10 different magnetic field strengths down to 0.3 Tesla. These measurements were done both for a micellar solution and for the cubic liquid crystalline phase. The α position was selected because the influence of the slow motion is greatest here, as a result of the relatively large order parameter for the α carbon (see Figure 8a). The results are presented in Figure 9 for the micelles and in Figure 11 for the cubic liquid crystalline phase (see below).

The spin-lattice and spin-spin relaxation rates for deuterium (spin quantum number I = 1) are given by[20]:

$$R_1 \equiv (1/T_1) = (3\pi^2/40)\cdot\chi^2\cdot(2\tilde{J}(\omega_D) + 8\tilde{J}(2\omega_D)) \qquad (9)$$

$$R_2 \equiv (1/T_2) = (3\pi^2/40)\cdot\chi^2\cdot(3\tilde{J}(0) + 5\tilde{J}(\omega_D) + 2\tilde{J}(2\omega_D)) \qquad (10)$$

χ is the quadrupole coupling constant for deuterium (set equal to 167 kHz[21]) and ω_D is the Larmor frequency for ^{2}H. In the two-step model for NMR relaxation the reduced spectral densities, $\tilde{J}(\omega)$, are given by eq.(6) assuming that the fast and slow motions can be described by single exponential correlation functions.

3.3.1 The Micellar Solution Phase.

For the micelles it is clear from Figure 9 that the two-step model describes the relaxation. Also included in the figure are relaxation data for the ^{14}N nucleus (I = 1) in the head group of DOTAC. The spin relaxation of ^{14}N follows equations (9) and (10) with ω_D replaced by ω_N, the Larmor frequency of ^{14}N. For ^{14}N a value of 116 kHz for χ was used[22]. With a slow correlation time, τ_c^s, of 3.9 ns and the other parameters as given in the figure text the theoretical lines in Figure 9 are calculated.

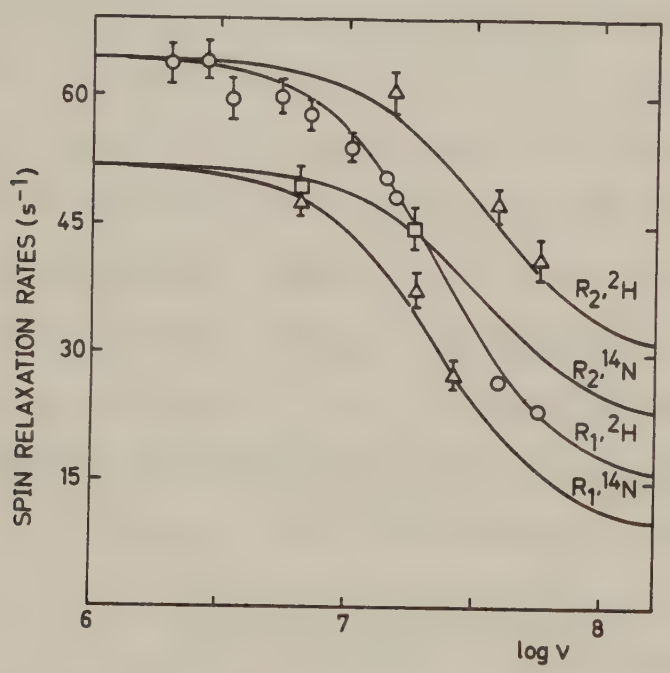

Figure 9. Spin-lattice and spin-spin relaxation rates for ^2H (○= R_1, △= R_2) and ^{14}N (△= R_1, □= R_2) for a micellar sample at 28°C of DOTAC (30 wt% DOTAC in water). The solid lines are fits of the two-step model to the data. τ_c^s = 3.9 ns, for ^2H the order parameter S = 0.17 and τ_c^f = 37 ps, and for ^{14}N S = 0.23 and τ_c^f = 52 ps.

Slower motions like micellar deformations may be present in these systems. Such processes do, however, not contribute to the NMR relaxation because the residual interaction left over by the fast (slightly anisotropic) motions is completely averaged out by the isotropic nanosecond motion.

Figure 10 explains why in paper II we find that slow correlation times extracted from ^{13}C relaxation data alone are so insensitive to changes in the micellar radius. ^{13}C spin-lattice relaxation is at the highest magnetic field strengths employed, mostly governed by the fast motion and therefore only part of the low frequency dispersion of $\tilde{J}(\omega)$ is probed. Due to the lower Larmor frequencies entering for deuterium and nitrogen the spin relaxation of these nuclei is more sensitive to the slow process. ^{13}C spin-lattice relaxation is, on the other hand, well determined by the order of the surfactant alkyl chains, and this information is accurately extracted from differences in spin-lattice relaxation rates at two or more different magnetic field strengths (see later).

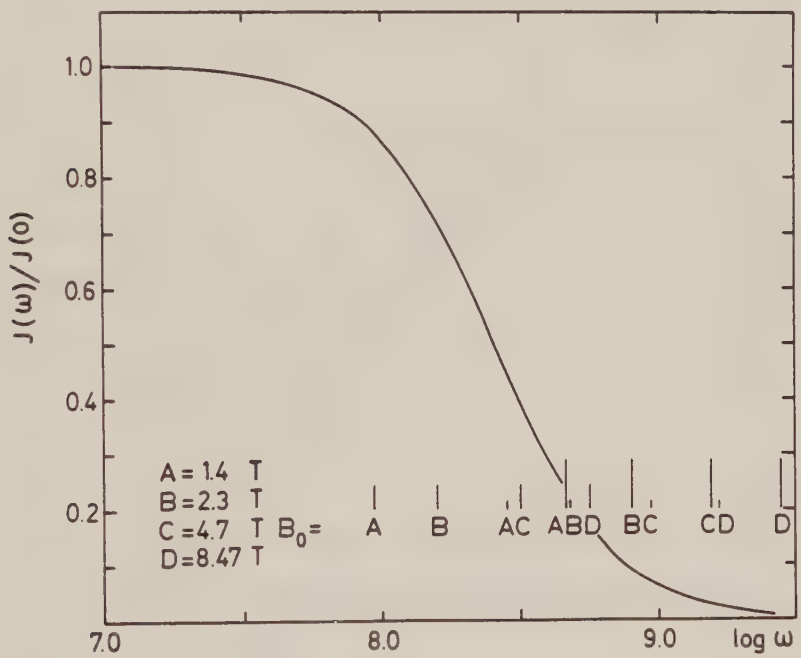

Figure 10. The reduced spectral density function for the slow motion assuming a single exponential correlation function and a slow correlation time of 3.9 ns. The vertical lines represent points on the curve sampled by a ^{13}C spin-lattice experiment. The height of the lines are proportional to the weight each value of $\tilde{J}(\omega)$ has in the equation for T_1(eq.(7)). The lines are positioned at the arguments ω_C, $\omega_H - \omega_C$ and $\omega_H + \omega_C$ (with increasing ω) for the spectral densities entering in the expression for ^{13}C T_1.

3.3.2 The Cubic Liquid Crystalline Phase.

The ^2H spin relaxation in the cubic liquid crystalline phase resembles that for the micellar system in that the spin-lattice relaxation rates level off to a plateau for low magnetic field strengths. However, in the cubic phase R_2 is not equal R_1 on the plateau but is nearly twice as large as R_1. This observation is contrary to the micellar case where R_1 and R_2 are equal on the plateau. Thus, the spin-spin relaxation picks up slower motions than does the spin-lattice relaxation for magnetic field strengths down to 0.3 Tesla. This effect is also seen for ^{14}N relaxation data in Figure 11 although this has not been measured at very low magnetic field strengths.

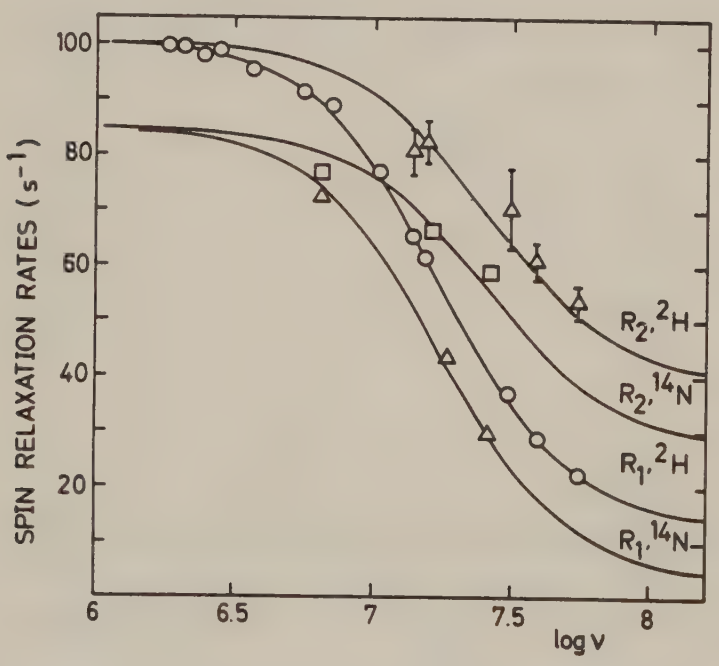

Figure 11. Spin-lattice and spin-spin relaxation rates for ^2H (○ = R_1, △ = R_2) and ^{14}N (△ = R_1, □ = R_2) for for a cubic (I_1) sample. The solid lines are fits of the three-step model to the data (see text). In order to obtain the experimental spin-spin relaxation rates a constant amount (95 s^{-1} for ^2H and 120 s^{-1} for ^{14}N) has to be added to the R_2 data given in the figure. τ_c^r = 5.21 ns; for ^2H S = 0.23 and τ_c^f = 35 ps, while for ^{14}N S = 0.32 and τ_c^f = 22 ps.

The frequency independent parts of the spin-spin relaxation enter via the $\tilde{J}(0)$ term in eq. (10). The two-step model is not able to account for the observed spin relaxation in this case and a generalization of the model is needed. We have based such a generalization on knowledge of the structure of this liquid crystalline phase.

Recently, a very detailed structure for this phase has been proposed, based on X-ray measurements[23] together with published self-diffusion data[24]. It is found that all data available can be accounted for if the aggregates are hemisphere capped cylinders with an axial ratio of around 2:1 and if these cylinders occupy a face-centered cubic lattice.

For rod-shaped micelles where the rotation around the length axis is much faster than the end-over-end tumbling the reduced spectral density can be written:

$$\tilde{J}(\omega) = (1-S^2)\,\tilde{J}^f(\omega) + (3/4)S^2\,\tilde{J}^r(\omega) + (1/4)S^2\,\tilde{J}^t(\omega) \qquad (11)$$

where the superscripts f, r and t denote fast motion, rotation and tumbling, respectively. The total motion is divided into three parts and the relaxation model is termed a "three-step model". For the cubic case the tumbling of the rods described by the last term in eq. (11) is so slow because of the packing constraints on the cylinders in the cubic lattice that it gives rise to a frequency independent part of the spin-spin relaxation for ^2H and ^{14}N and contributes nothing to the spin-lattice relaxation for these nuclei. Therefore, the first two terms of eq.(11) were inserted in equations (9) and (10) assuming exponential correlation functions for these processes. The solid lines in Figure 11 were then calculated with a rotational correlation time, τ_c^r, of 5.2 nanoseconds. The values for the other parameters are given in the figure text. These parameters have the same meaning in the two- and three-step models.

When this procedure is applied to ^{13}C spin-lattice relaxation data for all carbons along the alkyl chain, using 5.2 nanoseconds for the slow correlation time for all carbons, the order and fast dynamics so extracted closely resemble that found for simple micellar systems.

The rotational correlation time, τ_c^r, was used to extract the radius of the hemisphere capped cylindric aggregates from numerical solutions to this problem[25]. A radius of 13.9 Å appeared, in good agreement with 15 Å as determined from X-ray data[23].

As regards the slowest part of the total motion in this system it is hard to be very specific about its nature. We propose some kind of elastic deformations of the lattice originating from the highly collective motions of the cylindrical aggregates. Such processes are certainly not describable by single exponential correlation functions but we have not gone any deeper into this problem.

4. SURFACTANT HYDROCARBON CHAIN ORDER IN TWO LAMELLAR LIQUID CRYSTALLINE PHASES.

In paper IV the order of the hydrocarbon chain of sodium p-octylbenzenesulfonate (SOBS) in the lamellar liquid crystalline phases in the SOBS/pentan-1-ol/water, and SOBS/decan-1-ol/water systems is determined from ^{2}H quadrupole splittings of deuteriated SOBS. Interest is focussed on the effect of the aromatic head group and of the alcohol alkyl chain length on the surfactant hydrocarbon chain organization. Information is also obtained on the head group order.

This information is readily extractable for anisotropic systems. The fast local and (slightly) anisotropic motion of the chain segments reduces the total quadrupolar interaction to a level described by the order parameter, S (see part 3 of the summary). However, contrary to isotropic systems, the residual interaction is not averaged out on the NMR time scale. Therefore, a quadrupole splitting appears in e.g. ^{2}H NMR spectra of anisotropic systems. For a "powder" sample, i.e. a sample where the orientation of the microcrystallites is distributed at random, this splitting, Δ^{obs}, is given by[26]:

$$\Delta^{obs} = (3/4)\cdot\chi\cdot|S| \qquad (12)$$

where χ is the quadrupole coupling constant for ^{2}H and S is defined analogously to eq.(5) where the average now is taken over motions that are rapid compared to the inverse of the quadrupole interaction. If the symmetry axis of the electric field gradient is along the C-^{2}H bond axis then order parameters determined from deuterium spin relaxation or quadrupole splittings are equivalent to those extracted from ^{13}C spin relaxation data.

From observed splittings in ^2H NMR spectra the order parameters are extracted by means of eq.(12). For the lamellar system consisting of SOBS, pentan-1-ol and water it is found that the order parameter profiles show no plateau (see Figure 12a), while for the system SOBS/decan-1-ol/water the order parameter profile (Figure 12b) is more plateau-like. Such a plateau can be expected if the bilayers have maximum thickness.

This observation can be explained as follows. For high alcohol contents where the electrostatic repulsion between the charged head groups is largely reduced the difference in the surfactant and the alcohol alkyl chain length is an important stability factor. The pentanol compresses the bilayers to below maximum thickness while for the decanol system no such compression occurs (evidence from X-ray measurements). The surfactant alkyl chain is therefore beleived to be straightened in the decanol system as compared to the situation in the pentanol case. However, the relative large amphiphile head group can also influence the surfactant hydrocarbon chain order to some extent in these systems, thereby obscuring the effects of bilayer compression on observed order parameter profiles.

Also seen in Figure 12 is the odd-even effect described by Davis and Jeffrey[27]. It is thought that the effect is caused by the first C-C bond in the alkyl chain having an average orientation different from that of the bilayer normal. For SOBS this effect is introduced by the aromatic head group.

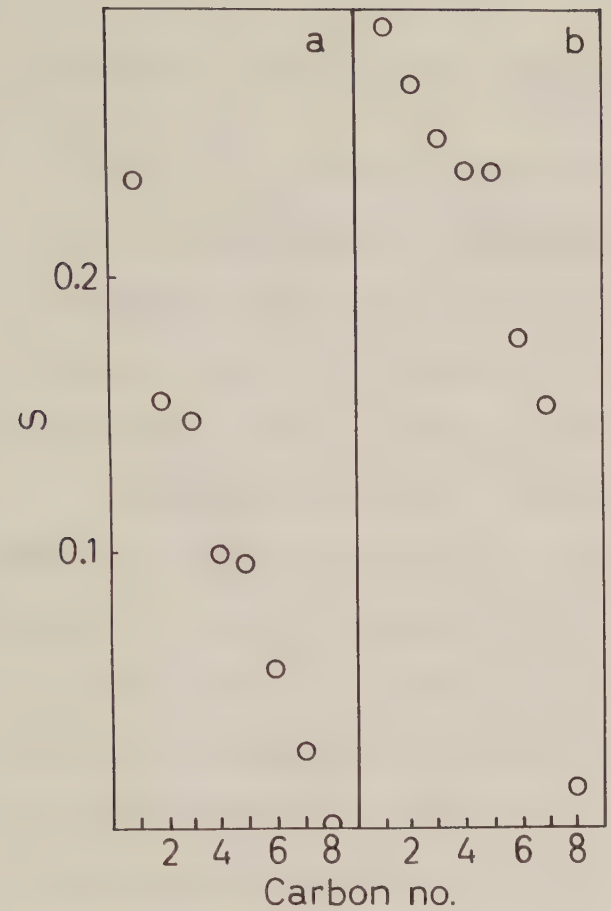

Figure 12. The order parameter profile for the hydrocarbon chain of SOBS in two lamellar phases of the systems
a: SOBS/pentan-1-ol/water
b: SOBS/decan-1-ol/water.

The observed quadrupole splittings from the head group deuterons are small, indicating that the angle θ_{MD} for these deuterons is close to the "magic angle", 54.74^{o}, for which the order parameter S = 0. This observation is also made for some isotropic solutions as extracted from ^{2}H and/or ^{13}C spin relaxation data. The isotropic systems were one micellar solution of SOBS in water, a three-component and a four-component "microemulsion" consisting of SOBS, butan-1-ol and water, and SOBS, butan-1-ol, water and toluene, respectively. It is found that the local order of the SOBS alkyl chain and head group is only weakly affected by the various kinds of aggregation in these systems. This conclusion is also valid for the local dynamics of the surfactant hydrocarbon chains in the isotropic systems. The head group becomes more mobile upon dilution of the systems with alcohol.

5. ^{13}C SPIN RELAXATION IN MICROEMULSIONS.

In papers V and VI two ^{13}C spin-lattice relaxation studies of so-called "microemulsion" systems are presented. Microemulsions are, according to a recent definition[28], thermodynamically stable isotropic single phase solutions of surfactant, oil (where "oil" is to be understood in a broad sense) and water. Often, also a so-called cosurfactant, a medium chain length alcohol, is present. Despite the substantial industrial and fundamental interest in microemulsion systems the molecular structures of these systems are only partly known at present. Oil-in-water situations where closed oil droplets are surrounded by surfactant in a water water continous medium, as well as water-in-oil systems, where the situation is reversed, are known. From the method of NMR self diffusion measurements[29] it has been found that for four-component microemulsions the alcohol alkyl chain length is an important factor in determining the type of microemulsion to be formed. It has been found that for medium chain length alcohols such as butanol, pentanol or hexanol, typical water and oil bicontinous microemulsions are formed over a wide range of compositions. A recent X-ray and neutron scattering study[30] shows that the hydrophobic/hydrophilic interfaces of Winsor type microemulsions have a zero mean curvature.

5.1 ^{13}C Spin-Lattice Relaxation in a Four-Component Microemulsion.

In paper V we investigate the four-component microemulsion system sodium p-octylbenzenesulfonate (SOBS)/butan-1-ol/water/toluene by means of ^{13}C spin-lattice relaxation of the hydrocarbon chain of SOBS. As for the micellar systems it is found that the spin-lattice relaxation rates are dependent on the magnetic field strength and that the nuclear Overhauser effects are reduced. Figure 13 shows this magnetic field strength

dependence in the relaxation rates for two carbon atoms in the alkyl chain of SOBS.

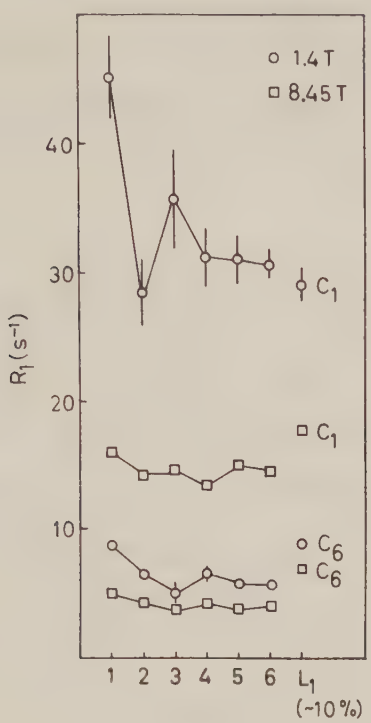

Figure 13. Observed ^{13}C spin-lattice relaxation rates as a function of composition of the microemulsion (see Figure 1 in paper V) for carbons no. 1 and 6 in the alkyl chain of SOBS at two different magnetic field strengths. Also shown are the corresponding data for a micellar solution (10 wt% SOBS in water) at $42^{o}C$. The temperature for the microemulsion is $25^{o}C$.

The two-step model for NMR relaxation is used to interpret the relaxation data. The order and fast dynamics for the hydrocarbon chain so extracted resemble that for simple micelles. The slow correlation times for the various samples investigated are around 1-2 nanoseconds and can be interpreted as the life-time for the anisotropy imposed on the alkyl chains by the hydrophobic/hydrophilic interface. This must then be in a highly dynamic state, accounting for the low viscosities of these systems. Part of the slow process can be monomer exchange between the different aggregates but probably this process contibutes only a minor part to the slow motion. It is, however, quite possible that the slow motion observed with ^{13}C spin-lattice relaxation is not completely isotropic and, furthermore, not describable by a single exponential correlation function. From our limited set of data we can not be very specific on this point at present. The slow motion problem is further dealt with in the next paragraph where another microemulsion system is studied.

5.2 ^{13}C Spin-Lattice Relaxation in a Three-Component Microemulsion.

In paper VI some ^{13}C spin-lattice relaxation investigations of the surfactant hydrocarbon chains in the L_2 phase of the system sodium di-2-ethylhexylsulfosuccinate (AOT)/water/p-xylene are presented. Figure 14 shows the phase diagram for this system.

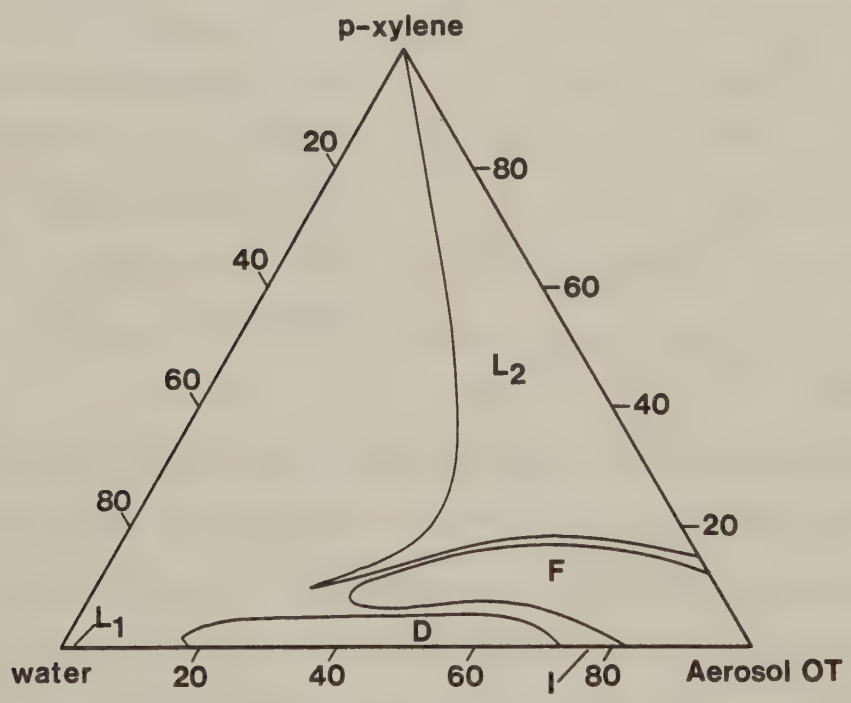

Figure 14. Phase diagram for the system AOT/water/p-xylene at 20°C.

AOT, which consists of two branched hydrocarbon chains, forms inverted structures and for low water contents in the L_2 phase region the structure is that of inverted micelles. With increasing water content the molecular structure is that of a typical water-in-oil (w/o) microemulsion (swollen reversed micelles) and this and related systems have been taken as model systems for microemulsions[31]. Figure 15 on the next page shows the structural formula of the AOT molecule.

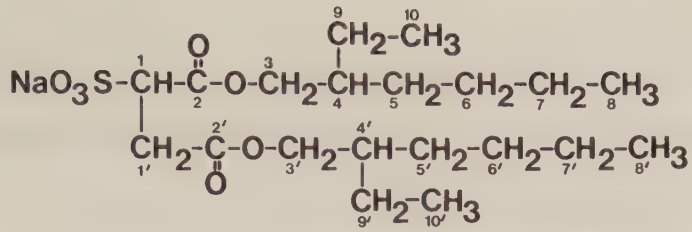

Figure 15. Structural formula of sodium di-2-ethylhexylsulfosuccinate (AOT).

The magnetic field strength dependence in the relaxation times is very high for the carbons close to the head group in both alkyl chains at low water contents and decreases upon dilution of the system with water. Table 1 shows ^{13}C relaxation times and nuclear Overhauser effects for three carbon positions and two compositions at two different magnetic field strenghts.

Table 1.

Spin-lattice relaxation times $(T_1)^a$ and nuclear Overhauser enhancements $(\eta)^b$ for three carbon positions in the alkyl chains of AOT at two different magnetic field strengths for systems containing 10 and 50 weight per cent water.

	10 wt% water			50 wt% water		
Carbon no.	T_1(1.4 T)	T_1(8.5 T)	η(8.5 T)	T_1(1.4 T)	T_1(8.5 T)	η(8.5 T)
1	0.047	0.230	0.36	0.081	0.257	1.06
5,5'[c]	0.117	0.284	1.07	0.249	0.415	1.46

(a): T_1 values quoted in seconds.
(a) and (b): Precision of ±10% or better.
(c): The individual NMR lines not resolved. See also figure 15 above.

When extracted by means of the two-step model the order is exceptionally high near the head group (order parameters as high as 0.5). There is a marked line broadening in both ^{13}C and ^{1}H NMR spectra for the segments

close to the head group which can not be accounted for by the simple two-step model. A generalization for the spectral density functions is suggested by the following equation[12]:

$$\tilde{J}(\omega) = (1-S_1^2)2\tau_c^f + (S_1^2 - S_2^2)2\tau_c^i/(1 + (\omega\tau_c^i)^2) + S_2^2 \cdot 2\tau_c^s/(1 + (\omega\tau_c^s)^2) \quad (13)$$

This equation describes three steps in the spin relaxation and two order parameters are needed. S_1 contains the same information as S in the two-step model while S_2 is the degree of the interaction being averaged out by the intermediate motion. In eq.(11) $S_1/S_2 = 3$ because of the symmetry in that case. Here we do not specify this proportion because of the lack of detailed information of the intermediate motion. Its correlation time is around 1 nanosecond and this motion is responsible for the magnetic field dependence in T_1 and reduced nuclear Overhauser effects (see Table 1). The intermediate correlation time, τ_c^i, is relatively independent of water content and therefore independent of the size of the aggregates in this system. The slowest motion possibly consists of aggregate reorientation and monomer lateral diffusion over the aggregate surface.

Even though the possibility exists that the intermediate motion can not be described by a single exponential correlation function it is demonstrated in paper VI that the order parameter <u>profile</u> for the hydrocarbon chains can be extracted from ^{13}C T_1's measured at only <u>two</u> different magnetic field strengths without assuming any particular form for the spectral density functions for the slow motions.

6. CONCLUDING REMARKS.

The method of NMR spin relaxation has been used to study properties of the surfactant hydrocarbon chains in a variety of situations. When small molecules like trans-Decalin (part 2 of the summary) is solubilized in simple micelles it is found that the reorientation of the solubilized molecules is described hydrodynamically with a viscosity of the hydrocarbon interior practically equal to the bulk viscosity of simple alkanes with the same alkyl chain length and at the same temperature. This observation gives further evidence for the picture of micelles with a very liquid-like interior.

The local properties of the surfactant alkyl chains of micelles and other isotropic aggregated surfactant systems have been extracted using ^{2}H, ^{13}C and ^{14}N spin relaxation data interpreted by means of a very simple two-step model for NMR spin relaxation. This model provides information on local order, quantified by an order parameter, and fast and slow dynamics, described by a fast and a slow correlation time, respectively. In some cases this model has been generalized to account for experimental relaxation data.

Local order thus extracted closely resembles that found in related anisotropic systems. The fast correlation times resemble those extracted from simple hydrocarbon liquids. Thus, the local properties of the surfactant alkyl chains do not depend critically on the type of aggregates formed.

It is also demonstrated that the slow overall motion of micelles is actually describable by a single exponential correlation function. In other cases the situation can be more complicated. However, some information on local structure of alkyl chains in isotropic aggregated surfactant systems can be extracted from spin relaxation data without assuming any particular form for the correlation functions for slow motions.

REFERENCES.

1. "Microemulsions", ed. L.M. Prince (Academic Press, New York 1977).
2. "Microemulsions", ed. I. Robb (Plenum Press, New York 1982).
3. "Surfactants in Solution", vol.3, eds. K.L. Mittal and B. Lindman (Plenum Press, New York 1984).
4. E. Vikingstad, Thesis, Bergen, 1979.
5. B. Lindman and H. Wennerström in Top. Curr. Chem., 87, 1 (1980); H. Wennerström and B. Lindman, Phys. Rep., 52, 1 (1979).
6. K. Fontell in "Liquid Crystals and Plastic Crystals", vol.2, eds. G.W. Gray and P.A. Winsor, Horwood, Chichester, 1974, chap.4.
7. M.E. Moseley, Chem. Scr., 16, 28 (1980).
8. D.E. Woessner, J. Chem. Phys., 37, 647 (1962).
9. W.T. Huntress, Adv. Magn. Reson., 4, 1 (1970).
10. R.T. Boeré and R.G. Kidd in "Annual Reports on NMR Spectroscopy", vol.13, ed. G.A. Webb, Academic Press, New York 1982, pp 319-85.
11. J. Seelig, Q. Rev. Biophys., 10, 3 (1977).
12. J.H. Davis, K.R. Jeffrey and M. Bloom, J. Magn. Reson., 29, 191 (1978).
13. T. Klason and U. Henriksson in "Solution Chemistry of Surfactants", eds. K.L. Mittal and E.J. Fendler, Plenum Press, New York 1982.
14. U. Henriksson, L. Ödberg, J.C. Eriksson and L. Westman, J. Phys. Chem., 81, 76 (1977).
15. B. Halle and G. Carlström, J. Phys. Chem., 85, 2142 (1981).

16. H. Wennerström, B. Lindman, O. Söderman, T. Drakenberg and J.B. Rosenholm, J. Am. Chem. Soc., 101, 6860 (1979).

17. D. Doddrell, V. Glushko and A. Allerhand, J. Chem. Phys., 56, 3683 (1972).

18. D.W.R. Gruen, J. Phys. Chem., 89, 146 (1985); D.W.R. Gruen, (ibid) p. 153.

19. J.M. Haile and J.P. O'Connell, J. Phys. Chem., 88, 6363

20. A. Abragam, "The Principles of Nuclear Magnetism", Clarendon, Oxford 1961.

21. L.J. Burnett and B.H. Muller, J. Chem. Phys., 55, 5829 (1971).

22. T.K. Protum and M.P. Klein, J. Magn. Reson., 53, 473 (1983).

23. K. Fontell, K.K. Fox and E. Hansson, submitted for publication.

24. P.O. Eriksson, A. Khan and G. Lindblom, J. Phys. Chem., 86, 387 (1982).

25. T. Yoshikazo and H. Yamakawa, J. Chem. Phys., 72, 57 (1980).

26. J.H. Davis, Biochim. Biophys. Acta, 737, 117 (1983).

27. J.H. Davis and K.R. Jeffrey, Chem. Phys. Lipids, 20, 87 (1977).

28. I. Danielsson and B. Lindman, Colloids and Surfaces, 3, 393 (1981).

29. B. Lindman and P. Stilbs in "Surfactants in Solution", eds. K.L. Mittal and B. Lindman, vol.3, p.1651, Plenum Press, New York 1984; P. Stilbs and B. Lindman, Progr. Colloid & Polymer Sci., 69, 39 (1984).

30. L. Auvray, J.P. Cotton, R. Ober and C. Taupin, J. Phys. Chem., 88, 4586 (1984).

31. H.F. Eicke and J. Rehak, Helv. Chim. Acta, 59, 2883 (1976); M. Zulauf and H.F. Eicke, J. Phys. Chem., 83, 480 (1979); M. Wong, J.K. Thomas and T. Nowak, J. Am. Chem. Soc., 99, 4730 (1977).

ACKNOWLEDGMENTS

First, and above all, I want to express my gratitude to my close friend Peter who introduced me to the novel Art of NMR in "early days" when I was an undergraduate student in Bergen, and to Björn for inviting me to his group in Lund.

Thanks also go to:

Olle: My close friend and co-worker/supervisor.

Torbjörn: For teaching me practical NMR.

Håkan and Joe: For valuable critizism on the final draft, and linguistic aid during the preparation of the Summary.

Bosse: See the Cover.

Our secretaries MajLis and Eva: For typing some of the manuscripts, and to the rest of the research group for the kind, stimulating and very informal atmosphere during these years.

Last, but not least, I want to acknowledge my beloved Annika for her patience with me during the preparation of my Thesis.

THANK YOU !

Reprinted from The Journal of Physical Chemistry, 1983, 87, 4762.
Copyright © 1983 by the American Chemical Society and reprinted by permission of the copyright owner.

Micellar Fluidity. A Deuterium Nuclear Magnetic Resonance Spin Relaxation Study of the Anisotropic Reorientation of Solubilized *trans*-Decalin-d_{18}

Peter Stilbs,*

Institute of Physical Chemistry, Uppsala University, S-75121 Uppsala, Sweden

Harald Walderhaug, and Björn Lindman

Physical Chemistry 1, Lund University, Chemical Center, S-22007 Lund, Sweden *(Received: April 8, 1983; In Final Form: May 16, 1983)*

The rotational diffusion tensor for micellarly solubilized *trans*-Decalin-d_{18} has been studied through deuterium NMR spin relaxation measurements. Quantitative information on the correlation times for reorientation of *trans*-Decalin around the principal rotational diffusion axes is obtained for a wide range of micellar systems. In this way, detailed insight into the dynamics of the interior of micelles is gained. This is found to resemble quantitatively that of simple solutions. More specifically, there is a close argument between the correlation times for reorientation of *trans*-Decalin in micelles on one hand and in hydrocarbon solvents with the same alkyl chain length as the surfactant hydrophobic part on the other. From a comparison with hydrodynamic theories it is concluded that the reorientation process is hydrodynamically related to a good approximation and thus can be quantified in terms of a "micellar viscosity". On the molecular level, the observations are interpreted in terms of the differing probabilities for intermolecular chain entanglement processes in micelles formed by surfactants with different alkyl chain lengths.

Introduction

The important question of the state of the hydrocarbon part of micelles and related aggregates has been considered ever since the pioneering work by Hartley.[1,2] Numerous recent discussions of experimental data on aqueous surfactant solutions are focused on structural aspects of this kind.[3–10] Presently there is general agreement that the micellar interior is "liquidlike". Several attempts by different techniques have been made to quantify this characteristic more fully.

In the transformation of macroscopic concepts like "fluidity, viscosity, rigidity, ..." to microscopic units of micellar size, several fundamental difficulties arise. Macroscopic material properties at a given temperature depend in a very complicated way on intermolecular and intramolecular forces and the dynamic molecular processes occurring on the molecular level in the system. Macroscopic and microscopic dynamic properties of microheterogeneous systems are only weakly correlated. This is evident from a vast source of experimental data, based on detailed insight into molecular motion through nuclear magnetic resonance methods.[10–17] Strikingly small differences in diffusion or reorientation behavior of small molecules or alkyl chains of constituents are found between normal low-viscosity solutions on one hand and macroscopically rigid systems like concentrated polymer solutions,[11–13,16] rubbers,[14] and certain cubic liquid crystalline mesophases[15,17] (which physically resemble Plexiglas) on the other. The macroscopic rigidity of microheterogeneous systems is merely a reflection of long-range order; local mobility is often only weakly hindered by these conditions.

The situation is quite different in liquids made up by small to medium-size molecules. Here one finds a close correspondence between concepts such as bulk viscosity and molecular transport processes. The familiar Debye–Stokes–Einstein equation

$$\tau_{\mathrm{rot}} = 4\pi\eta a^3/(k_{\mathrm{B}}T) \qquad (1)$$

for example, provides a surprisingly good description of reorientational phenomena in these solutions. Originally derived for a sphere in a continuum, this equation was later extended to asymmetric tops by Perrin.[18] Numerous other refinements of these theories have been published, partly accounting for details of molecular motion in solution, as opposed to the continuum model leading to expressions

(1) G. S. Hartley, "Aqueous Solutions of Paraffin Salts", Hermann, Paris, 1936.
(2) G. S. Hartley, *J. Chem. Soc.*, 1968 (1938).
(3) R. J. E. M. de Weerd, J. W. de Haan, L. J. M. van de Ven, and H. M. Buck, *J. Phys. Chem.*, **86**, 2528 (1982).
(4) T. S. Brun, H. Høiland, and E. Vikingstad, *J. Colloid Interface Sci.*, **63**, 89 (1978).
(5) H. Wennerström, B. Lindman, O. Söderman, T. Drakenberg, and J. B. Rosenholm, *J. Am. Chem. Soc.*, **101**, 6860 (1979).
(6) R. E. Stark, M. L. Kasakevitch, and J. W. Granger, *J. Phys. Chem.*, **86**, 335 (1982).
(7) J. C. Eriksson, U. Henriksson, T. Klason, and L. Ödberg in "Solution Chemistry of Surfactants", K. L. Mittal and E. J. Fendler, Eds., Plenum Press, New York, 1982, pp 907–19; U. Henriksson, T. Klason, E. Florin, and J. C. Eriksson, *NATO Adv. Study Inst. Ser., Ser. C*, **61**, 681 (1980).
(8) B. Lindman and H. Wennerström in "Solution Chemistry of Surfactants", K. L. Mittal and E. J. Fendler, Eds., Plenum Press, New York, 1982, pp 3–25; B. Lindman and H. Wennerström in *Top. Curr. Chem.*, **87**, 1 (1980); H. Wennerström and B. Lindman, *Phys. Rep.*, **52**, 1 (1979).
(9) K. Fontell in "Liquid Crystals and Plastic Crystals", Vol. 2, G. W. Gray and P. A. Winsor, Eds., Horwood, Chichester, 1974, Chapter 4.
(10) E. Williams, B. Sears, A. Allerhand, and E. H. Cordes, *J. Am. Chem. Soc.*, **95**, 4871 (1973).
(11) M. E. Moseley and P. Stilbs, *Polymer*, **19**, 1133 (1978).
(12) J. R. Lyerla, Jr., and G. C. Levy in "Topics in Carbon-13 NMR Spectroscopy", Vol. 1, G. C. Levy, Ed., Wiley, New York, 1974, Chapter 3.
(13) B. D. Boss, E. O. Stejskal, and J. D. Ferry, *J. Phys. Chem.*, **71**, 1501 (1967).
(14) E. von Meerwall and R. D. Ferguson, *J. Appl. Polym. Sci.*, **23**, 3657 (1979).
(15) P.-O. Eriksson, A. Khan, and G. Lindblom, *J. Phys. Chem.*, **86**, 387 (1982).
(16) W. Brown and P. Stilbs, *Chem. Scr.*, **19**, 161 (1982); B. Nyström, M. E. Moseley, P. Stilbs, and J. Roots, *Polymer*, **22**, 218 (1981); M. E. Moseley and P. Stilbs, *Chem. Scr.*, **16**, 114 (1980); W. Brown, P. Stilbs, and T. Lindström, *J. Appl. Polym. Sci.*, in press.
(17) H. Walderhaug, O. Söderman, and P. Stilbs, to be published.
(18) F. Perrin, *J. Phys. Radium, Ser. VII*, **5**, 497 (1934).

0022-3654/83/2087-4762$01.50/0 © 1983 American Chemical Society

of the Debye–Stokes–Einstein type.[19] Moseley has summarized and tested current hydrodynamic theories for reorientation in solution in a recent paper.[20] A review paper on the subject has also very recently been published.[21]

In contrast to direct motional information on alkyl chain motion within a micelle (which is readily available through nuclear magnetic resonance methods), motional information on a suitable probe molecule would be expected to provide a useful measure of the overall characteristics of the micellar interior. This "motional probe approach", of course, has been extensively used before in many different techniques and applications, also for micelles.[6,22–24] However, in our opinion previous studies on micelles by these techniques are generally unsatisfactory in one or more respects with regard to the information sought. The probe approach is always associated with a number of fundamental problems. Its application to micellar systems adds complicating factors to this list

(i) The probe molecules perturb the micellar structure. This effect is unavoidable but can be minimized. It should be noted, however, that the probed micelles will always contain at least one probe molecule/micelle, despite any efforts to lower the probe concentration.

(ii) The probe molecules may be water soluble and only partly located in the micelles, leading to considerable problems with regard to the interpretation of any acquired data.

(iii) The probe molecules may be unevenly distributed in the micelles, perhaps not even solubilized in the hydrocarbon core, the focus of interest here.

(iv) Motional information on the probe molecules may be difficult to extract from the measurements made for practical or fundamental reasons.

(v) The motional information, when extracted, may be difficult to translate into macroscopic concepts like "viscosity" or related characteristics. For example, probe molecule motion may be restricted due to factors other than "hydrodynamic" ones (ordering in the micelle and specific molecular interactions). When such information is treated uncritically, one may "find" highly misleading measures of local fluidity or viscosity. Order and specific interactions have no relation to hydrodynamics and there is usually no simple relation between order and dynamics in any system.

We believe that these difficulties have been considered and eliminated to a great extent in the present work.

This work is focused on the reorientational behavior of *trans*-Decalin (Figure 1) in solution and when solubilized in micelles. This molecule is rigid and of relatively small size. In contrast to benzene it is almost water insoluble and can safely be assumed to be extensively located in the micellar interior. Since it is a small alicyclic hydrocarbon with no functional groups, one can furthermore anticipate that the perturbations on the micellar structure will be minimized.

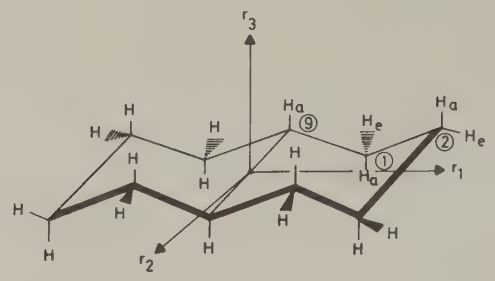

Figure 1. Atom numbering and orientation of the rotational diffusion tensor in *trans*-Decalin.

As described in the Experimental Section, detailed motional information on this molecule in solution is readily accessible through measurements of its carbon-13 or deuterium spin relaxation rates. Reorientational correlation times along the principal axes of the rotational diffusion tensor (as extracted from spin relaxation measurements) can then be related to the viscosity of the environment through hydrodynamic theories, as described in Moseley's paper,[20] or through direct comparison with corresponding experimental data on nonmicellar solutions. It should be noted that of course the reorientational correlation times themselves contain direct information on molecular dynamics, which is not dependent on models.

Experimental Section

Compounds and Sample Preparation. Perdeuterated *trans*-Decalin[25] was prepared from a cis–trans mixture of Decalin-d_{18} (EGA-Chemie, Albuch, West Germany) through the procedure described by Seyer and Yip.[26] The conversion process was monitored by carbon-13 NMR and was found to be considerably slower for the deuterio compound. The conversion of an initially 70:30 cis–trans mixture was observed to be essentially complete after 1 week at 42 °C. Apparently, a retarding isotope effect of about a factor of 7 is operative in this conversion process.

All commercial chemicals were of good quality (puriss or equivalent).

The sodium alkyl sulfate surfactants were purchased from Merck AG. Alkyltrimethylammonium bromide surfactants were purchased from Fluka AG or Eastman Kodak. The corresponding chlorides were prepared from aqueous solutions of these bromides through ion exchange (Dowex 21K resin) over an intermediate hydroxide form. This hydroxide solution was then neutralized with dilute HCl and then filtered and freeze-dried. We thank Dr. Ali Khan for instructions with regard to these ion-exchange procedures for the preparation of alkyltrimethylammonium chlorides from the bromides.

Alkanes and alkylbenzenes were purchased from Fluka AG.

Samples were prepared through weighing and were allowed to equilibrate at room temperature for 24 h before the measurements, and a further hour at the measurement temperature. The Krafft point for two of the surfactants is close to 25 °C, so an elevated measurement temperature

(19) Modern computing facilities and methods have made possible the direct simulation of thermal motion imposed on the molecular force fields in solution, through the so-called methods of molecular dynamics. Although molecular dynamics methods represent much more satisfactory approaches to solution dynamics than hydrodynamic ones, they are of no value in the present context as there is no direct counterpart in these simulations to the quantities sought here.

(20) M. E. Moseley, *Chem. Scr.*, **16**, 28 (1980).

(21) R. T. Boeré and R. G. Kidd in "Annual Reports on NMR Spectroscopy", Vol. 13, G. A. Webb, Ed., Academic Press, New York, 1982, pp 319–85.

(22) A. S. Waggoner, O. H. Griffith, and C. R. Cristensen, *Proc. Natl. Acad. Sci. U.S.A.*, **57**, 1198 (1967).

(23) M. Grätzel and J. K. Thomas, *J. Am. Chem. Soc.*, **95**, 6885 (1973); M. Chen, M. Grätzel, and J. K. Thomas, *Chem. Phys. Lett.*, **24**, 65 (1974); K. Kalyanasundaram, M. Grätzel, and J. K. Thomas, *J. Am. Chem. Soc.*, **97**, 3915 (1975).

(24) M. Shinitzsky, A. C. Dianoux, C. Gitler, and G. Weber, *Biochemistry*, **10**, 2106 (1971).

(25) Due to lack of suitable NMR instrumentation at the time, this work was initially planned to be based on carbon-13 spin relaxation measurements on *trans*-Decalin. This approach turned out to be impractical, primarily for sensitivity reasons. Preliminary data from these studies agree well with the deuterium relaxation data presented in the present paper.

(26) W. F. Seyer and C. W. Yip, *Ind. Eng. Chem.*, **41**, 378 (1949).

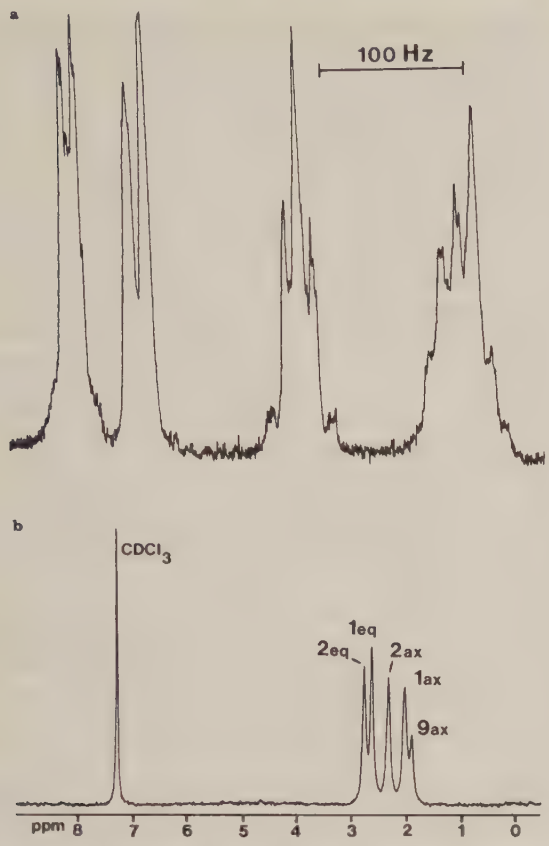

Figure 2. (a) The 360-MHz proton spectrum of (normal) *trans*-Decalin in deuteriochloroform at 27 °C. (b) The 15.3-MHz deuterium spectrum of a dilute solution of *trans*-Decalin-d_{18} and deuteriochloroform in benzene at 25 °C. Shifts are referenced to the internal deuteriochloroform, assigned to a shift of 7.30 ppm. Please note that the line widths are only weakly instrumentally determined. The widths (and heights) closely reflect the respective spin–spin relaxation rates. The different relaxation rates are a result of the anisotropic tumbling of the molecule. (1 symbolizes the 1-, 4-, 5-, and 8-deuterons, 2-, the 2-, 3-, 6-, and 7-deuterons, and 9 the 9- and 10-deuterons). In Hz/ppm at 15.3 MHz the signal shifts are 42.1/2.75, 39.9/2.60, 35.1/2.29, 30.4/1.98, and 28.4/1.85 counting from the low-field side, when using the same shift reference.

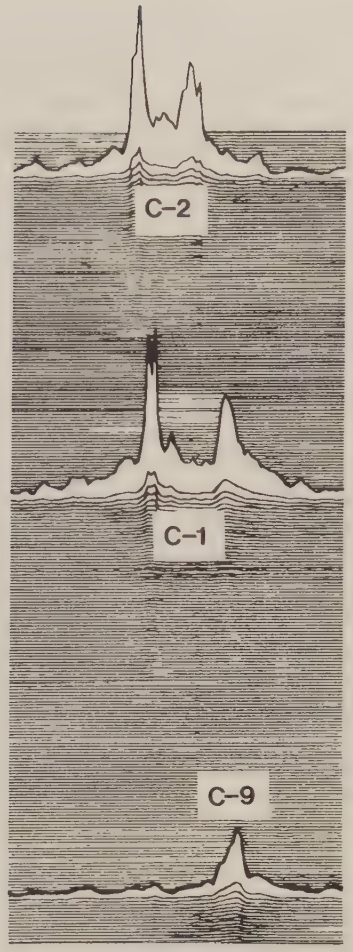

Figure 3. Chemical shift correlation between protons and carbon-13, as obtained by 2D techniques at 8.45-T magnetic field strength; 1000 Hz of the horizontal proton frequency axis and about 1690 Hz of the vertical carbon-13 frequency axis are displayed. The field increases from left to right and from the lower to the upper trace. Quadrature detection was employed in both time dimensions. The projection onto the *x* axis approximately corresponds to the proton/deuterium spectrum but is of course "distorted" by second-order effects (see ref 30 and 31).

of 35 °C was chosen for the main measurement series described below.

Spin Relaxation Measurements. Deuterium relaxation measurements at 15.29 MHz were made on a JEOL FX-100 NMR spectrometer in a special 10-mm deuterium probe, using lithium-7 "internal" lock on a LiCl–water capillary. The external lithium-7 lock facility on this spectrometer is too unstable for this particular application, which requires a frequency stability better than 0.3 Hz over a single measurement series. The corresponding 55.54-MHz measurements were made without field/frequency lock (stabilizer only) on a Nicolet NM-360 high-field (superconducting), wide-bore NMR spectrometer, using a wide-band, 12-mm probe head with 12-mm tubes. This measurement setup has adequate field/frequency stability for the measurements.

The inversion–recovery method in the Fourier transform mode[27] was used for spin–lattice relaxation (T_1) on both systems. Field homogeneity spoiling pulses of 1-ms length after the initial 180° radiofrequency pulse were applied in the 15-MHz measurements to destroy residual transverse magnetization before the observation pulse. Spin–spin (T_2) relaxation of deuterium at 15 MHz was studied through the Carr–Purcell–Meiboom–Gill method[28] in the Fourier transform mode. A low 5-ms interval between successive 180° pulses was employed to minimize artificial effects from sample spinning and translational diffusion on these measurements.[29] Artifacts from off-resonance effects were minimized by performing the measurements as closely as possible (within 8 Hz) on-resonance.

Data Evaluation. Except for the 9-deuteron with half the intensity of the other peaks, the deuterium NMR spectrum of *trans*-Decalin-d_{18} (Figure 2b) is not directly assignable. The corresponding proton spectrum (Figure 2a) is rather intractable even at 360 MHz (even with spin decoupling of selected bands), so there is no way to use the close proton–deuterium shift scale correspondence for an indirect assignment. An unambiguously correct assignment of the deuterium spectrum is a prerequisite for any further evaluation of relaxation rates and rotational diffusion tensor components. The carbon-13 can be shift cross-correlated with the proton spectrum through the modern 2D-NMR techniques,[30,31] as illustrated in Figure 3. Since the carbon assignment is simple and exists be-

(27) R. L. Vold, J. S. Waugh, M. P. Klein, and D. E. Phelps, *J. Phys. Chem.*, **48**, 3831 (1968).

(28) H. Y. Carr and E. M. Purcell, *Phys. Rev.*, **94**, 630 (1954); S. Meiboom and D. Gill, *Rev. Sci. Instrum.*, **29**, 688 (1958).

(29) R. Freeman and H. D. W. Hill, in "Dynamic Nuclear Magnetic Resonance Spectroscopy", L. M. Jackman and F. A. Cotton Eds., Academic Press, New York, 1975, pp 131–62.

forehand, one can combine the 2D map with the established relative high-field shift for axial geminal protons/deuterons with respect to equatorial ones[32] and thus by this doubly indirect way finally assign the deuterium spectrum. The result is shown in Figure 2b.

Spin relaxation rates at 15 MHz were evaluated through iterative nonlinear least-squares procedures, directly on the raw peak intensities, using the Fortran V program UNIFIT (P. Stilbs, unpublished). Confidence intervals were estimated through the Monte Carlo procedure described in ref 33. The 55-MHz spin–lattice relaxation data were evaluated on-line with the standard Nicolet three-parameter, nonlinear least-squares software.

Due to partial signal overlap as a result of the small deuterium shift range, data at 15 MHz are less reliable than those at 55 MHz.[34] The 15-MHz data were collected primarily for purposes of comparison of spin relaxation at different magnetic fields (see the discussion below). All final results in this paper are based on the 55-MHz data.

Possible Complications from trans-Decalin Ordering in the Micelles. Wennerström and co-workers have recently[5] demonstrated that spin relaxation in micellar systems may be very significantly influenced by the overall tumbling of the micelles, the rate of which is not far from the Larmor frequency of the NMR experiment. The extent of this relaxation effect is related to the degree of ordering of the molecular fragment in question and can be related to first approximation to the reduced spectral density of motion at the Larmor frequency by a relation of the form

$$\tilde{J}(\omega) = S^2\frac{2\tau_s}{1 + (\omega\tau_s)^2} + (1 - S^2)\frac{2\tau_f}{1 + (\omega\tau_f)^2} \qquad (2)$$

where S is the usual Saupe order parameter (here referred to a local director oriented perpendicularly to the micellar surface) and τ_s and τ_f represent the ("slow") correlation time for reorientation of the micelle and the local ("fast") effective correlation time, respectively. This approach has found support in recent experimental studies, where a very significant magnetic field dependence on the carbon-13 relaxation of the alkyl chain carbons of surfactant micelles was demonstrated, despite being in the typical "extreme narrowing" range (as judged from the relaxation rates alone). An analysis of these field-dependent relaxation data makes possible detailed insight into ordering and alkyl chain dynamics[5,35] in micelles. For the present purpose the possible influence on the spin relaxation of the solubilized probe from the "slow" component of motion is a serious complication and would invalidate the analysis given below. The full analysis of the combined effects of anisotropic probe motion, superimposed on partial (unknown) ordering in the micelles, represents a truly formidable theoretical challenge in the field of spin relaxation theory, in addition to the evident experimental and evaluational problems involved in such a study.

We are convinced that the results presented here are insignificantly influenced by effects of this nature for the following reasons: (i) As seen in Table II, there is no significant field dependence on the relaxation times of the probe. (ii) The spin–lattice and spin–spin relaxation times at 15 MHz in the same table are equal within experimental error. (iii) *trans*-Decalin, when solubilized in liquid crystalline mesophases, formed in certain water/surfactant ratios by these surfactants exhibits only small (typically 3 kHz) deuterium quadrupolar splittings, corresponding to order parameters in these phases in the 0.01 range.

It should be noted in this context that Eriksson and co-workers[7] did find a very significant difference between deuterium spin–lattice and spin–spin relaxation for deuteriobenzene-d_6, when solubilized in cetyltrimethylammonium bromide micelles. No similar effects were observed for solubilized deuteriocyclohexane-d_{12}. Also, benzene quadrupolar splittings in the corresponding mesophases were much larger than for cyclohexane. These effects were qualitatively explained in terms of a relation of the form given in eq 2.

Stark et al., in their study of aniline and nitrobenzene reorientation in micelles,[6] found by light-scattering measurements that on the average (unfortunately, the technique cannot specifically monitor the probed micelles) these micelles were geometrically unperturbed by the solubilizates. Due to lack of high-field NMR instrumentation, they were unable to include a test of possible effects of ordering of the solubilizates in their investigation, however. Aromatic solubilizates are definitely more prone to micellar orientation than is *trans*-Decalin, as is evident in the studies by Eriksson et al.[7] on the solubilization of aromatics, and also from many other investigations (see, e.g., work cited in ref 8). Neither of the compounds aniline or nitrobenzene can be expected to be evenly distributed in the micelles; they are likely to be preferentially located in the micellar surface region.[8] (A noneven micellar distribution need not be a result of the aromaticity only, but can also be argued to result from nonglobularity and general geometric constraints for the incorporation of nonaliphatic molecules into micelles.) Particularly for aromatics in alkyltrimethylammonium bromide micelles very clear evidence for this exists.[36] As motional probes, aniline and nitrobenzene are therefore unlikely to properly sample the hydrocarbon core of the micelles. According to our investigations (through the techniques described in ref 37), aniline is furthermore very incompletely solubilized in micellar solution, making it impossible to deduce the desired motional information from such spin relaxation measurements.

Evaluation of the trans-Decalin Rotational Diffusion Tensor Components. Woessner, in 1962, derived the equations relating intramolecular spin relaxation in an anisotropically and diffusionally reorienting rigid ellipsoid to its rotational diffusion tensor.[38] Since that time, these equations have been extensively used, sometimes in situations where they are not applicable. We have commented on this in an earlier paper.[39] As pointed out by Huntress,[40] it is important to note that for most molecules in solution the orientation of the principal axes of the rotational diffusion tensor is not known. In general, it is not the same as that of the moment of inertia tensor (whose orientation is readily evaluated through methods of classical me-

(30) A. A. Maudsley and R. R. Ernst, *Chem. Phys. Lett.*, **50**, 368 (1977); G. Bodenhausen and R. Freeman, *J. Magn. Reson.*, **28**, 471 (1977); A. A. Maudsley, L. Müller, and R. R. Ernst, *ibid.*, **28**, 463 (1977).

(31) A. Bax, "Two-dimensional Nuclear Magnetic Resonance in Liquids", Delft University Press and D. Reidel Publishing Co., Dordrecht and Boston, 1982.

(32) L. M. Jackman and S. Sternhell, "Applications of Nuclear Magnetic Resonance Spectroscopy in Organic Chemistry", 2nd ed., Pergamon Press, Braunschweig, 1969.

(33) P. Stilbs and M. E. Moseley, *J. Magn. Reson.*, **31**, 55 (1978).

(34) In principle, one could improve the evaluation of the 15-MHz spin relaxation data through complete bandshape fitting procedures for all acquired, partially relaxed, spectra. However, the necessary computerware for these extensive data transfers from the spectrometer computer to a computer center is not available to us at the time of writing.

(35) H. Walderhaug, O. Söderman, and P. Stilbs, *J. Phys. Chem.*, in press.

(36) J. C. Eriksson and G. Gillberg, *Acta Chem. Scand.*, **20**, 2019 (1966).

(37) P. Stilbs, *J. Colloid Interface Sci.*, **87**, 385 (1982).

(38) D. E. Woessner, *J. Chem. Phys.*, **37**, 647 (1962).

(39) P. Stilbs and M. E. Moseley, *J. Magn. Reson.*, **33**, 209 (1979).

(40) W. T. Huntress, *Adv. Magn. Reson.*, **4**, 1 (1970).

TABLE I: Deuterium Spin-Lattice Relaxation Times at 55.5 MHz for *trans*-Decalin in Alkane and Alkylbenzene Solution and the Corresponding Rotational Diffusion Tensor Components and Rotational Correlation Times

solvent	temp, °C	viscosity, cP	spin relaxation times[a]			
decane	22.5	0.87	0.55	0.70	0.51	0.50
dodecane	22.5	1.44	0.44	0.58	0.37	0.37
nonylbenzene	35	2.29	0.368	0.46	0.295	0.298
decylbenzene	35	2.72	0.351	0.47	0.265	0.267
hexadecane	22.5	3.27	0.295	0.398	0.195	0.214
decylbenzene	22.5	3.59	0.257	0.353	0.196	0.196
dodecylbenzene	35	3.77	0.266	0.353	0.204	0.201
tridecylbenzene	35	4.40	0.251	0.351	0.181	0.184
pentadecylbenzene	35	5.88	0.211	0.28	0.145	0.154
tridecylbenzene	22.5	6.08	0.200	0.262	0.13	0.13

solvent	temp, °C	rotational diffusion coeff[b,c]			correlation times[d]		
decane	22.5	57 (54-61)	25 (23-27)	56 (50-61)	2.9	6.7	3.0
dodecane	22.5	45 (41-47)	16.1 (15.2-18.7)	51 (49-54)	3.8	10.3	3.3
nonylbenzene	35	33 (32-34)	14.7 (13.9-15.6)	42.8 (40.8-43.9)	5.0	11.3	3.9
decylbenzene	35	33 (31-37)	10.6 (8-11)	45 (44-48)	5.0	15.7	3.7
hexadecane	22.5	26 (24-28)	7.7 (6-9)	42 (39-45)	6.4	21.6	4.0
decylbenzene	22.5	25 (23-27)	7.2 (6.8-8.7)	34 (31-37)	6.7	23.1	4.9
dodecylbenzene	35	25 (23-26)	8.3 (7.2-9.9)	34 (33-36)	6.7	20.1	4.9
tridecylbenzene	35	24 (23-26)	6.1 (5.0-6.9)	35 (33-37)	6.8	27.5	4.8
pentadecylbenzene	35	19 (16-21)	6.0 (5.0-7.3)	29 (28-31)	8.9	27.7	5.8
tridecylbenzene	22.5	16 (14-18)	5.3 (4.3-6.3)	29 (27-31)	10.4	31.4	5.7

[a] In seconds, in the order 1, 2, 3, and 4–5 (average or combined), counting from the low-field side. [b] In rad²/ns in the order R_1, R_2, R_3. [c] The error limits correspond to 80% confidence intervals. [d] In picoseconds, based on the least-squares estimate of the corresponding diffusion tensor component, through the relation $\tau_i = 1/6R_i$.

chanics). For *trans*-Decalin, however, the orientation follows from symmetry arguments and is identical with that of the moment of inertia tensor.

Woessner's equations have primarily been used for the analysis of intramolecular, purely dipolar–dipolar (from attached or nearby protons) carbon-13 spin relaxation under complete proton broad-band decoupling.[12] Under extreme narrowing conditions each such proton (i) contributes to the carbon (j) relaxation by an amount equal to[12,41]

$$\frac{1}{T_1^{DD}} = \frac{\gamma_H^2\gamma_C^2\hbar^2}{r_{ij}^6}\frac{1}{2}\left[\frac{C_1}{4R_1+R_2+R_3} + \frac{C_2}{4R_2+R_3+R_1} + \frac{C_3}{4R_3+R_1+R_2} + \frac{C_4}{6[R+(R^2-L^2)^{1/2}]} + \frac{C_5}{6[R-(R^2-L^2)^{1/2}]}\right] \quad (3)$$

where the R's represent the diagonal components of the rotational diffusion tensor in the principal axis system, R represents $(R_1 + R_2 + R_3)/3$, and L^2 represents $(R_1R_2 + R_2R_3 + R_3R_1)/3$. The C's are complicated geometric expressions in terms of directional cosines of the respective C–H bond vectors in the principal axis system. This sum of dipolar interactions rapidly converges, and one need not consider either C–H interactions beyond 0.25-nm distance or intermolecular contributions for carbons with directly attached protons. For the evaluation of rotational diffusion

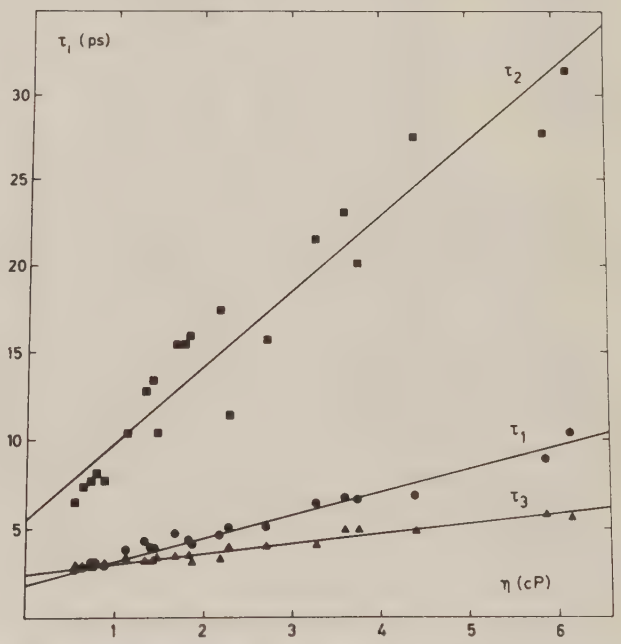

Figure 4. Experimentally determined relation between the respective rotational correlation times for *trans*-Decalin in solutions of different viscosity (see text).

data,[43] two additional factors are of importance. The exact dipolar–dipolar relaxation contribution (although normally dominant) to the relaxation rates must be carefully evaluated through proton–carbon nuclear Overhauser effect measurements. This is rather time-consuming and difficult experimentally. The presence of several geometrically related contributions to the spin relaxation tends to "smear

(41) Many different versions and forms of these equations can be found in the literature, and it appears that the factor $^1/_2$ in eq 3 is often mistakenly left out. For isotropic reorientation, the quantity within the brackets (which corresponds to the usual τ_C^{eff} for the reorientation process) converges (it is undefined for exactly isotropic reorientation) to $1/3R$, not to $1/6R$, which is the common definition of τ_C^{eff}. The origin of this error (which is unimportant for an application of the comparative nature found in the present paper) is unknown to us. For identical input atom coordinate data and eq 3 in that form, the WOESNR program gives the same results as the MOTION program of Grant and co-workers.[42]

(42) S. M. Berger, F. R. Kreissl, D. M. Grant, and J. D. Roberts, *J. Am. Chem. Soc.*, **97**, 1805 (1975). For a simulation on *trans*-Decalin by an earlier procedure, see D. M. Grant, R. J. Pugmire, E. P. Black, and K. A. Christensen, *J. Am. Chem. Soc.*, **95**, 8465 (1973).

(43) Of course, the evaluation of the different R_i requires, in addition to knowledge of the orientation of the rotation diffusion tensor, that at least three carbon types with geometrically different interactions exist in the molecule under investigation. The *trans*-Decalin has three different carbons and five different deuterium atoms. However, three of these deuteriums have identical spin relaxation parameters, resulting in only three different observables also in deuterium spectra.

TABLE II: Observed Deuterium Spin Relaxation Times for Micellarly Solubilized *trans*-Decalin

surfactant[d,e]	temp, °C	NMR freq	relax type	spin relaxation times[a-c]			
C10TAC	35.0	15.3	spin-lattice	0.29 ± 0.01	0.38 ± 0.02	0.24 ± 0.02	0.22 ± 0.01
C10TAC	35.0	15.3	spin-spin	0.19 ± 0.10	0.33 ± 0.05	0.23 ± 0.004	0.23 ± 0.04
C10TAC	35.0	55.5	spin-lattice	0.280 ± 0.010	0.422 ± 0.009	0.225 ± 0.008	0.229 ± 0.006
C10TAB	35.0	15.3	spin-lattice	0.32 ± 0.01	0.41 ± 0.01	0.23 ± 0.01	0.22 ± 0.01
C10TAB	35.0	15.3	spin-spin	0.30 ± 0.02	0.39 ± 0.04	0.20 ± 0.03	0.27 ± 0.03
C10TAB	35.0	55.5	spin-lattice	0.310 ± 0.004	0.443 ± 0.004	0.219 ± 0.002	0.227 ± 0.002
C10SS	35.0	15.3	spin-lattice	0.31 ± 0.01	0.42 ± 0.02	0.23 ± 0.02	0.23 ± 0.02
C10SS	35.0	15.3	spin-spin	0.32 ± 0.04	0.50 ± 0.10	0.30 ± 0.04	0.29 ± 0.03
C10SS	35.0	55.5	spin-lattice	0.315 ± 0.009	0.46 ± 0.01	0.225 ± 0.002	0.251 ± 0.003
C12TAB	35.0	15.3	spin-lattice		0.36 ± 0.03	0.19 ± 0.01	0.18 ± 0.01
C12TAB	35.0	15.3	spin-spin	0.21 ± 0.03	0.39 ± 0.04	0.23 ± 0.04	0.22 ± 0.03
C12TAB	35.0	55.5	spin-lattice	0.310 ± 0.004	0.419 ± 0.006	0.203 ± 0.002	0.207 ± 0.003
C12SS	35.0	15.3	spin-lattice	0.29 ± 0.02	0.40 ± 0.02	0.20 ± 0.02	0.20 ± 0.01
C12SS	35.0	15.3	spin-spin	0.28 ± 0.01	0.37 ± 0.02	0.21 ± 0.01	0.22 ± 0.03
C12SS	35.0	55.5	spin-lattice	0.270 ± 0.006	0.391 ± 0.009	0.191 ± 0.004	0.207 ± 0.003
C14TAC	35.0	15.3	spin-lattice	0.25 ± 0.02	0.33 ± 0.02	0.21 ± 0.03	0.17 ± 0.01
C14TAC	35.0	15.3	spin-spin		0.40 ± 0.06	0.21 ± 0.04	0.23 ± 0.03
C14TAC	35.0	55.5	spin-lattice	0.24 ± 0.01	0.34 ± 0.02	0.155 ± 0.004	0.162 ± 0.005
C14TAB	35.0	15.3	spin-lattice	0.24 ± 0.01	0.34 ± 0.01	0.16 ± 0.01	0.15 ± 0.01
C14TAB	35.0	15.3	spin-spin		0.41 ± 0.07	0.20 ± 0.02	0.22 ± 0.03
C14TAB	35.0	55.5	spin-lattice	0.290 ± 0.002	0.420 ± 0.008	0.164 ± 0.003	0.168 ± 0.003
C14SS	35.0	15.3	spin-lattice	0.24 ± 0.01	0.33 ± 0.02	0.16 ± 0.01	0.16 ± 0.01
C14SS	35.0	15.3	spin-spin	0.15 ± 0.05	0.40 ± 0.12	0.21 ± 0.03	0.18 ± 0.02
C14SS	35.0	55.5	spin-lattice	0.258 ± 0.004	0.423 ± 0.005	0.158 ± 0.003	0.167 ± 0.002
C16TAC	35.0	15.3	spin-lattice		0.30 ± 0.01	0.14 ± 0.01	0.13 ± 0.01
C16TAC	35.0	15.3	spin-spin		0.27 ± 0.02	0.14 ± 0.02	0.14 ± 0.02
C16TAC	35.0	55.5	spin-lattice	0.228 ± 0.003	0.337 ± 0.005	0.140 ± 0.002	0.144 ± 0.001
C16TAB	35.0	15.3	spin-lattice	0.24 ± 0.01		0.11 ± 0.01	
C16TAB	35.0	15.3	spin-spin	0.28 ± 0.04			0.123 ± 0.006
C16TAB	35.0	55.5	spin-lattice	0.206 ± 0.004	0.301 ± 0.005	0.130 ± 0.007	0.123 ± 0.006
C18TAC	35.0	15.3	spin-lattice	0.23 ± 0.01		0.10 ± 0.02	
C18TAC	35.0	15.3	spin-spin	0.25 ± 0.01		0.13 ± 0.02	
C18TAC	35.0	55.5	spin-lattice	0.201 ± 0.003	0.307 ± 0.004	0.108 ± 0.002	0.112 ± 0.001
C12SS[f]	(22.7)	55.5	spin-lattice	0.236	0.363	0.158	0.160
	(31.7)	55.5	spin-lattice	0.288	0.445	0.191	0.192
	(42.0)	55.5	spin-lattice	0.338	0.502	0.226	0.230
C12SS[g]	(22.7)	55.5	spin-lattice	0.232	0.361	0.155	0.151
	(31.7)	55.5	spin-lattice	0.282	0.444	0.194	0.190
	(42.0)	55.5	spin-lattice	0.338	0.502	0.226	0.230
C16TAC[h]	(22.7)	55.5	spin-lattice	0.157	0.247	0.086	0.088
	(31.7)	55.5	spin-lattice	0.199	0.307	0.113	0.106
	(42.0)	55.5	spin-lattice	0.243	0.406	0.146	0.151

[a] In the order 1, 2, 3, and 4-5 (combined, due to signal overlap), counting from the low-field side in the deuterium spectrum. The assignments are given in Figure 2a. [b] In seconds. [c] All 15.3-MHz data suffer from peak overlap (see Experimental Section), resulting in noticeable evaluational artifacts. A blank entry signifies that the corresponding signal was too poorly resolved for a meaningful evaluation of its associated relaxation time. For some of the C16 and C18 micellar solutions, only an apparent (combined) relaxation time could be evaluated at 15.3 MHz. [d] C*IJ* denotes an *n*-alkyl chain with *IJ* carbons, TAC an alkyltrimethylammonium chloride, TAB an alkyltrimethylammonium bromide, and SS a sodium sulfate. [e] Sample composition (weight percent): surfactant (12.1), *trans*-Decalin-d_{18} (0.5), H_2O (86.5), and D_2O (for field shimming purposes) (0.9) unless otherwise noted. [f] C12SS (27.1), *trans*-Decalin-d_{18} (0.7), H_2O (66.2), D_2O (6.0). [g] C12SS (18.1), *trans*-Decalin-d_{18} (0.5), H_2O (79.2), D_2O (2.2). [h] C16TAC (16.6), *trans*-Decalin-d_{18} (0.5), H_2O (80.6), D_2O (2.3).

out" the information on motional anisotropy in the observed relaxation rates.

Deuterium relaxation studies, as applied here, have several advantages over carbon-13-based ones in these particular applications. The probe molecule is the major deuterium-containing species in solution (essentially the only one). Therefore, there is no problem with signal overlap in any system, regardless of complexity. Deuterium relaxation is 1 order of magnitude more rapid than carbon-13 relaxation, thus speeding up the measurements. For deuterium ($I = 1$), the completely dominating relaxation mechanism is intramolecular, as required, and of quadrupolar origin.[44] The motional process affecting deuterium relaxation in solution is the reorientation of the principal axes of the electric field gradient tensor at the deuterium nucleus. For hydrocarbons the largest component of the axially symmetric field gradient tensor is oriented along the C–D bond.[44]

For deuterium spin relaxation the factor $\gamma_H^2\gamma_C^2\hbar^2/r^6$ in eq 3 is simply replaced by $(3/8)(e^2qQ/\hbar)^2$ where e^2qQ/h is the deuterium quadrupole coupling constant. Deuterium quadrupolar relaxation is thus dependent on molecular motion in exactly the same way as carbon dipolar relaxation arising from attached protons. The advantage lies in shorter relaxation times, an overwhelmingly dominating relaxation mechanism, and the fact that there is one single quadrupolar contribution instead of many dipolar ones. It turns out that the motional information in the observed relaxation rates is very much better defined than for carbon-13 for this reason.

All computer simulations were made with the iterative Fortran V WOESNR program (P. Stilbs, unpublished) on VAX 11/780 or UNIVAC 1100/70 computers using the same procedures as described previously.[11,20,39] The error analysis in WOESNR is of the same Monte Carlo type as that

(44) H. H. Mantsch, H. Saito, and I. C. P. Smith, *Prog. Nucl. Magn. Reson. Spectrosc.*, 11, 211 (1977).

TABLE III: Rotational Diffusion Coefficients and Correlation Times for Micellarly Solubilized *trans*-Decalin, as Based on 55-MHz Deuterium Spin Relaxation Data

surfactant[d]	temp, °C	rotational diffusion coeff[a,b]			correlation times[c]		
C10TAC[e]	35.0	33.6 (31.0–34.8)	5.98 (5.24–7.54)	36.9 (34.7–39.7)	5.0	27.9	4.5
C10TAB[e]	35.0	29.8 (27.2–30.8)	7.48 (6.92–9.09)	45.9 (44.2–48.1)	5.6	22.3	3.6
C10SS[e]	35.0	34.4 (28.6–42.9)	7.04 (4.02–10.54)	42.8 (36.5–50.4)	4.8	23.7	3.9
C12TAB[e]	35.0	26.4 (24.8–29.7)	7.33 (5.35–8.31)	46.3 (43.2–49.5)	6.3	22.7	3.6
C12SS[e]	35.0	28.3 (24.1–33.0)	5.92 (3.62–7.77)	37.6 (33.8–40.5)	5.9	28.2	4.4
C14TAC[e]	35.0	22.0 (18.9–22.9)	4.66 (4.14–6.49)	37.0 (35.6–39.0)	7.6	35.9	4.5
C14TAB[e]	35.0	24.2 (22.9–24.8)	3.52 (2.87–4.29)	52.1 (50.8–55.2)	6.9	47.3	3.2
C14SS[e]	35.0	27.9 (24.8–30.4)	1.03 (0.01–3.03)	46.1 (43.5–46.1)	6.0	(161)	3.6
C16TAC[e]	35.0	21.1 (19.2–22.2)	3.01 (2.81–4.74)	38.4 (36.9–40.4)	7.9	55.0	4.3
C16TAB[e]	35.0	18.3 (17.4–21.9)	2.75 (0.53–3.42)	35.3 (34.3–38.7)	9.1	60.6	4.7
C18TAC[e]	35.0	17.6 (16.9–18.0)	1.12 (0.95–1.92)	39.1 (38.1–40.6)	9.5	(139)	4.3
C12SS[f]	(22.7)	24.6 (23.3–25.3)	2.87 (2.76–3.68)	38.0 (35.3–39.2)	6.9	58.1	4.3
	(31.7)	29.8 (27.7–32.6)	3.23 (1.66–4.13)	47.2 (45.3–51.9)	5.6	51.6	3.5
	(42.0)	31.3 (29.2–32.9)	7.58 (6.27–8.74)	62.1 (58.9–63.4)	5.3	22.0	2.7
C12SS[g]	(22.7)	24.0 (22.0–25.0)	2.34 (1.85–3.41)	38.7 (37.0–40.3)	6.9	71.2	4.3
	(31.7)	30.5 (28.9–32.4)	2.85 (1.96–3.82)	45.9 (43.5–48.4)	5.5	58.5	3.6
	(42.0)	33.6 (31.6–35.2)	5.27 (3.81–6.44)	53.0 (51.0–55.2)	5.0	31.6	3.2
C16TAC[h]	(22.7)	14.4 (13.5–15.2)	0.56 (0.01–1.28)	30.9 (29.7–32.9)	11.6	(298)	5.4
	(31.7)	17.5 (14.7–18.7)	0.94 (0.01–2.58)	39.3 (36.8–43.7)	9.5	(177)	4.2
	(42.0)	26.3 (24.6–26.7)	0.28 (0.01–1.35)	45.4 (42.2–48.6)	6.3	(595)	3.7

[a] In rad²/ns in the order R_1, R_2, R_3. [b] The error limits correspond to 80% confidence intervals. [c] In picoseconds, based on the least-squares estimate of the corresponding diffusion tensor component, through the relation $\tau_i = 1/6R_i$. [d] *CIJ* denotes an *n*-alkyl chain with *IJ* carbons, TAC an alkyltrimethylammonium chloride, TAB an alkyltrimethylammonium bromide, and SS a sodium sulfate. [e] Sample composition (weight percent): surfactant (12.1), *trans*-Decalin-d_{18} (0.5), H_2O (86.5), and D_2O (for field shimming purposes) (0.9). [f] C12SS (27.1), *trans*-Decalin-d_{18} (0.7), H_2O (66.2), D_2O (6.0). [g] C12SS (18.1), *trans*-Decalin-d_{18} (0.5), H_2O (79.2), D_2O (2.2). [h] C16TAC (16.6), *trans*-Decalin-d_{18} (0.5), H_2O (80.6), D_2O (2.3).

used by the UNIFIT program described above. The WOESNR program is capable of a simultaneous simulation of carbon-13 and deuterium relaxation and also of nitrogen-14 (with the restriction of an axially symmetric geometric environment for nitrogen, as, for example, in pyridine). The atomic coordinates for *trans*-Decalin were obtained from a molecular mechanics simulation using the BIGSTRN program[45] utilizing the force field for saturated hydrocarbons, developed 1970–1972 by Allinger et al.

In *trans*-Decalin there are five different deuteriums, not necessarily with exactly equal coupling constants. In the present work we have assumed the coupling constants to be equal and "calibrated" *trans*-Decalin carbon-13 relaxation rates to those of the deuterium nuclei through the common rotational diffusion tensor using the WOESNR program. An excellent agreement between carbon-13 (with the geometry from the force field simulation) and deuterium data was found for a common quadrupole coupling constant of 178 kHz, which is a very reasonable value in the range quoted for alicyclic compounds.[44]

As pointed out above, three of the deuteriums in *trans*-Decalin have geometrically identical relaxation parameters. Experimentally, it was indeed found that precisely these three deuteriums (corresponding to the three high-field signals) had equal relaxation rates within the experimental uncertainty in all systems. These observations therefore also give support to the assumption of a common quadrupole coupling constant for all five deuterium types.

Establishing a Relationship between Macroscopic Viscosity and Rotational Correlation Times for trans-Decalin in Solution. For this purpose, deuterium spin relaxation measurements were made on a series of dilute solutions (5 mg/mL) of *trans*-Decalin-d_{18} in various hydrocarbons. The results, together with evaluated rotational diffusion data, are summarized in Table I. According to hydrodynamic theories for reorientation, the different correlation times for reorientation of an asymmetric top like *trans*-Decalin should closely follow relations of the form[20,21]

$$\tau_i = C_i\eta + \tau_i^{(0)} \tag{4}$$

Moseley[20] found a good agreement between his experimental data and this equation for the different τ_i's for *trans*-Decalin in mixtures of similarly sized molecules. We have extended his experimental set to higher viscosities with the data in Table I. The combined result is shown in Figure 4. Clearly, the agreement with a function of the form of eq 4 is good. It should be stressed at this point that it is surprising that hydrodynamic theories for reorientation hold so well in a situation where one is far from continuum solution conditions. With regard to the experimental data, one should also note that some of the data in Figure 4 lie outside the linear relation by amounts somewhat greater than their statistical uncertainty. However, for the present purposes, we conclude that it is meaningful to describe the reorientation of *trans*-Decalin in solution in terms of a hydrodynamic picture, involving the viscosity of the local environment.

Results and Discussion

Spin relaxation data for micellarly solubilized *trans*-Decalin is summarized in Table II. Table III summarizes the evaluated rotational diffusion coefficients and correlation times.[46]

A general trend is readily apparent; the reorientation rate for solubilized *trans*-Decalin decreases with increasing

(45) J. D. Andose and K. Mislow, *J. Am. Chem. Soc.*, **96**, 2168 (1974).

(46) Our results for "the micellar viscosity" are lower and differ by approximately a factor 2 from those of Stark et al. in ref 6. This is in part due to the temperature difference in our studies but could also be a reflection of the complications (see Experimental Section) in their study. A possible evaluational difference also exists between our experimental/evaluational designs, as pointed out by one of the referees; nitrogen-14 relaxation in aniline and nitrobenzene was utilized by Stark et al. to obtain the combined relaxation information necessary to evaluate the three rotational diffusion correlation times. Nitrogen-14 is a "low-frequency" nucleus and its spin relaxation might be more affected by the possible low-frequency motional processes from the overall tumbling of the micelles than carbon-13 or deuterium nuclei.

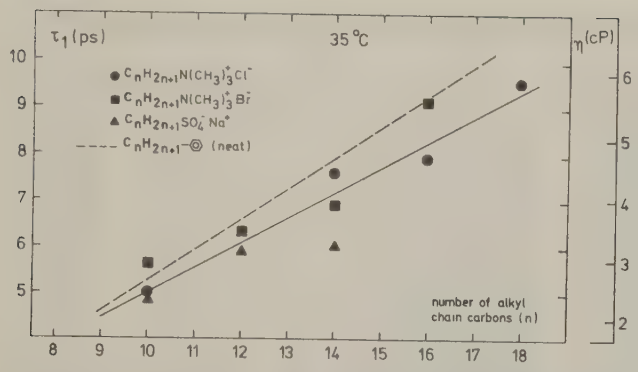

Figure 5. Relation between τ_1 and the number of alkyl chain carbons in the micellar surfactants. The linear relation for alkylbenzene solutions is shown for comparison.

surfactant chain length for all three surfactant types. Furthermore, one finds that the three reorientation rates for micellar *trans*-Decalin show similar absolute values and trends with increasing chain length as do normal alkane or alkylbenzene solutions. For this reason one can conclude that it is meaningful to also consider the reorientation of *trans*-Decalin in micelles to be hydrodynamically related.

The close correlation between *trans*-Decalin rotational behavior in normal solutions and micelles is further illustrated in Figure 5. In general, analogous diagrams of the different individual τ_i do not lead to the same estimate of the micelle viscosity. This is to a great extent due to the highly nonlinear error propagation from the original spin relaxation rates, through Woessner's equations (eq 3) to the inverted rotational diffusion coefficients entering into eq 4. The best estimate (in the unweighted least-squares sense[47] of the micellar viscosity is evaluated and presented in Figure 6.

Again, it should be emphasized that the evaluated correlation times, as such, are model independent. The approximately linear behavior, according to eq 4 and Figure 5, is a reflection of a good correspondence with a hydrodynamic reorientational model, involving concepts related to the quantity sought here: viscosity. Viscosity, as related

(47) The quantity $\sum_{i=1,3}((\tau_i(\text{obsd}) - \tau_i(\text{calcd}))/(\tau_i(\text{obsd})))^2$ has been minimized. τ_i(obsd) symbolizes the respective values for the particular micelle type, as given in Table III, and τ_i(calcd) is taken to be the values predicted by the linear relations shown in Figure 4. The directly measured alkylbenzene viscosities are shown for comparison.

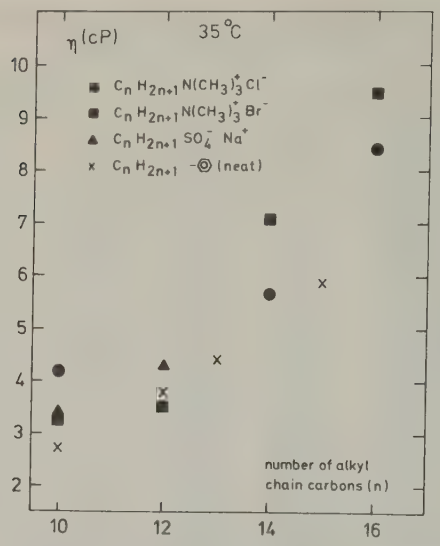

Figure 6. Result of a least-squares fit[47] of the rotational correlation times in Table III to the viscosity concept, when using the linear relations between the τ_i and viscosity, shown in Figure 4.

to molecular motion, is merely a reflection of intermolecular interactions of various kinds. For alkane or polymer solutions, viscosity is primarily a result of interchain entanglements.

The final conclusion would be that, as in normal hydrocarbon liquids, the viscosity of the local environment in the micellar hydrocarbon core increases with increasing alkyl chain length as a result of an increased probability for these interchain entanglement processes. Consequently, this work therefore indicates that the "fluidity" of a particular micelle type approaches that of a hydrocarbon liquid, composed of molecules having alkyl chains of the same length as the surfactant in question.

Acknowledgment. This work has been financially supported by the Swedish Natural Sciences Research Council.

Registry No. Deuterium, 7782-39-0; *trans*-Decalin, 493-02-7; decane, 124-18-5; dodecane, 112-40-3; nonylbenzene, 1081-77-2; decylbenzene, 104-72-3; hexadecane, 544-76-3; tridecylbenzene, 123-02-4; pentadecylbenzene, 2131-18-2; C10TAC, 10108-87-9; C10TAB, 2082-84-0; C10SS, 142-87-0; C12TAB, 1119-94-4; C12SS, 151-21-3; C14TAC, 4574-04-3; C14TAB, 1119-97-7; C14SS, 1191-50-0; C16TAC, 112-02-7; C16TAB, 57-09-0; C18TAC, 112-03-8.

Reprinted from The Journal of Physical Chemistry, 1984, *88*, 1655.
Copyright © 1984 by the American Chemical Society and reprinted by permission of the copyright owner.

Micellar Dynamics and Organization. A Multifield ^{13}C NMR Spin–Lattice Relaxation and $\{^1H\}^{13}C$ Nuclear Overhauser Effect Study

Harald Walderhaug, Olle Söderman,*

Physical Chemistry 1, Lund University, S-220 07 Lund, Sweden

and Peter Stilbs

Institute of Physical Chemistry, Uppsala University, S-751 21 Uppsala, Sweden *(Received: June 27, 1983)*

An extensive ^{13}C spin-relaxation study is presented for four micellar systems. These are dodecyltrimethylammonium chloride, hexadecyltrimethylammonium chloride, potassium palmitate, and sodium *p*-octylbenzenesulfonate. The spin relaxation data are analyzed with a relaxation model that takes into account the complexity of molecular motions in surfactant systems. The results show that the internal motions in the micelles are quite fast, occurring on a time scale of 10^{-11} s, which is similar to that found for liquid hydrocarbons of comparable chain lengths. The motional restrictions imposed by the aggregate–water interface resemble those found in other types of surfactant aggregates. A correlation time associated with the motions of the whole aggregate is extracted. The value of this correlation time implies that, apart from the rotational tumbling and monomer diffusion, the micelles undergo additional motions.

Introduction

The measurements of nuclear magnetic resonance (NMR[1]) relaxation times are an important method in studying molecular motions in solutions. Carbon-13 relaxation (T_1, T_2, and nuclear Overhauser enhancement (NOE[1])) is particularly useful in this respect, since it is almost exclusively related to intramolecular reorientational processes.

One particular area where extensive ^{13}C NMR relaxation studies have been made is that of surfactant systems.[2,3] Surfactants, dispersed in water, form a whole hierarchy of aggre-

(1) Abbreviations used: NMR, nuclear magnetic resonance; NOE, nuclear Overhauser effect; DOTAC, dodecyltrimethylammonium chloride; CTAC, hexadecyltrimethylammonium chloride; CTAB, hexadecyltrimethylammonium bromide; PPALM, potassium palmitate; SOBS, sodium *p*-octylbenzenesulfonate.

(2) R. E. London and J. Avitabile, *J. Am. Chem. Soc.*, **99**, 7765 (1977).
(3) D. Canet, J. Brondeau, H. Nery, and J. P. Marchal, *Chem. Phys. Lett.*, **72** (1980).

0022-3654/84/2088-1655$01.50/0 © 1984 American Chemical Society

gates.[4,5] In general, spherical micelles initially form above a certain critical micelle concentration, followed by more complex aggregates such as rodlike or prolate or oblate micelles and ultimately liquid-crystalline mesophases of various kinds. An overall description of molecular motion for micellarly bound molecules, the subject of the present paper, is by no means simple. Consequently, the interpretation of spin relaxation data in surfactant–water systems is not straightforward either. Motional models for micelles have been suggested that have in common a separation of "fast" internal alkyl chain motions and "slow" motions, ascribed to tumbling of the whole aggregate and/or diffusion of surfactant monomers over the micellar surface. Several suggested spin-relaxation models are based on a time scale separation of this kind.[2,3,6,7]

In the present paper the motional model suggested in ref 7 is applied to micellar dynamics in solution, as derived from NMR spin-relaxation data. Parameters entering into that theory are directly comparable with structural and dynamic data for other types of surfactant systems. It is then possible to directly evaluate the influence of aggregate shape on the state of the hydrocarbon chains. With the dual purpose of testing the NMR spin-relaxation model[7] and obtaining structural and dynamic information about micellar systems, we have performed a multifield ^{13}C NMR T_1 relaxation and $\{^1H\}^{13}C$ NOE study on the alkyl chains for four different micellar systems. Dodecyltrimethylammonium chloride (DOTAC)[1] and hexadecyltrimethylammonium chloride (CTAC)[1] were chosen for study of the effect of different chain lengths on the motional/organizational parameters entering into the spin-relaxation model. In addition, DOTAC micelles were studied at three temperatures to monitor the temperature dependence of these parameters. Potassium palmitate (PPALM)[1] was chosen for study since the lamellar lyotropic liquid-crystalline phase of this system has been extensively investigated by ^2H NMR band-shape methods. This allows a direct comparison of the alkyl chain state. Sodium *p*-octylbenzenesulfonate (SOBS)[1] was selected, with particular interest focused on the influence of the aromatic head group on the micellar dynamics and organization. It should be pointed out that all these amphiphiles have low cmc's.[8] Therefore, at all the experimental concentrations used in this work, the contributions to relaxation from free monomers are negligible and need not be taken into account.[9]

Theory

With the usual assumption that the relaxation of a ^{13}C nucleus is given solely by the dipole–dipole interaction to directly bonded protons, the general expressions for T_1 and the nuclear Overhauser enhancement η (NOE) are given by[10] (SI units)

$$(T_{1i})^{-1} = (N_i/20) \times \left[\frac{\mu_0\gamma_H\gamma_C\hbar}{4\pi r_{C\text{-}H}^3}\right]^2 (\tilde{J}(\omega_H - \omega_C) + 3\tilde{J}(\omega_C) + 6\tilde{J}(\omega_H + \omega_C)) \quad (1a)$$

$$\eta_i = (1/20)\gamma_H^3\gamma_C\left[\frac{\mu_0\hbar}{4\pi r_{C\text{-}H}^3}\right]^2 (N_iT_{1i}) \times (6\tilde{J}(\omega_H + \omega_C) - \tilde{J}(\omega_H - \omega_C)) \quad (1b)$$

where T_{1i} and η_i are the spin–lattice-relaxation time and NOE for carbon i along the alkyl chain, respectively, μ_0 is the permeability of vacuum, γ_H and γ_C represent the magnetogyric ratios of proton and carbon, and $r_{C\text{-}H}$ denotes the C–H bond length (see below). The $\tilde{J}(\omega)$'s are various reduced spectral densities, N_i is the number of directly bonded protons to carbon i, $\hbar$ is Planck's constant divided by 2π, and ω_H and ω_C are the angular Larmor frequencies of protons and carbons at a given magnetic field.

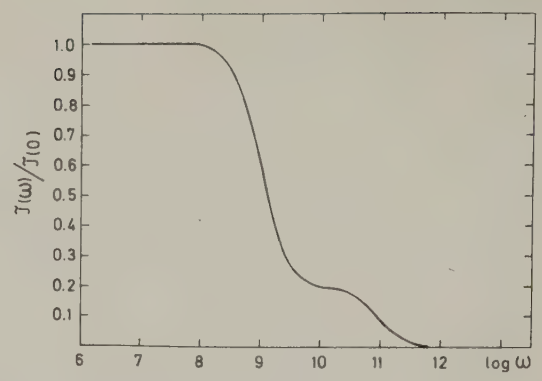

Figure 1. $\tilde{J}(\omega)/\tilde{J}(0)$ as a function of log ω for $S = 0.2$, $\tau_c^f = 1 \times 10^{-11}$ s, and $\tau_c^s = 1 \times 10^{-9}$ s.

Combining the result of Wennerström et al.[7] with those of Halle and Wennerström,[11] we arrive at the following reduced spectral densities for molecular motions:

$$\tilde{J}(\omega) = (1 - S^2)2\tau_c^f + S^2\left(\frac{2\tau_c^s}{1 + (\omega\tau_c^s)^2}\right) \quad (2)$$

where τ_c^f is the correlation time for the fast local motion in the alkyl chain. It is assumed that this motion is sufficiently fast to fall within the extreme narrowing range; i.e., $(\omega\tau_c^f)^2 \ll 1$. τ_c^f is the correlation time for a much slower process occurring in the nanosecond (10^{-9} s) range. The parameter S is defined as

$$S \equiv (1/2)\langle 3\cos^2\theta_{LD} - 1\rangle_f \quad (3)$$

where θ_{LD} is the angle between the C–H bond vector and the local director, which is perpendicular to the micellar surface. The symbol $\langle\ \rangle_f$ means an average of the quantity inside the brackets over a time long enough to average the fast local motion. It is assumed that the fast local motions occur in an environment that has, on the average, a threefold or higher symmetry and that the symmetry axis is the local director. Thus, only one order parameter, S, suffices to describe the methylene group organization.

The physical picture behind the model that leads to eq 2 is the following. Since the amphiphiles are anchored at the aggregate–water interface, the motion of a chain segment is not isotropic; i.e., a C–H bond vector does not sample all directions with respect to the external magnetic field with equal probability. This leaves a residual anisotropy, clearly seen for lyotropic liquid crystals where it gives rise to static effects in the spectra, e.g., the quadrupolar splittings of deuteron signals of deuterated amphiphiles.[12,13] However, in micellar systems no such splittings are observed, indicating that there must also be superimposed isotropic motions that average this residual anisotropy to zero. If these motional processes can be described by correlation times of the same order of magnitude as the inverse Larmor frequencies, they will contribute to the spin–lattice relaxation. Such a model is termed a "two-step model" because the relaxation is thought to be caused by processes occurring on different time scales (see Figure 1). It is by no means restricted to ^{13}C relaxation. The same approach has been used for the ^{17}O nucleus of water,[11] ^{14}N,[14] ^2H,[15] and to ionic quadrupolar nuclei[16] NMR data of amphiphile–water sys-

(4) H. Wennerström and B. Lindman, *Phys. Rep.*, **52C**, 1 (1980).
(5) G. J. T. Tiddy, *Phys. Rep.*, **57C**, 1 (1980).
(6) Y. K. Levine, N. J. M. Birdsall, A. G. Lee, J. C. Metcalfe, P. Partington, and G. C. K. Roberts, *J. Chem. Phys.*, **60**, 2890 (1974).
(7) H. Wennerström, B. Lindman, O. Söderman, T. Drakenberg, and J. B. Rosenholm, *J. Am. Chem. Soc.*, **101**, 6860 (1979).
(8) P. Mukerjee, and K. J. Mysels in "Critical Micelle Concentrations of Aqueous Surfactant Systems", National Bureau of Standards, Washington, DC, 1970.
(9) T. Ahlnäs, H. Walderhaug, O. Söderman, and B. Lindman in "Surfactants in Solution", K. L. Mittal and B. Lindman, Eds., Plenum Press, New York, in press.
(10) D. Doddrell, V. Glusko, and A. Allerhand, *J. Chem. Phys.*, **56**, 3683 (1972)
(11) B. Halle and H. Wennerström, *J. Chem. Phys.*, **75**, 1928 (1981).
(12) T. Klason and U. Henriksson in "Solution Chemistry of Surfactants", K. L. Mittal and E. J. Fendler, Eds., Plenum Press, New York, 1982.
(13) J. Seelig, *Q. Rev. Biophys.*, **10**, 3 (1977).
(14) U. Henriksson, L. Ödberg, J. C. Eriksson, and L. Westman, *J. Phys. Chem.*, **81**, 76 (1977).
(15) G. W. Stockton, C. F. Polnaszek, A. P. Tulloch, F. Hasan, and I. C. P. Smith, *Biochemistry*, **15**, 954 (1976).

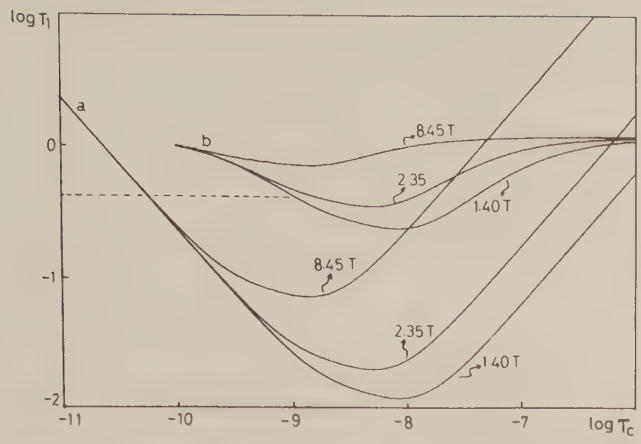

Figure 2. Theoretical predictions of ^{13}C T_1 for a CH_2 group at three magnetic fields. The curves under (a) represent the single isotropic motion model, while those under (b) represent the two-step model. In the latter case, S is given the value 0.2, while τ_c^f is set at 2×10^{-11} s. The dashed line indicates a typical micelle T_1.

tems. It should be mentioned here that Lipari and Szabo[17] have recently arrived at eq 2 using different arguments.

It is instructive to plot the T_1's given by the two-step model and the simple isotropic model where the relaxation is determined by a correlation time for a single isotropic process.[10] This is illustrated in Figure 2. As can be seen, a typical experimental micellar T_1 would be predicted by the two-step model to depend on the magnetic field. The single isotropic motion model does not predict this field dependence. In ref 3, 7, and 9 it is demonstrated that T_1's for typical micellar systems are indeed field dependent, thus supporting a two-step relaxation model over the single isotropic model.

Within the two-step picture, three parameters determine ^{13}C relaxation in a micelle. To extract these parameters, at least three independent measurements of T_1 and/or NOE are required. We have measured T_1's at three different magnetic fields and NOE's at one field. In addition, to further test the model itself, we have measured T_1's and NOE's for one system at a fourth magnetic field.

Experimental Section

Materials and Methods. CTAC was prepared from the corresponding bromide (CTAB)[1] as described in ref 18. CTAB was from Merck (99% purity). PPALM was made by neutralization of palmitic acid, BDH (99% purity), with potassium ethoxide in absolute ethanol. DOTAC was from Eastman (99% purity). It was dissolved in methanol and treated with active charcoal, filtered, and dried in vacuum. SOBS was prepared as described in ref 19. Three different concentrations of each of these surfactants were prepared. All measurements were made under conditions of internal field/frequency lock on the D_2O solvent (Ciba Geigy, 99% enriched).

The T_1 measurements were performed at three different magnetic fields, i.e. at 8.5, 2.3, and 1.4 T on a Nicolet 360 spectrometer, a Varian XL-100 spectrometer, and a JEOL FX-60 spectrometer, respectively, all working in the Fourier transform mode. In addition, T_1 and NOE experiments on the most concentrated of the DOTAC samples (30% by weight) were performed at a field strength of 4.7 T on a Varian XL-200 spectrometer.

Spin relaxation times were measured by using the so-called fast inversion-recovery technique[20] with a pulse repetition time of 1–3 T_1 depending on the particular carbon's T_1 and an adequate number of dummy scans to generate a steady-state magnetization before data acquisition. Around 15 τ values were generally used, and the intensities of the peaks were fitted to the function

$$I = I_0(1 - A \exp(-\tau/T_1)) \quad (4)$$

where I is the intensity as measured by the height of the peak at the time τ between the 180 and 90° pulses, I_0 is the equilibrium intensity, and A is a constant depending on the steady-state Z magnetization immediately before the 90° rf pulses. The fitting procedure is based on a general nonlinear least-squares procedure (directly on the nonlinearized raw data) and was performed by the UNIFIT Fortran V computer program.[21] We used the Monte Carlo error analysis described in ref 21 to estimate confidence intervals for the fitted parameters, as presented in the tables and figures below. Special precautions were made to achieve high-quality raw spin-relaxation data. The inversion-recovery method in its basic form suffers from noncorrectable phase errors in the transformed spectra under certain circumstances. These errors occur as a result of refocusing effects from incomplete transverse relaxation between the rf pulses. Effects of this kind are considerably enhanced in the fast inversion-recovery mode. Phase alternation techniques eliminate these refocusing effects to a large extent. We have used alternation of the 90°-pulse phase for the two lowest fields and a composite 180° pulse together with phase alternation of this pulse for the highest field. Heating effects, as a result of the broad-band decoupling, constitute and additional complication especially at high magnetic fields. This was avoided by using the bilevel decoupling scheme (see below).

All the T_1's of the resolved carbons were measured at the same time with a carefully selected range of pulse intervals, appropriately chosen to cover all different relaxation rates. The experimental T_1's are judged to be accurate to within ±5% at the higher fields and within ±10% at the lower fields. When running an experiment several times for the same sample, we found no significant differences in the measured T_1's.

The NOE's were determined on the 8.5-T spectrometer and, for the most concentrated of the DOTAC samples, on the 4.7-T Varian XL-200 spectrometer as well. The NOE's were determined by the so-called dynamic NOE technique.[22] This is a combined T_1 and NOE experiment. The proton decoupler is off during a time interval equal to or greater than 10 times the longest T_1. Subsequently, the decoupler is turned on for a variable time interval τ to partially build up the NOE; a 90° observation pulse is then applied followed by acquisition of the fid. To avoid heating the samples, the following pulse sequence was used. The power of the decoupling field is carefully adjusted so that it just suffices to build up the NOE during the time interval τ. During the acquisition following the 90° pulse, the decoupler power is increased to totally decouple the protons. In this way heating effects, which can cause serious problems in these kinds of measurements, are reduced to a minimum.

After Fourier transformation the intensity data are again fitted to a three-parameter function:

$$I = I_0(1 + \eta - \eta \exp(-\tau/T_1)) \quad (5)$$

where η is the NOE and the other symbols are explained in the text above. Here, I_0 is the intensity of a peak with no NOE. The fitting procedure is based on the UNIFIT program[21] (see above). The discrepancies between the T_1 values from the NOE and fast inversion-recovery experiments did not exceed ±10%.

The experimental temperatures were checked by a calibrated copper/constantan thermocouple or a thermometer calibrated against such a thermocouple. We judge the uncertainty in the temperatures to be ±0.5 °C. For DOTAC and CTAC the assignments of the spectra are based on ref 23 with the added assumption that T_1 increases continuously when going from the

(16) H. Wennerström, G. Lindblom, and B. Lindman, *Chem. Scr.*, **6**, 97 (1974).
(17) G. Lipari and A. Szabo, *J. Am. Chem. Soc.*, **104**, 4546 (1982).
(18) A. Khan, K. Fontell, and G. Lindblom, *J. Phys. Chem.*, **86**, 383 (1982).
(19) F. W. Gray, J. F. Gerecht, and I. J. Krens, *J. Org. Chem.*, **20**, 511 (1955).
(20) D. Canet, G. C. Levy, and I. R. Peat, *J. Magn. Reson.*, **18**, 199 (1975).
(21) P. Stilbs and M. E. Moseley, *J. Magn. Reson.*, **31**, 55 (1978).
(22) R. Freeman, H. D. W. Hill, and R. Kaptein, *J. Magn. Reson.*, **7**, 327 (1972).
(23) E. Williams, B. Sears, A. Allerhand, and E. H. Cordes, *J. Am. Chem. Soc.*, **95**, 4871 (1973).

TABLE I: Experimental and Theoretical Slow Correlation Times

		$10^9\tau_c^s$(expt), s			$10^9\tau_c^s$(calcd), s			
SOBS	5%	1.1 (0.9–1.4)						$r_M = 20$ Å[a]
	8%	1.0 (0.9–1.3)				2.9		$D = 1 \times 10^{-10}$ [b]
	12%	0.7 (0.4–1.1)						$T = 315$ K (42 °C)
								$\eta = 0.68 \times 10^{-3}$ [c]
		27 °C	40 °C	55 °C	27 °C	40 °C	55 °C	
DOTAC	20%	1.9 (1.7–2.1)	1.6 (1.2–2.0)	1.6 (1.6–1.9)				$r_M = 18$ Å[a]
	25%	1.9 (1.6–2.5)	1.8 (1.5–2.0)	2.1 (1.8–2.6)	4.4	3.0	2.2	$D_{27} = 2.4 \times 10^{-11}$,[b] $\eta = 0.93 \times 10^{-3}$
	30%	2.7 (2.3–3.2)	1.8 (1.4–2.0)	2.0 (1.8–2.1)				$D_{40} = 4.6 \times 10^{-11}$,[b] $\eta = 0.72 \times 10^{-3}$
								$D_{55} = 6.5 \times 10^{-11}$,[b] $\eta = 0.55 \times 10^{-3}$
CTAC	11%	3.1 (1.8–3.9)						$r_M = 23$ Å[a]
	19%	3.1 (2.4–4.0)				9.7		$D = 1.2 \times 10^{-11}$ [b]
	23%	2.3 (2.0–2.5)						$T = 301$ K (28 °C)
								$\eta = 0.91 \times 10^{-3}$ [c]
PPALM	8%	2.1 (1.8–2.4)						$r_M = 22$ Å[a]
	12%	3.8 (3.1–5.1)				5.4		$D = 2.1 \times 10^{-11}$ [b]
	16%	2.2 (2.0–3.9)						$T = 320$ K (47 °C)
								$\eta = 0.63 \times 10^{-3}$ [c]

[a] Estimated values from ref 39. [b] Estimated diffusion coefficients in units of m^2/s. SOBS is from ref 40. DOTAC, CTAC, and PPALM are from ref 41 assuming that the diffusion coefficients of CTAC and PPALM are comparable to that of hexadecyltrimethylammonium fluoride (CTAF). Extrapolations to the experimental temperatures have been made assuming a simple activation process for the diffusion. [c] Viscosities for heavy water in units of kg/m·s.

head group toward the end of the hydrocarbon chain. This latter criterion has been used for carbons that are not resolved in ref 23 but that are resolved here, owing to the higher field strengths used in this study. PPALM and SOBS spectra have been assigned solely by means of T_1 data. For CTAC and PPALM not all carbons are resolved even at the highest field. In these cases the number of carbons assigned to each peak in the central part of the spectra is somewhat arbitrary.

Computational Procedure for the Evaluation of τ_c^f, τ_c^s, and S. To evaluate the individual fast correlation times and order parameters and the common slow correlation time invoked in the present model, the experimental data were subjected to a least-squares analysis. In this process the error sum (6) was evaluated

$$\text{ERRSUM} = \sum \frac{(R_1(\text{obsd}) - R_1(\text{calcd}))^2}{R_1(\text{obsd})^2} + \sum \frac{(\eta(\text{obsd}) - \eta(\text{calcd}))^2}{\eta(\text{obsd})^2} \quad (6)$$

and minimized. The quantities R_1(calcd) and η(calcd) are defined in eq 1 ($R_1 = T_1^{-1}$). The individual observations are thus normalized so as to give equal weight to all available data. The minimization of the error sum was achieved by a specially written Fortran 77 computer program (TWOSTP) (P. Stilbs, unpublished) on UNIVAC 1110 or VAX 11/780 computers. The TWOSTP program utilizes the general minimization subroutine STEPIT, as supplied by the Quantum Chemistry Program Exchange organization.[24] After the minimization process (providing the "best" estimates of the correlation times and order parameters in the least-squares sense), statistical confidence intervals were examined by using the Monte Carlo technique outlined in ref 21. Confidence intervals given in Table I and Figures 6–9 correspond to an approximately 80% level and are based on a slightly modified computational approach where probable errors are added to the least-squares estimates of the observables, not to the original observations, as in the original procedure.

It should be pointed out that although a least-squares minimization of this kind involves 27 parameters in the case of 13 carbons, these parameters are only weakly covariant and that estimates of individual (τ_c^f, S) pairs are almost orthogonal to each other in that they only couple through τ_c^s.

Discussion

This discussion has been divided into three parts. In the first we discuss in some detail the parameters of eq 1 and 2 and how they are evaluated. Secondly, we will discuss the obtained data for the four different micellar systems, and, finally, we will compare our results with two theoretical models for the packing of amphiphiles in micelles.

The Parameters τ_c^f, τ_c^s, and S. ^{13}C T_1 studies on micellar systems are abundant in the literature.[23,25–30] When analyzing data from such studies, the concept of effective correlation times is often used. However, in order to write an observable correlation time as a harmonic mean of two or more correlation times, two criteria have to be fulfilled.[31] Firstly, the motions characterized by these correlation times have to be independent, and, secondly, they have to average the *same* part of the interaction. For the case of a micelle with fast, slightly anisotropic internal motions and slower isotropic motions, the first of these conditions is met while the second one is clearly not fulfilled. Therefore, spectral densities of the type in eq 2 have to be used when analyzing the relaxation data.

As stated in the Theory section, the relaxation model used in the present work predicts that the relaxation for the carbons in the alkyl chain of the aggregated amphiphiles is determined by three parameters, i.e. a correlation time for fast local motion of a chain segment τ_c^f, an order parameter S describing the anisotropy of this motion, and a correlation time τ_c^s for a slower overall process involving the whole aggregate.

The order parameter is analogous to the order parameter measured with ^2H NMR on lyotropic liquid crystals formed by surfactants at higher concentrations of amphiphile. Thus, it is a measure of the ensemble averaged conformations of the hydrocarbon chain and does not contain any detailed information on the dynamics of the chains. For liquid crystals, it reflects the fact that motions at frequencies higher than the static quadrupole coupling constant (167 kHz) are prevalent. Apart from that, the order parameter contains no information on the actual rate of the hydrocarbon chain motions. This information appears solely in the fast correlation time.

The motions of the chains are complex. In general, they reorient by rotations around carbon–carbon bonds (gauche–trans isom-

(24) Program No. 307, "Quantum Chemistry Program Exchange", Department of Chemistry, Indiana University, Bloomington, IN 47401. (Author: J. P. Chandler, Oklahoma State University, Stillwater, OK).

(25) H. Maeda, S. Ozeki, S. Ikeda, H. Okabayashi, and K. Matsushita, *J. Colloid Interface Sci.*, **76**, 532 (1980).
(26) R. A. Burns, Jr., and M. F. Roberts, *Biochemistry*, **19**, 3100 (1980).
(27) R. A. Burns, Jr., J. M. Friedman, and M. F. Roberts, *Biochemistry*, **20**, 5945 (1980).
(28) E. I. Franses, H. T. Davis, W. G. Miller, and L. E. Scriven, *J. Phys. Chem.*, **84**, 2314 (1980).
(29) H. Okabayashi, T. Yoshida, Y. Terada, and K. Matsushita, *J. Colloid Interface Sci.*, **87**, 527 (1982).
(30) M. J. Minch and G. N. La Mar, *J. Phys. Chem.*, **86**, 1400 (1982).
(31) B. Halle, personal communication (see also ref 11).

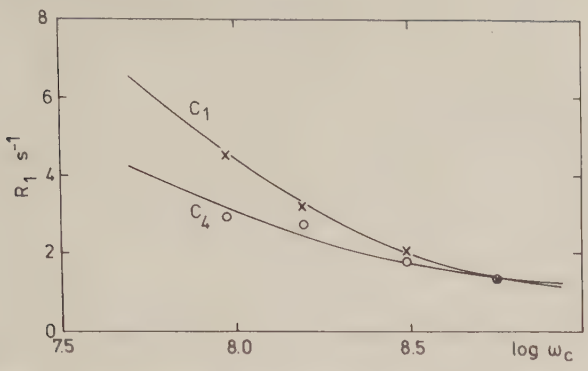

Figure 3. The lines show the calculated relaxation rate R_1 ($=T_1^{-1}$) for carbons 1 and 4 of DOTAC[1] as functions of log ω. The parameters τ_c^f, S, and τ_c^s have been evaluated from T_1 data for all resolved carbons at four fields. Also given are the experimental values for the same carbons ((×) carbon 1, (O) carbon 4).

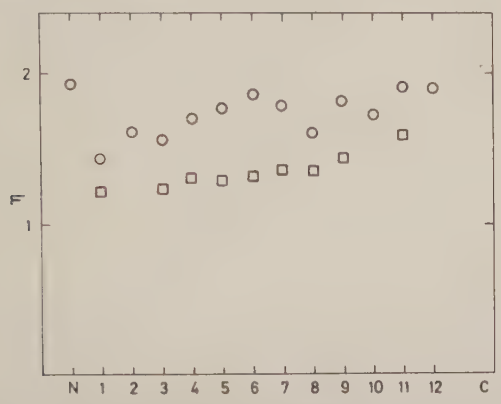

Figure 4. (□) Experimental and (O) predicted NOE's at 8.5 T for all carbons in DOTAC[1] (30%) at 28 °C when parameters extracted from T_1 measurements only are used.

erizations). Due to the presence of neighboring chains, the rotations in one chain can also be expected to be correlated with those of other chains.[32] Therefore, we feel that the interpretation of τ_c^f's using a particular model for the motion is not warranted. However, we believe that the fast correlation times give us a qualitative picture of the motions that the hydrocarbon chain undergoes in a micelle.

The slow correlation time gives the characteristic time for the motions that average the residual anisotropy left by the fast motions to zero. As a first approximation, these motions are interpreted as aggregate tumbling and/or diffusion of monomers over the curved surface of the micelle. Other motions occurring on a time scale comparable to the Larmor frequency of carbon or proton can also contribute to the slow correlation time, however (see further discussion on this topic below).

Cross-Correlation. In a CH_2 or a CH_3 group, the so-called cross-correlation spin relaxation effects can play an important role.[33] The two-step model giving eq 2 does take care of cross-correlation effects due to the slower motions. In no experiments performed in this work did the recovery curves for the magnetization depart significantly from an exponential form. This would suggest that cross-correlation is unimportant in the present study.

Evaluation of Data. For one of the systems studied (DOTAC 30% by weight at 27 °C) we have measured T_1's at four fields and NOE's at two fields in order to carefully evaluate the parameters. If one uses the T_1 data, an excellent fit is obtained. This is shown in Figure 3 where we have calculated the theoretical frequency dependence for R_1 from T_1 data obtained at four fields. With these T_1 data it is possible to calculate the outcome of a NOE experiment. Figure 4 shows the result, and, as can be seen,

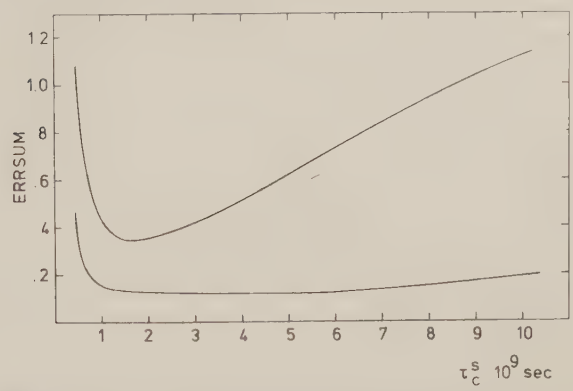

Figure 5. Error sums (see Computational Procedure...) as functions of τ_c^s for DOTAC[1] 30% (see Evaluation of Data). For the upper curve NOE's are included; for the lower curve T_1's only have been used. Data for all carbons are used in the calculations.

the actual experimental values differ quite significantly from the predicted ones. The reason for this can be found in Figure 5, where we have assigned various values to τ_c^s and made a two-parameter fit to the T_1 data. The error sum (see under Computational Procedure...) is presented in Figure 5 as a function of the given value for τ_c^s. As can be inferred from Figure 5, the T_1 data are relatively insensitive to the value of the slow correlation time. If, however, the experimental NOE's are included, a clear minimum in the error sum is found, also shown in Figure 5. Consequently, it appears that while T_1's are rather insensitive to the values of the slow correlation time, the NOE's depend somewhat more on this parameter. This demonstrates that it is important to include NOE data when evaluating τ_c^s from NMR relaxation data.

For all the results quoted in the present work we have used a carbon–proton bond length of 1.09 Å, the value normally used for a sp^3-hybridized carbon. The only exception is the bond length in the phenyl ring of SOBS where a value of 1.07 Å was used. It has been pointed out that the value 1.09 Å for the bond length is rather small, since effects of vibrational averaging must be taken into account.[34] In order to assess the influence of the r_{C-H} value on the obtained parameters, we have taken one set of T_1's and NOE's and evaluated the parameters using 1.09 and 1.12 Å for r_{C-H}. The value 1.12 Å is obtained from molecular mechanics calculations.[35] The differences for the parameters calculated from these two values for r_{C-H} are marginal.

The SOBS–Water System. Three concentrations of this system have been studied, namely 5%, 8%, and 12% by weight at a temperature of 42 °C. The order parameter and fast correlation time profiles along the amphiphilic molecule for one of these concentrations are shown in Figure 6a,b. The profiles are insensitive to concentration within the uncertainties of the evaluated parameters. Hence, the increased concentration of surfactant does not change the chain packing or the chain dynamics in these micelles, strongly suggesting that the micelles do not change shape over the concentration interval studied. In ref 36 it is concluded that at 33 °C SOBS micelles are spherical up to 0.15 m (5% by weight). The order parameter profile for the hydrocarbon chain shows a characteristic S shape. The value of the order parameter is highest for the carbon closest to the phenyl ring, fairly constant for the next four carbons, and then drops rapidly for the last three carbons. For comparison, the order parameter profile for a lamellar liquid-crystalline phase in the system water–SOBS–pentan-1-ol is shown in Figure 6a.[37] The profiles follow each other closely with the one for the lamellar phase displaced to lower values, especially for the carbons close to the end of the chain. This is presumably caused by the presence of pentan-1-ol near

(32) O. Edholm and C. Blomberg, *Chem. Phys.*, **53**, 185 (1980); O. Edholm, *Chem. Phys. Lipids*, **29**, 213 (1981).
(33) L. G. Werbelow and D. M. Grant, *Adv. Magn. Reson.*, **9**, 189 (1977).
(34) R. L. Vold, R. R. Vold, and D. Canet, *J. Chem. Phys.*, **66**, 1202 (1977).
(35) S. Andersson, Thesis, Lund, Sweden, 1982.
(36) B. Lindman, M. C. Puyal, N. Kamenka, B. Brun, and G. Gunnarsson, *J. Phys. Chem.*, **86**, 1702 (1982).
(37) O. Söderman and H. Walderhaug, to be submitted for publication.

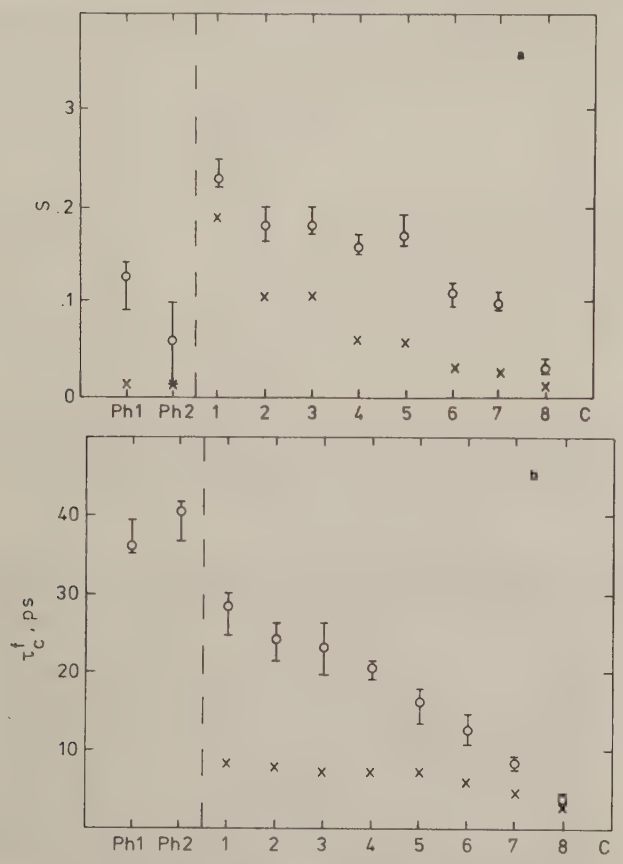

Figure 6. (a): (O) The order parameter for SOBS[1] as a function of chain position at 42 °C. Ph 1 and Ph 2 denote the two different protonated carbons of the phenyl ring; (X) the corresponding order parameters for SOBS in the lamellar D phase of the system water–SOBS–pentan-1-ol at 30 °C (from ref 37). (b): (O) The fast correlation time as a function of chain position in SOBS at 42 °C; (X) the corresponding correlation times for octylbenzene in acetone at 30 °C.

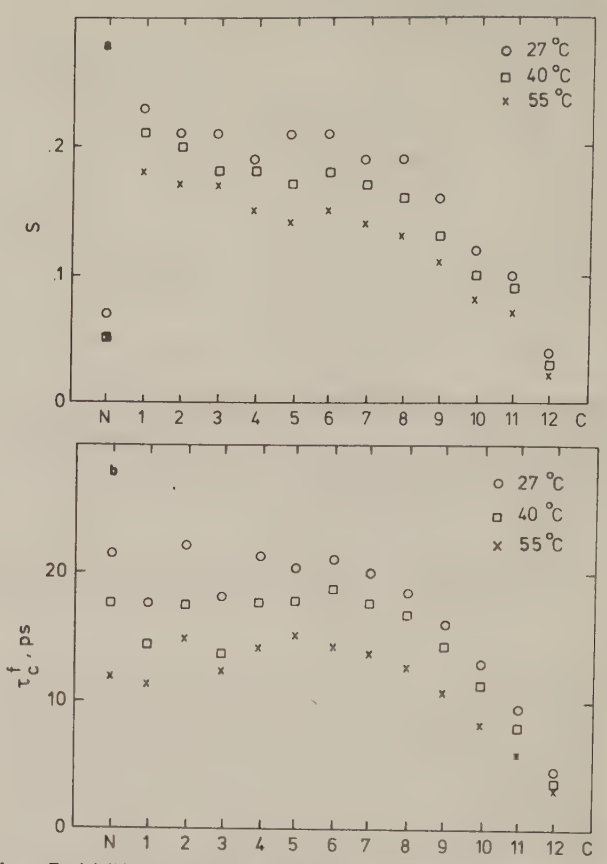

Figure 7. (a) The order parameter as a function of chain position for the system DOTAC 30% at three different temperatures. N denotes the methyl groups of the ammonium head group. (b) The fast correlation time as a function of chain position for the same system and at the same temperatures as in (a).

the lamellar surface. One parameter determining the values of the order parameters in a lamellar phase is the thickness of the bilayer.[38] With decreasing thickness a larger number of molecular conformations become available, since the area under the polar head group increases with decreasing thickness of the bilayer, thus increasing the amplitude of motions that each chain can undergo. Due to its shortness, pentanol tends to compress the bilayer. Finally, the order parameter for the protonated carbons in the phenyl ring (ortho and meta) is quite close to 0.125, which is expected if all the phenyl rings are oriented with the SO_3 para carbon direction perpendicular to the micellar surface and rotating about the axis defined by this direction.

Turning to the fast correlation time, one finds (Figure 6b) that it falls off in an almost continuous fashion. Also shown in Figure 6b are the correlation times for octylbenzene in acetone (data from ref 37). It is evident that the fast correlation times are longer in the micelles; the difference is largest for the carbons closest to the polar head group and decreases toward the methyl group, where essentially no difference is observed. This reflects the fact that the carbons close to the head group are motionally restricted due to the anchoring of the polar head group at the water–micelle interface, but the restriction is slight and the motions are indeed fast in the micelle (see further discussion below). The evaluated slow correlation times are summarized in Table I. Also shown are the theoretical correlation times defined by

$$(\tau_c^s)_{theor}^{-1} = (\tau_c^s)_{rot}^{-1} + (\tau_c^s)_{diff}^{-1} \quad (7)$$

In eq 7 the assumption is made that the slow motions include rotation of the micelle and amphiphile diffusion over the curved surface of the micelle. $(\tau_c^s)_{rot}^{-1}$ is calculated from the Debye–Stoke–Einstein equation

$$(\tau_c^s)_{rot}^{-1} = 3kT/(4\pi r_M^3\eta) \quad (8)$$

and $(\tau_c^s)_{diff}^{-1}$ is calculated from the diffusion equation

$$(\tau_c^s)_{diff}^{-1} = 6D/r_M^2 \quad (9)$$

Here k is the Boltzmann constant, T is the absolute temperature, r_M is the radius of the micelle, η is the viscosity of the medium (heavy water), and D is the lateral diffusion coefficient of the amphiphiles. As can be seen, the slow correlation time is shorter than that expected from micelle rotation and amphiphile diffusion over the surface of the micelle. This observation is discussed further below.

The TAC Systems. Three different concentrations were used for the TAC systems. For DOTAC 20%, 25%, and 30% by weight solutions were used, while the corresponding figures for CTAC were 11%, 19%, and 23%. Again, no dependence on the concentration was found for τ_c^s and S. Thus, no apparent change in the micellar shape takes place over the concentrations used for DOTAC or CTAC. Data for DOTAC at 30% by weight and three temperatures and CTAC at 23% by weight and 28 °C are shown in Figures 7a,b and 8a,b, respectively. The order parameter profiles show the typical S-shape with the methyl groups in the head group having a lower value, due to its rotation around the C–N bond. As can be seen in Figure 7a, there is a slight temperature dependence for the order parameters. As the temperature increases, the profile is displaced to lower values of S. This reflects an increased configurational disorder in the micelles with increasing temperature. The fast correlation times show a slight increase toward the middle of the hydrocarbon chain, and for the DOTAC systems they decrease with increasing temperature,

(38) J. H. Davis and K. R. Jeffrey, *Chem. Phys. Lipids*, **20**, 87 (1977).
(39) C. Tanford in "The Hydrophobic Effect", 2nd ed., Wiley, 1980.
(40) B. Lindman, N. Kamenka, T. M. Kathopoulis, B. Brun, and P. G. Nilsson, *J. Phys. Chem.*, **84**, 2485 (1980).
(41) P. O. Eriksson, A. Khan, and G. Lindblom, *J. Phys. Chem.*, **86**, 387 (1982).

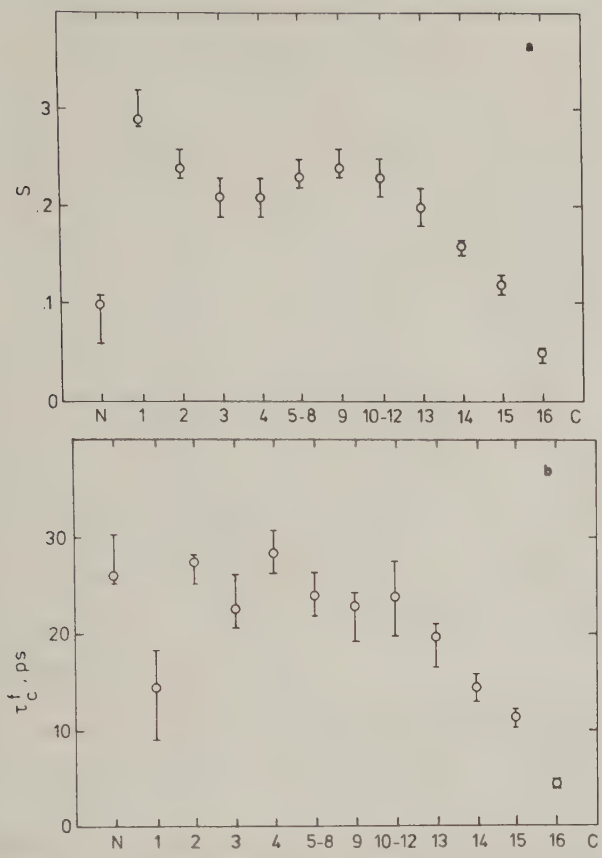

Figure 8. (a) The order parameter as a function of chain position for CTAC.[1] N denotes the methyl groups of the ammonium head group. The carbons 5–8 and carbons 10–12 have not been resolved, and therefore only an average value of S can be ascribed to these. (b) The fast correlation time as a function of chain position for CTAC.

reflecting the increased mobility of the chains with temperature. Within the experimental error, there are no changes in the slow correlation times for the DOTAC system. Nor does it increase significantly when the length of the hydrocarbon chain is increased to CTAC (see Table I).

The PPALM System. Three concentrations were also studied for PPALM. These were 8%, 12%, and 16% by weight. As for the other systems studied, there is no apparent concentration dependence on τ_c^f or S. The order-parameter profile for PPALM at 8% and 47 °C is shown in Figure 9a together with literature values for a lamellar sample of perdeuterated PPALM.[38] The data are generally somewhat higher than for the lamellar phase, but the differences are slight. Our evaluated fast correlation times are displayed in Figure 9b together with literature data from deuterium T_1's measured for a lamellar phase of perdeuterated PPALM.[42] The fast correlation time for the lamellar sample has been evaluated here from the T_1 data of ref 42 with the assumption that the correlation time for the slow motion is infinite in eq 2. As can be seen, the fast correlation times for the lamellar sample are a factor of about 5 longer than for the micellar case. This is quite a large difference, and it is contrary to the notion that both the rate and the amplitude of the motions should be more or less independent of the aggregate type for amphiphilic systems. Leaving aside the problem of evaluating T_1's from spectra of this kind, this discrepancy could be due to the presence of additional slower motions in the bilayer. If such motions are present then, obviously, the correlation time for the fast motion in the bilayer would be shorter. There are indications that such motions are indeed present in PPALM bilayers. It has been found[43] that there is a $1/\omega^{1/2}$ dependence for the relaxation rate for ^{1}H in the lamellar

(42) J. H. Davis, K. R. Jeffrey, and M. Bloom, *J. Magn. Reson.*, **29**, 191 (1978).
(43) K. R. Jeffrey, T. C. Wong, E. E. Burnell, M. J. Thompson, T. P. Higgs, and N. R. Chapman, *J. Magn. Reson.*, **36**, 151 (1979).

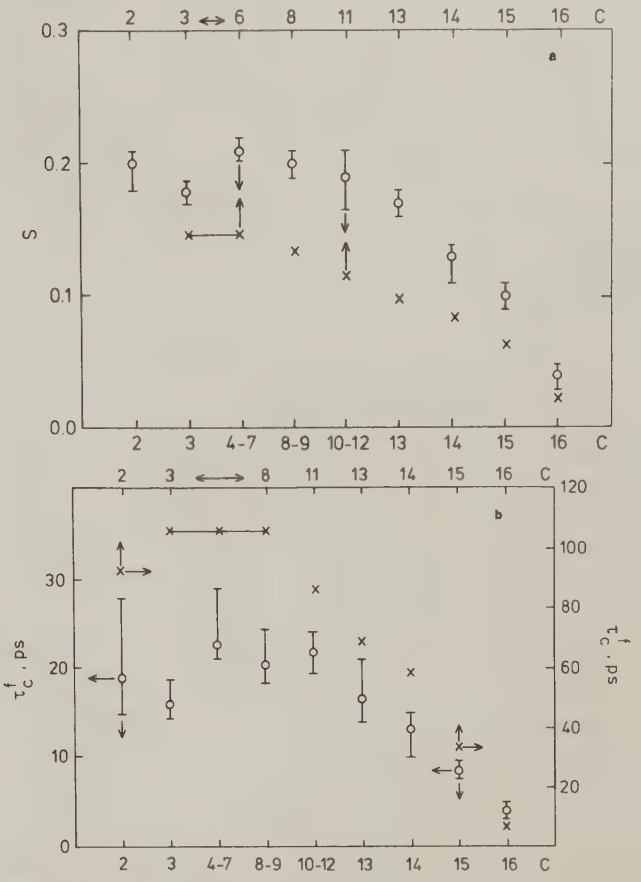

Figure 9. (a) The order parameter as a function of chain position for PPALM[1] at 47 °C. O are values for the micellar case, and the numbering of carbons is indicated on the lower axis. Carbons 4–7, 8–9, and 10–12 are not resolved. × are the values of the order parameters of PPALM extracted from deuterium quadrupole splittings in the lamellar D phase at 42 °C (from ref 38). The numbering of carbons is indicated on the upper axis. Carbons 3–6 are not resolved. (b) The fast correlation time as a function of chain position for PPALM. O are values for the micellar case, and × are values for the lamellar system (from ref 42). In this case carbons 3–8 are not resolved for the lamellar system where the temperature was 45 °C.

phase of PPALM. This indicates the presence of order fluctuations, a motion that could contribute to the spin–lattice relaxation of deuterium, providing it has frequency components at ω_0 and $2\omega_0$ for deuterium. A frequency dependence of T_1 has also been found in lipid bilayers,[44] indicating the presence of additional motions in these phases as well. This is in line with the conclusion reached in ref 45. Of course, the possibility exists that at least part of the differences in τ_c^f's result from isotope effects.

The slow correlation time for PPALM is found to be 2.2 ns, again a value that lies under the value derived from the combination of the Debye–Stoke–Einstein and the diffusion equations (7), (8), and (9). As can be seen in Table I, this is a general conclusion, valid for all the systems studied in this work. One important point is that rotational diffusion and monomer diffusion will *always* be present. Since these motions are isotropic, slower motions will not contribute to the spin relaxation. Thus, an exchange of monomers between micelles and solution can be ruled out, since typical time constants for this process fall in the microsecond regime.[46] Theoretical considerations lead to the conclusion that micelles are rather easy to deform.[47] The cost of energy for a slight change of the micelle from spherical to prolate or oblate shape seems to be very minor. A deformation

(44) M. F. Brown and J. H. Davis, *Chem. Phys. Lett.*, **79**, 431 (1981).
(45) M. F. Brown, *J. Chem. Phys.*, **77**, 1576 (1982).
(46) E. A. G. Aniansson, S. N. Wall, M. Almgren, H. Hoffmann, I. Kielmann, W. Ulbricht, R. Zana, J. Lang, and C. Tondre, *J. Phys. Chem.*, **80**, 905 (1976).
(47) B. Jönsson, personal communication.

of this kind would change the direction of the director and thus contribute to the relaxation.

To summarize, the present work gives the following picture of micelles. The anchoring of the polar head group at the micelle–water interface gives rise to an orientational ordering of the hydrocarbon chains. The order parameter quantifying this order varies somewhat both regarding the profile along the chain and the absolute values from those obtained in other types of amphiphilic aggregates. This is to be expected since, after all, the packing of chains into aggregates depends on the geometry of the aggregates.

The internal motions, as described by the parameter τ_c^f, are fast and only slightly affected by micellization. They all fall around 10^{-11} s, a value that is in good agreement with the correlation times that can be calculated from ^{13}C T_1 data for *n*-alkanes[6,48] of comparable chain lengths. Therefore, the dynamic state of the interior of a micelle resembles that of the corresponding *n*-alkanes. The same conclusion is reached in ref 45 for hydrocarbon chain motions in bilayers. Indeed, the result quoted there for the fast internal motions is 10^{-11} s. Thus, the dynamic state of hydrocarbon chains is rather unaffected by the shape of the surfactant aggregate it resides in. It is important, and should be stressed again, to realize that the order parameter itself does not give any information about the actual rate of motions that segments in the hydrocarbon chain undergo. This picture of the micelle is in good agreement with conclusions in a number of studies.[49–51]

Comparison with Theoretical Descriptions of Amphiphile Chain Packing in Micelles. One of the reasons for performing this work was to provide experimental data that can be used to test the various theoretical models for packing of amphiphile chains. For anisotropic phases, the order parameters are readily obtained from the deuterium spectra of deuterated amphiphiles. However, for isotropic phases, the spectra show no static effects and the order parameters have to be evaluated by an analysis like that presented above. Of the various models presented for chain packing in micelles,[49,52–54] Dill and Flory[53] and Gruen[54] present calculated order parameters that can be directly compared with those from this work. When comparing with Gruen's order parameters (which are defined for a CH_2 group by using the angle between the vector perpendicular to the plane spanned by the two C–H vectors and the director), the order parameters of this work must be multiplied by a factor of 2[55] (note that we cannot determine the sign of the order parameters). If this is done the experimental order-parameter profiles for a C-12 chain (see Figure 7a) resemble those predicted by Gruen, as regards both the shape and the magnitude of the individual order parameters. However, they disagree with the results of Dill and Flory, whose order parameters increase when going down the hydrocarbon chain.

One finds in the literature a vast number of theoretical treatments of the state of hydrocarbon chains in bilayers, both using mean-field approximations and Monte Carlo simulations. Recently, the method of molecular dynamics has been applied to bilayer systems.[56] The present authors feel that this latter method might prove very fruitful, since it provides information concerning *both* dynamic and static properties of the system. In particular, the interpretation of the fast correlation time extracted from NMR measurements of the present kind can be directly supported by molecular dynamics simulations of amphiphilic systems.

Acknowledgment. We thank Gunnar Grönberg, M.Sc., for performing the measurements at 4.7 T on the XL-200 spectrometer. This spectrometer was placed at our disposal through the courtesy of Svenska Sockerfabriks AB, Malmö, Sweden.

Registry No. DOTAC, 112-00-5; CTAC, 112-02-7; PPALM, 2624-31-9; SOBS, 6149-03-7.

Supplementary Material Available: Tables of T_1's and NOE's for the four micellar systems studied (6 pages). Ordering information is given on any current masthead page.

(48) J. R. Lyerla, Jr., H. M. McIntyre, and D. A. Torchia, *Macromolecules*, **7**, 11 (1974).
(49) B. Cabane, *J. Phys.* (*Orsay, Fr.*), **42**, 847 (1981).
(50) M. Schara, F. Pusnic, and M. Sentjurc, *Croat. Chem. Acta*, **48**, 147 (1976).
(51) J. Ulmius and H. Wennerström, *J. Magn. Reson.*, **28**, 309 (1977).
(52) P. Fromherz, *Chem. Phys. Lett.*, **77**, 460 (1981).
(53) K. A. Dill and P. Flory, *Proc. Natl. Acad. Sci. U.S.A.*, **78**, 676 (1981).
(54) D. Gruen, *J. Colloid Interface Sci.*, **84**, 281 (1981).
(55) J. Seelig and W. Niederberger, *J. Am. Chem. Soc.*, **96**, 2069 (1974).
(56) P. van der Ploeg and J. J. C. Berendsen, *J. Chem. Phys.*, **76**, 3271 (1982).

III

NMR RELAXATION IN ISOTROPIC SURFACTANT SYSTEMS. A ^{2}H, ^{13}C AND ^{14}N NMR STUDY OF THE MICELLAR (L_1) AND CUBIC(I_1) PHASES IN THE DODECYLTRIMETHYLAMMONIUM CHLORIDE/WATER SYSTEM.

Olle Söderman*(1), Harald Walderhaug (1),

Ulf Henriksson (2) and Peter Stilbs (3)

1. Division of Physical Chemistry 1, Lund University, P.O.B. 124, Chemical Center, S-220 07 Lund 7, Sweden

2. Department of Physical Chemistry, The Royal Institute of Technology, S-100 44 Stockholm 70, Sweden

3. Institute of Physical Chemistry, Uppsala University, Box 532, S-751 21 Uppsala, Sweden

(*) To whom correspondence should be adressed.

ABSTRACT

A ^{2}H, ^{13}C and ^{14}N NMR spin relaxation study of micellar solutions and cubic liquid crystalline phases formed in the two-component system dodecyl trimethylammonium chloride (DOTAC)(1)/water is presented. In particular, based on multifield ^{2}H NMR relaxation data, covering the frequency range 1.8 - 55.2 MHz, it is concluded that the NMR spin relaxation in ordinary micelles is determined by the fast local motion (trans- gauche isomerizations) of the $C-D_2$ segment of the hydrocarbon chains of the monomers and the rotational tumbling of the micelles and diffusion of monomers over the (curved) micellar surface. There is no need to invoke other motions to explain the spin relaxation over a wide frequency range for the micellar case. For the cubic phase at high water content, the relaxation data are interpreted in favour of a novel structure, recently presented for this phase. The data also indicate that the interior of the amphiphilic aggregates is liquid-like and that the orientational order imposed by the hydrophobic-hydrophilic interface depends only weakly on the geometry of the aggregates.

INTRODUCTION

Carbon-13 Nuclear Magnetic Resonance (NMR) (1) relaxation studies have been used extensively in studies of isotropic surfactant solution systems such as ordinary and reversed micelles and microemulsions (for recent reviews see refs.2-4). A general observation in these studies is that of rather long spin-lattice relaxation times that depend on the magnetic field strength, a reduced nuclear Overhauser enhancement and narrow NMR-lines (5-9). This observation immediately suggests that more than one motion causes relaxation and that one of these motions must occur on a time scale on the order of the inverse of the Larmor frequency in order to cause the observed field dependence. This makes the interpretation of NMR relaxation experiments on these systems complicated, but this complication can be turned into an advantage, since from studies of the frequency dependence of the relaxation rather detailed information about these systems can be obtained.

In a previous work (7) we used the so-called "two-step" model (10,11) to interpret extensive ^{13}C relaxation data at several magnetic field strengths, and showed that it was indeed possible to deduce significant properties of micellar systems from such studies. We have previously suggested (10) that the slow motions causing the frequency dependence, consist of the rotational tumbling of the micelle and/or monomer diffusion over the curved micellar surface. However, in ref.7 we found that the slow motion, when extracted from ^{13}C relaxation data, was invariably faster than that predicted from the Debye-Stokes-Einstein and diffusion equations for micellar tumbling and monomer diffusion. We therefore suggested that some other motions, e.g. micellar shape deformations, contributed to the relaxation. In order to further investigate this suggestion we synthesized α-deuterated dodecyltrimethylammonium chloride (DOTAC) (1); one of the surfactants used in ref.7 and present here ^{2}H relaxation data at no less than 10 field strengths as well as some ^{13}C and ^{14}N relaxation data for DOTAC micelles. In addition, to further investigate the influence of the slow motion, we have done analogous measurements on the cubic liquid crystalline phase I_1 (see Figure 1) which is formed between the micellar and the hexagonal phase of the binary DOTAC/water system.

During the course of this work a novel structure for this cubic phase has been suggested (13) , and the present NMR study gives further proof for this suggested structure.

THEORY

In the present work we will discuss NMR measurements on the micellar (L_1) and cubic (I_1) (see Figure 1) phases of binary DOTAC/water mixtures. Both these systems give rise to isotropic NMR spectra, i.e. spectra that show no static effects. The relevant relaxation equations are given below. For a nucleus X with spin I = 1 the longitudinal and transverse relaxation rates are (14):

$$R_1 = (3\pi^2/40)\cdot\chi^2\cdot(2\tilde{J}(\omega_x) + 8\tilde{J}(2\omega_x)) \qquad (1)$$

$$R_2 = (3\pi^2/40)\cdot\chi^2\cdot(3\tilde{J}(0) + 5\tilde{J}(\omega_x) + 2\tilde{J}(2\omega_x)) \qquad (2)$$

while for carbon "i" along the hydrocarbon chain the ^{13}C longitudinal and transverse relaxation rates and the nuclear Overhauser effect (n.O.e) (1), η, are given by (15):

$$R_1 = (N_i/20)[\mu_o\gamma_H\gamma_C\hbar/4\pi r^3_{C-H}]^2(\tilde{J}(\omega_H - \omega_C) + 3\tilde{J}(\omega_C) + 6\tilde{J}(\omega_H + \omega_C)) \qquad (3)$$

$$R_2 = (N_i/40)[\mu_o\gamma_H\gamma_C\hbar/4\pi r^3_{C-H}]^2(\tilde{J}(\omega_H - \omega_C) + 3\tilde{J}(\omega_C) + 6\tilde{J}(\omega_H + \omega_C) + 4\tilde{J}(0) + 6\tilde{J}(\omega_H)) \qquad (4)$$

$$\eta = (1/20)(\gamma_H{}^3\gamma_C)[\mu_o\hbar/4\pi r^3_{C-H}]^2(N_iT_1)(6\tilde{J}(\omega_H + \omega_C) - \tilde{J}(\omega_H - \omega_C)) \qquad (5)$$

Here χ is the quadrupolar coupling constant, μ_0 is the permeability of vacuum, γ_H and γ_C represent the magnetogyric ratios of proton and carbon and r_{C-H}, set equal to 1.09 Å, (see ref.7), denotes the C-H bond length. $\tilde{J}(\omega)$ are various reduced spectral density functions, ω_x ($x = {}^2H$, ${}^{14}N$), ω_C and ω_H are the Larmor frequencies of deuterium, nitrogen, carbon and proton at the actual magnetic field strengths and $\hbar$ is the reduced Planck's constant. N_i is the number of protons directly bonded to carbon "i". It is implied in equations (1) and (2) that the asymmetry parameter of the electric field gradient tensor is zero. As regards nitrogen, this assumption is discussed further on in the text while for a C-D group it has been demonstrated theoretically and experimentally (16,17).

As stated above the interpretation of relaxation data from isotropic surfactant systems is complicated since the relaxation is caused by several different types of motions of which at least one is anisotropic. In the present investigation we shall consider two cases. The first is the case where we have a fast, slightly anisotropic, motion and superimposed on that, a slow, isotropic motion. For such a case the relevant reduced spectral densities are (7,10,11):

$$\tilde{J}(\omega) = (1-S^2)\tilde{J}^f(\omega) + S^2\tilde{J}^s(\omega) \qquad (6)$$

where f and s denote the spectral densities for the fast and slow motion, respectively. S is defined as $S \equiv (1/2)\langle 3\cos\theta - 1\rangle_f$ where the average is taken over a time that is long enough to average the fast local motion but so short that the average is not affected by the slow motion. θ is the angle between the C-H or C-D vector and the local director, taken to be normal to the surface of the aggregate. S is termed order parameter and is completely analogous to the order parameter measured by deuterium or nitrogen NMR in anisotropic phases. If the fast and slow motions are described by single exponential correlation functions then

$$\tilde{J}^{f,s}(\omega) = 2\tau_c^{f,s}/(1 + (\omega\tau_c^{f,s})^2) \qquad (7)$$

where $\tau^{f,s}$ is the correlation time for the fast or slow motion. By assuming that the fast motion fulfils the extreme narrowing condition and inserting eq.(7) into eq.(6) we obtain eq.(2) in ref.7.

The second case we need to consider is that which pertains to rod-shaped micelles. Let us assume that the axial ratio of the micelles is such that the rotation about the length axis of the rod is much slower than the fast local motion but much faster than the end-over-end tumbling of the rods. For such a case the reduced spectral density is (18):

$$\tilde{J}(\omega) = (1 - S^2)\tilde{J}^f(\omega) + (3/4)S^2\tilde{J}^r(\omega) + (1/4)S^2\tilde{J}^t(\omega) \qquad (8)$$

Here superscripts r and t denote the spectral densities for the rotation and end-over-end tumbling, respectively.

We will end this section with two remarks. First,the motional model described by eq.(6) has been termed a "two-step" model. Consequently, the situation described in eq.(8) is termed a "three-step" model. Secondly, both eq.(6) and eq.(8) express the general fact that if the relaxation is caused by two or more anisotropic motions occuring on very different time scales then the spectral density can be written as a sum of terms, one for each time scale separated motion or set of motions. Each term is a product of a factor quantifying the amount of the interaction being averaged out by that particular motion or set of motions and a spectral density for that/these motion/motions (19,20).

EXPERIMENTAL SECTION

Materials.

DOTAC for ^{13}C and ^{14}N NMR was purchased from Eastman Kodac (99% purity). It was dissolved in methanol and treated with active charcoal, filtered and dried in a vacuum. DOTAC-1,1 ^{2}H was synthesized from dodecanoic acid chloride which was treated with dimethylamine to produce the corresponding amide. The amide was subsequently reduced with LiAl-$(^{2}H)_4$, producing the α-deuterated dodecyldimethylamine. The final product was then obtained by reacting the dimethylamine with methyl chloride. The synthesis was performed by "Syntestjänst", Chemical Center, Lund. High resolution proton NMR spectra showed that more than 98% of the α-protons were replaced with deuterons. Samples were prepared by weighing the appropriate amounts of surfactant and water directly into NMR tubes. The micellar samples were equilibrated for at least two weeks at 25°C while the cubic samples were sealed and kept at an elevated temperature (70°C) for 48 hours. They were then stored at 25°C for at least two weeks before any NMR measurements were made. The composition of the cubic phase was 50 wt % DOTAC in H_2O.

Methods.

^{13}C relaxation measurements were performed at four magnetic field strengths, 8.45 T, 4.70 T, 2.35 T and 1.40 T, as described in ref.7. ^{2}H measurements were performed at 8.45 T, 6.00 T, 4.70 T, 2.35 T and 2.11 T on a NICOLET 360 Spectrometer, a home-built spectrometer equipped with an Oxford wide bore superconducting magnet, a highly modified BRUKER CXP 200 spectrometer, a JEOL FX 100 spectrometer and a BRUKER CXP 100 spectrometer equipped with a fluxstabilizer HS 90 var., respectively. Further measurements at field strengths between 2.1 T and 0.27 T were performed by varying the field strength on the BRUKER CXP 100 system.

Finally, ^{14}N measurements were performed at 8.45 T, 6.0 T and 2.1 T on the same spectrometers as for ^{2}H. ^{2}H and ^{14}N spin-lattice relaxation measurements were performed with the standard inversion-recovery experiment, while the

spin-spin relaxation measurements were performed with the Carr-Purcell-Meiboom-Gill method for narrow lines and deduced from the line width after suitable corrections for magnetic field inhomogenities for broad lines. Data evaluation was performed as described in ref.7. All given confidence intervals in measured and evaluated quantities correspond to approximately an 80% level of confidence. Only random errors are considered. The temperature was, unless stated otherwise, 28°C. We estimate the difference in temperature between the various experiments to be less than 1°C.

RESULTS AND DISCUSSION.

For the sake of clarity we will discuss the results for the micellar and the cubic phases separately.

The Micellar Phase.

Presented in Figure 2a-c are deuterium R_1 and R_2 and ^{13}C relaxation data at two and three different field strengths, respectively, as a function of DOTAC concentration. There is a marked field dependence in the ^{13}C R_1 data as has already been demonstrated in ref.7. Furthermore, the deuterium R_1's for the α-carbon also depend on the field strength and are not equal to R_2. As a function of concentration within the micellar phase there is an increase in R_1 for ^{13}C and ^{2}H at the lower fields as the concentration increases,while at the higher fields it stays fairly constant. The same observation can be made for ^{2}H R_2, although there is a slight increase in R_2 at 6.0 T. With the data in Figure 2a-c and eqs.(1), (2) and (3) it is possible to calculate the parameters τ_c^f, S and τ_c^s ; this was the procedure used for ^{13}C data in ref.7. However, as pointed out in the introduction, the τ_c^s's obtained in this way were shorter for four different micellar systems than what would be expected from the tumbling of the micelle and monomer diffusion over the curved micellar surface. Furthermore, when the parameters were evaluated we assumed an exponential correlation function for the slow motion. It has been suggested that so-called order-director fluctuations would be the origin of the slow motion (5,6). The correlation function for these motions produces a spectral density that depends on $(\omega_0)^{-1/2}$ (21). With relaxation data at only 3-4 different magnetic field strengths it is not possible to distinguish between the two types of spectral densities. Consequently, the evaluated parameters depend on the model chosen for the slow motion. With this in mind we have performed ^{2}H R_1 measurements on a 30% wt/wt α-deuterated DOTAC sample at 10 different magnetic field strengths. These data together with ^{2}H R_2 and ^{14}N R_1 and R_2 at three magnetic field strengths are presented in Figure 3. The solid lines in Figure 3 have been obtained in the following way. First, the parameters S, τ_c^f and τ_c^s were obtained by fitting eqs.(1),(2),(6) and (7) to the ^{2}H R_1 and R_2 data (assuming that the extreme narrowing condition applies for the fast motion) using the value χ = 167 kHz for

the deuterium quadrupole coupling constant. This procedure produces the solid lines through the deuterium data. Secondly, the ^{14}N data were treated in the same way with τ_c^s kept at the value obtained from the ^{2}H fit, since this parameter will be the same for the two nuclei. When treating the ^{14}N data we have set χ equal to 116 kHz. Before commenting on the result of the fits in Figure 3 we will diverge somewhat and discuss the value chosen for the ^{14}N quadrupole coupling constant.

In the literature there are several suggestions for the value of the quadrupole coupling constant in molecules containing the following group:

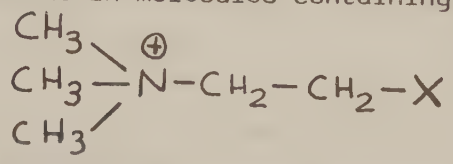

Siminovitch et al. (22) computed the order parameter for the N-C_α bond from the deuterium quadrupole splitting for a deuterated choline methylene group in dipalmitoylphosphatidylcholine (DPPC) (1) and then proceeded to compute χ from the ^{14}N quadrupolar splitting. They arrived at a value of 135 kHz. Using a similar analysis for dioleylphosphatidylcholine Rothgeb and Oldfield deduced a value of 131 kHz (23). However, this analysis presupposes that the asymmetry parameter $\eta = (V_{xx} - V_{yy})/ V_{zz}$ where V_{ii} (i=x,y,z) are the components of the electric field gradient tensor in its principal axis system, is zero. Furthermore, the z-axis of the principal axis system has to coincide with the N-C_α bond axis. This is not strictly true since the N-C_α bond axis is not a three-fold (or higher) axis of symmetry. Therefore the analysis in refs.(22,23) is not strictly correct. The deviation from three-fold symmetry is probably quite small and it is quite possible that 135 kHz is a good approximation for χ in phosphatidylcholines. A more serious objection to the use of this value for DOTAC is that in the phosphatidylcholines there are only two methylene groups in the hydrocarbon attached to the nitrogen. It has been demonstrated that the length of the hydrocarbon chain is important up to 5 methylenes but for longer chains the length does not appear to have any influence on χ (24). Therefore, we have chosen to use the value for χ obtained from broadline ^{14}N NMR on decyltrimethylammonium bromide (DTAB) in the solid state (25). When obtaining χ from solid-state NMR it is possible that there are intermolecular contributions to the electric field gradient. In fact, Protum and Klein obtained a χ some 15% lower for the C-16 analogue of DTAB indicating that there are indeed such contributions. However, 116 kHz is close to the value 111 kHz obtained earlier by one of us (26) from ^{14}N relaxation studies and we have therefore chosen the former value. Furthermore, we shall assume that the asymmetry parameter, η, is close to zero and hence neglect it.

Returning to the results presented in Figure 3 , the parameters obtained from the fits are given in Table 1. As can be inferred from Figure 3 the experimental data suggest that the slow motion is indeed well described by a single exponential correlation function. We have also tried to fit the data to $(\omega)^{-1/2}$ and it is evident from the insert in Figure 3 that such a form for the spectral density is at variance with the experimental results.

Turning to the values in Table 1, the fast correlation time is 37 ps for the deuterium and somewhat longer for nitrogen. The value for the latter depends on the choice of χ but it is reasonable that it should not deviate much from the value for the α-CD_2. After all, the dynamics of the N-C_α bond are not expected to differ much from those for the C_α-D bond.

The fast local motion of the C_α-D bond, indeed of any C-D vector along the chain, is presumably complex. There will be rotations around the carbon-carbon bonds, torsions, diffusion etc. To put the value of τ_c^f into perspective it would be interesting to compare it with that for monomeric DOTAC in aqueous solution. Unfortunately, the low c.m.c.(1) of DOTAC prevents any such relaxation measurements from being made. However, the C-8 analogue, i.e. octyltrimethylammonium bromide (OTAB)(1) has a c.m.c. high enough to allow such a measurement. From the ^{13}C T_1 work of Williams et al. (27) we calculate τ_c^f = 10 ps for the α-carbon of OTAB at 34°C. For the monomer we will have, in addition to the motions described above, motions of the molecule as a whole. Moreover, the temperature was 6°C higher in the monomer experiment. Thus, it appears that the rate of these motions is only weakly affected by the micellization.

From the data of Brown et al. (28) it is possible to estimate τ_c^f = 20 ps for the C_α-carbon in DPPC (1) vesicles at 50°C. Taking into consideration the difference in temperature and system, the difference between the DOTAC and DPPC is slight, indicating that the surfactant and phospholipid system, at least in this respect, behave very much the same.

The order parameter,S, is 0.17 for deuterium and 0.23 for nitrogen. This can be compared with the values deduced from quadrupolar splittings in the hexagonal phase of DOTAC/water for which case data are given in Table 2. In order to compare the order parameter in the hexagonal phase with those derived from relaxation measurements, the former have to be multiplied by a factor of 2 (30). The values of S are somewhat lower in the micelles both for the N-C_α bond and the C_α-D bond, but the difference is slight. This gives further evidence for

the notion that the local molecular properties for surfactants depend only weakly on the geometry of the aggregate they reside in (31,32).

When treating ^{13}C relaxation data from micelles formed by alkylammonium chlorides Canet et al. (5,33), using an approach similar to the "two-step" model, make an assumption which amounts to setting the C_α-D order parameter equal to 0.33. It is assumed that the N-C_α bond is parallel to the director and, furthermore, except for rotations around the C_α-N bond, that there are no further fast motions. Clearly, in line with what has been said above, this is an over-simplification, and the experimental verification that this assumption is erroneous is seen in Table 1.

Finally, we turn to the slow correlation time τ_c^s. Its value obtained from the ^2H relaxation data is 3.9 ± 0.4 ns. Assuming that the slow motion is the micellar tumbling and the diffusion of surfactant molecules over the curved aggregate surface the slow correlation time is given by :

$$1/\tau_c^s = 1/\tau_c^{rot} + 1/\tau_c^{diff} \qquad (9)$$

$$\tau_c^{rot} = 4\pi R^3\eta/3kT \qquad (10)$$

$$\tau_c^{diff} = R^2/6D \qquad (11)$$

Here R is the radius of the spherical micelle, D is the diffusion coefficient for the surfactant molecule in the aggregate, η is the viscosity of the medium and the other quantities in eq.(10) have their usual meaning. The value for the diffusion coefficient D in micelles is not known. However, it has been measured in the cubic liquid crystalline phase (I_2 in Figure 1) to be $0.76\times10^{-11}m^2s^{-1}$ at 26^oC (29). Assuming a rodlike structure for this cubic phase, the diffusion coefficient to be used in eq.(11) should be multiplied by a factor of 3 (see also the Discussion in ref. 29). We assume that the translational motion within the aggregates does not depend on the aggregate geometry (34,35) and hence use this value. In setting the radius R that appears in equation (11) equal to the micellar radius we have assumed that it is the electrostatic interactions in the head group region that determine the rate of diffusion. From the experimental value of τ_c^s we then calculate a micellar radius R = 17.7 ± 0.6 Å from eqs.(9)-(11). Theoretical considerations imply that the radius of the micelle should be the length of an all-trans chain (36) which for DOTAC is equal to 16.6 Å to the mid point of the bond connecting the α-carbon and the nitrogen (37).

Adding 2 Å for the head group we obtain a value of 18.6 Å for the micellar radius, in very good agreement with the experimental finding, especially considering the assumptions made in eqs.(10) and (11) (vide supra). It is also in good agreement with a neutron scattering study on the same system (38).

To sum up, the slow motion is described by a single exponential correlation function and there is no need to invoke other slow motions than the rotational tumbling and monomer diffusion over the curved surface to explain the ^2H NMR relaxation data. A further critical test of these conclusions would be to perform a similar experiment on micelles of different (say larger) radius. If the experiment then picks up the increase in τ_c^s due to the change in R and D predicted by eqs.(10) and (11) this would certainly give further evidence for these conclusions. We are presently performing such an experiment on the cetyltrimethylammonium chloride (CTAC), the C-16 analogue of DOTAC.

The order parameter and fast correlation time profiles for 30% DOTAC in water are presented in Figure 4a-b. These data have been obtained from ^{13}C R_1's at four field strengths, ^{13}C n.O.e's at two field strengths (data from ref.7) and ^2H R_1's and R_2's for the α-CD_2 group given in Figure 3. In ref.7 the same parameters were extracted from ^{13}C relaxation data alone. Except for the α-carbon the results agree within the experimental error.

We now proceed to discuss why the slow correlation time τ_c^s extracted from ^{13}C R_1 relaxation data deviates from the value 3.9 ns obtained from ^2H relaxation rates (see Table 1). In Figure 5 we show the reduced spectral density function for the slow motion with a correlation time of 3.9 ns. Also shown are the points on the curve where ^{13}C R_1's sample the spectral density for the four magnetic field strengths used in ref.7. It is clear that ^{13}C R_1's sample the spectral density predominantly at high frequencies and thus, the R_1's are not very sensitive to the slow motion. Deuterium relaxation data, on the other hand, sample frequencies in the range 1.2×10^7 - 6.9×10^8 rad/s. For longer chain surfactants, giving larger τ_c^s, the curve in Figure 5 is shifted to lower frequencies making ^{13}C R_1 measurements even less sensitive to the slow motion. This explains why in ref.7 no dependence on τ_c^s was found as the micellar radius was increased. Consequently, when going to shorter chain surfactants the curve in Figure 5 is displaced to higher frequencies. Now, a larger portion of the spectral density curve is probed and the ^{13}C data depend more strongly on τ_c^s. This is presumably the reason why the slow correlation time derived from sodium octanoate micelles (39) is in good agreement with that predicted from eqs.(10) and (11). This suggestion is also in line with the concentration dependence of

the relaxation data, depicted in Figure 2. At higher field strengths both the ^{13}C and ^{2}H R_1's do not depend on the concentration and do not change when entering the cubic phase (vide infra), while at lower fields strengths there is a concentration dependence. For the micellar case this reflects an increase in τ_c^S, due to either an increase in micellar size or an increased intermicellar interaction or a combination of both, with increasing concentration of surfactant. This increase of τ_c^S is picked up at the lower field strengths but not at the higher ones where the relaxation to a large extent is given by the fast motion. It also follows from the unsensitivity in R_1 at higher field strengths upon entering the cubic phase, that the fast motion is not sensitive to the particular phase the aggregates form (vide infra).

Before terminating the discussion of the micellar results we will make one final remark. As is seen in Figure 3 the ^{2}H R_1's level off to a plateau at low frequencies. On the plateau R_1 equals R_2. This effect is even more noticeable for the ^{14}N data. This is a consequence of the fact, which was stressed in ref.7, that no motions slower than the fastest isotropic motion can contribute to the NMR relaxation, a fact that has not always been appreciated (5,33). See also the discussion on pages 4552 and 4565 of the papers by Lipari and Szabo (40).

The Cubic Phase I_1.

The binary system DOTAC/water is interesting since it has two composition regions in which cubic liquid crystalline phases are formed, one on either side of the hexagonal liquid crystalline phase (see Figure 1). In the present work we have studied the cubic phase I_1 which occurs between the micellar and hexagonal phases with the intention of examining if it is possible to probe with NMR relaxation measurements, whether any changes take place in the molecular or aggregate dynamics as one goes from the micellar to the cubic phase. This liquid crystalline phase is very attractive for NMR studies in that it, contrary to most liquid crystalline phases, gives rise to high resolution NMR spectra (see Figure 6). Note that at the field strength used in Figure 6 all the carbons are resolved. This is somewhat surprising at first sight, since the phase is hard as plexiglass, but it is a consequence of the short range disorder and the cubic symmetry of the phase. As is seen in Figure 2 ^{13}C and ^{2}H R_1 increases somewhat as one goes into the cubic phase at the lower field strengths; but the increase is small and, in fact, approximately linear with concentration over the combined micellar + cubic phase region. At the higher field strengths R_1 is constant

(vide supra). However, there is a marked line broadening for ^2H as one enters the cubic phase. One convenient and fast method to detect the presence of slow motions in surfactant systems is to record the ^1H NMR spectrum, since line broadening of the peaks indicates that slow motions contribute to the NMR relaxation of the protons (6,32,42). In Figure 7 we show the proton signals from the methylenes and the ω-methyl in the hydrocarbon chain for a micellar and a cubic sample at 28°C. As can be inferred from Figure 7 there is a detectable NMR line broadening upon entering the cubic phase, indicating the presence of slow motions contributing to the NMR linewidth in the cubic phase. In fact, as early as 1973 Bull and Lindman reported a marked increase in ^1H R_2 upon entering the cubic phase (42). These workers did unfortunately not realize the importance of their observation. Of more recent date is a study by Eriksson et al.(29) who report an analogous increase in the ^{14}N R_2.

In Figure 8 we show ^2H R_1's at 13, ^2H R_2's at 5 and ^{14}N R_1's and R_2's at 3 different field strengths. It is clear that the deuterium R_1's level off and do not depend on the magnetic field strength below ~0.3 T (approx. 2 MHz for deuterium). However, contrary to the micellar solution, R_1 is not equal R_2 on the plateau (cf. Figure 2 and Figure caption 8). Therefore there must be at least three types of motion causing the NMR relaxation, viz. the fast local motion, an intermediate anisotropic motion causing the frequency dependence in R_1 and, finally, one or more slow motions which, when combined, are isotropic.

Before going into a more detailed analysis of the data in Figure 8 a few words about the structure of the cubic I_1 phase are necessary. NMR diffusion measurements show conclusively that this phase has discontinous hydrocarbon regions, i.e. it consists of closed amphiphilic aggregates (29,42). Based on ^{14}N NMR data, Eriksson et al.(29) suggest a structure consisting of closely packed spherical micelles. These workers use a two-step model and assign the slow motion to monomer diffusion over the curved surface. However, the analysis is based solely on ^{14}N R_1 and R_2 at one single field strength. With reference to Figure 8 this analysis is clearly incomplete. A further, perhaps more serious objection to a structure with closely packed spherical micelles is that X-ray data for this model predict a sphere with radius considerably longer than the extended hydrocarbon chain (13). To reconcile the NMR diffusion data with the X-ray data Fontell et al.(13) have suggested that the structure of the liquid crystalline phase I_1 of DOTAC/water belongs to the space group Pm3n and has the same structure as that of solid γ-O_2 and β-F_2 at 50K. Each unit cell is composed of 8 hemisphere capped rods with an axial ratio of 2. A picture of the structure is shown in Figure 9. Of the 8 aggregates in the unit cell X-ray data imply that

6 are restricted to end-over-end rotation in only one plane or are statistically disordered in this plane while 2 are either freely rotating or statistically disordered at several orientations. All 8 aggregates are free to rotate around their long axis. We suggest that this latter motion plus monomer diffusion around the rod is the cause of the frequency dependence in R_1. As is evident from Figure 9 the aggregates in the unit cell are tightly packed, indicating that any end-over-end rotation of the rods will be highly collective and thus considerably slower than the same motion for an isolated aggregate in water (vide infra).

This situation is equivalent to that of a rod-shaped micelle with an axial ratio such that the end-over-end rotation is considerably slower than the rotation around the rod's length axis and the monomer diffusion around the rod. This justifies the use of a three-step model, viz. eq. (8), for the relaxation in the cubic liquid crystalline phase I_1. The various solid lines in Figure 8 have been obtained in the following way. First, we note that the ^2H R_1 levels off to a plateau value below approximately 2 MHz. Thus, the third step in the total spectral density curve will not contribute to the spin-lattice relaxation times determined at the frequencies shown in Figure 8. We have therefore used eq.(1) and eq.(8) except the last term on the right-hand side in the fitting to the ^2H R_1 data. This procedure gives the parameters τ_c^f, τ_c^r and S and also the solid line through the ^2H R_1 data in Figure 8 as well as a line for the predicted R_2 from the first two steps in the spectral density function. The experimental ^2H R_2 values are according to eq.(2) determined by the value of the spectral density function at zero frequency, at the Larmor frequency and at twice the Larmor frequency. Since the third term in the spectral density function in eq.(8) does not contribute to R_1 in the frequency range used in this work, it gives only a frequency independent contribution to R_2 via the zero frequency term in eq.(2). From each experimental R_2 value this contribution, δ_D, was determined by subtraction of the R_2 value obtained by using the parameters extracted from the R_1 fitting and the first two terms in eq.(8), i.e. the values obtained from the solid line for R_2 ^2H in Figure 8. The ^{14}N relaxation data are treated in an analogous manner whereby the value of the intermediate correlation time, τ_c^r, is fixed to the value determined by the fit to the ^2H R_1 data. The parameters determined from the fitting procedures together with the frequency independent contributions, δ_D and δ_N, from the slowest motion to R_2 are presented in Table 3. As is evident from Figure 8 and from the quite small standard deviations in the parameters in Table 3 the fit to the ^2H R_1 data is remarkably good. It is also clear from the insert in Figure 8 that the data are not compatible with a spectral density function proportional to $(\omega_o)^{-1/2}$.

From eqs.(2) and (8) it follows that the constants δ are given by:

$$\delta = (3\pi^2/40)\cdot\chi^2\cdot(S^2/4)3\tilde{J}^t(0) \qquad (12)$$

and the ratio between δ_N and δ_D is given by:

$$\delta_N/\delta_D = [\chi_N\cdot S_N / \chi_D\cdot S_D]^2 \qquad (13)$$

This ratio can be determined from experimental ^{14}N and ^{2}H quadrupole splittings. The experimental quadrupole splittings from the hexagonal phase presented in Table 2 give the value $\delta_N/\delta_D = 97$. The average value for this ratio determined from the relaxation data (Table 3) is 126. Considering the uncertainty in the ^{14}N fitting and possible variations in the ratio between the quadrupole splittings with phase structure and composition we believe that the agreement is satisfactory.

A further test is provided by the ^{13}C T_2 value for the α-carbon whose ^{13}C signal at 1.4 T in the cubic phase is broad enough to permit a rather accurate determination of the linewidth. Using eq.(4) and the data in Table 3 it is predicted to be 83 milliseconds. The value obtained from the linewidth is 64 $\pm$ 4 milliseconds. (We have corrected for magnetic field inhomogenities and unresolved J-couplings by subtracting the ^{13}C linewidth for the terminal methyl from the observed linewidth). The experimental ^{13}C T_2 value contains a contribution from the ^{14}N scalar coupling to the ^{13}C nucleus which is given by (14):

$$(1/T_2^{sca}) = (8\pi/3)J_{N-C}\, T_1(^{14}N) \qquad (14)$$

Taking $T_1(^{14}N)$ = 12.5 milliseconds from Figure 8 and J_{N-C} = 3.8 Hz (43) from the related compound iso-butylammine we arrive at a value, after subtraction of the scalar contribution, for the experimental T_2(dipolar) equal to 92 $\pm$ 6 milliseconds. Again the agreement is satisfying.

When using the three-step model to fit the R_1 data we are essentially ignoring end-effects on the rods. This is clearly an approximation in the present case with an axial ratio as small as 2 to 1. In principle, the diffusion of the monomers over the hemispheres at the end of the rods will also contribute to the relaxation. Since diffusion over a hemisphere leaves no residual anisotropy (11) one would expect that more of the interaction would be averaged

out by motions of intermediate rate. This amounts to replacing the factor 3/4 in eq.(8) with a number larger than 3/4 but smaller than 1, and adding another term to the spectral density, describing the intermediate motion. Changing the factor 3/4 does not change the goodness of the fit; it merely decreases the value of S. The reported value of S is therefore an upper limit. The addition of another Lorenzian term in $\tilde{J}^r(\omega)$ does not improve the fit either. Thus, and for reasons of simplicity, we have chosen to ignore end effects.

Turning to the individual parameters in Table 3 it is clear that the fast correlation time for ^2H is the same in the micellar and cubic phases within the uncertainty of the fit. The rate of the fast motion is consequently not changed at all when entering the cubic phase. The order parameters increase somewhat - 15% and 25% compared with the hexagonal and micellar phases, respectively. Keeping in mind that the S's reported in Table 3 are upper limits, these changes are small. To sum up, both as regards the rate of the fast, anisotropic motion and the magnitude of the anisotropy induced by the hydrophobic-hydrophilic interface the influence of the aggregate geometry is very small. The local motion is rapid and although the head-group is restricted to move more or less in the surface of the interface, it is in no way constrained to a given position. In addition to lateral diffusion it undergoes presumably complex motions, e.g torsional oscillations. A picture of a liquid-like amphiphilic aggregate emerges, well in the line with several other studies (see ref.44 and references therein). The corresponding values of τ_c^f and S for ^{14}N support the reasoning above, although they are much less well determined due to fewer experimental data points.

As regards the intermediate correlation time, τ_c^r, it is roughly one nanosecond longer than the slow correlation time for the micellar case. This small change and the smoothness of change in the R_1 values when going from the micellar to the cubic phase indicate that it is the same type of motion in both cases; it is merely somewhat slower in the cubic phase. We suggested above that the intermediate motion in the cubic phase could be attributed to the rotation of the rod around its long axis and monomer diffusion around the rod. The correlation time for the second type of motion is given by:

$$\tau_c^{diff} = R^2/4D \qquad (15)$$

where R is the radius of the rod and D the monomer diffusion coefficient, while no analytical expression exists for the rotation of a hemisphere capped cylinder.

However, Yoshizaki and Yamakawa (45) give numerical solutions for this case. Combining data from ref.45 with eq.(15) we compute a value for the radius R equal to 13.9 Å (axial ratio of 2:1) from our experimental intermediate correlation time, τ_c^r. X-ray data give 15 Å (13). As for the micellar case, when considering the approximations involved in obtaining this radius, the agreement is remarkably good. It should be noted that in the above calculation we are neglecting intermicellar interactions which presumably are present, and which are then mediated by the solvent.

It remains to explain the last part of the spectral density function in eq.(8), i.e. the part causing the frequency independent contribution $\tilde{J}^t(0)$ to R_2. First we note that this last step does not contribute to R_1 at 2 MHz for deuterium. Thus $(\omega\tau_c^t) > 1$ where τ_c^t is the correlation time for the slowest motion (assuming exponential correlation functions, see below), that is $\tau_c^t > 10^{-6}$s. Using the value from Table 3 for δ_D and eq.(12) we calculate $\tau_c^t = 6\times10^{-8}$s, a value which is short enough to contribute to R_1 at 2 MHz. We will suggest three possible reasons for this inconsistency. First, recall that in the three-step model applied (eq.(8)) 25% of the residual anisotropy left after the fast motions was averaged out by the slowest motion. If, for any reason, less than 25% is averaged by this slow process then, clearly, the correlation time must be longer. Secondly, if the slow motion takes place in more than one step then the correlation times involved will be longer. Lastly, if the slowest motion is not describable by an exponential correlation function (vide infra) but rather by a function that falls off less rapidly than a single exponent, then the slow motion may not contribute to the longitudinal relaxation (R_1) at 2 MHz for deuterium.

It is clear that from the present data set it is not possible to be very precise about the nature of the slow process. In a similar investigation of the corresponding cubic phase formed by the 1-palmitoyllysophosphatidylcholine/water system Eriksson et al.(46) record a superposition of an anisotropic and isotropic signal for ^2H, ^{14}N and ^{31}P. It is suggested that the isotropic signal is due to spherically disordered micelles (vide supra), while the anisotropic signal is due to the cylindrically disordered micelles, providing strong evidence for the suggested phase structure in ref.13. For this to be valid the rate of exchange of the monomers between micelles must be slower than the intrinsic relaxation rates. If the exchange is fast in the lysolecithin case the spectrum would not be a superposition of two spectra but it would still show anisotropic effects, other things being equal. In the present case we record no superimposed spectra; thus the monomer exchange for DOTAC is faster than for the lysolecithin.

Furthermore, for the DOTAC case the spectrum shows no anisotropic effects; thus in this case the fastest isotropic motion must occur on a time scale shorter than the inverse of the quadrupole interactions expressed in Hz while the opposite holds for lysolecithin. Taking into consideration the difference between the two systems this is clearly reasonable. The lifetime for a lysolecithin molecule in an amphiphilic aggregate is certainly longer than for DOTAC (47). As regards the slow motion Eriksson et al. suggest the following candidates: lipid exchange, end-over-end rotations of the aggregates and collective translations of whole aggregates between different positions in the lattice. To this list we would add long range plastic deformations of the crystallites. All these types of motion will be highly collective and most likely not decribable by single exponential correlation functions. Furthermore, it is conceivable that very subtle effects such as changes in the temperature, small amounts of impurities etc. may drastically change the rate of these types of motion. Indicative of this is the fact that, for α-deuterated DOTAC, ^{2}H T_1 increases by approximately 10% as the temperature is increased from 25°C to 35°C while the T_2 increases by ~100% (data not shown).(Recall that T_1 was determined by the rotational tumbling and monomer diffusion). In this temperature interval X-ray data indicate that the structure of the cubic phase does not change (48). The same temperature dependence in the relaxation was found for ^{14}N by Eriksson et al.(32). In order to achieve a fuller understanding of the slow process one would have to perform R_1 measurements below 1 MHz. Here, the technique of $T_1\rho$ off resonance would perhaps prove useful. Such experiments are underway.

Taken together we feel that the NMR data presented in ref.46 and in the present work give strong support for the structure proposed by Fontell et al. (13). In particular, the data presented in Figure 8 are not compatible with a structure consisting of closely packed spheres, since in such a case one would predict a single step in the correlation function for the slow motions. The data of ref.46 rather convincingly demonstrate the presence of two different kinds of aggregates in the lysolecithin system.

Finally, in Figure 10 we present the profile for the order parameter and the fast correlation time along the hydrocarbon chain of DOTAC for the cubic phase. These data have been obtained from ^{13}C R_1's at four field strengths (8.45 T, 4.7 T, 2.3 T and 1.4 T), ^{13}C n.O.e's at one field strength (8.45 T) and ^{2}H R_1 data from Figure 8. Compared with the micellar case the order parameters are displaced to slightly higher values, but the differences are slight. The profile for the fast correlation time is almost identical in the two cases. The uncertainty is larger for the cubic phase which, as discussed above, results from

the longer slow correlation time in the cubic phase.

We will end this section with a general remark. It should be evident from Figure 8 that one has to be careful when extracting information about surfactant or lipid systems from R_1 and R_2 at a single magnetic field strength, since by doing this one is attempting to extract the whole spectral density function from only two data points (29,49,50).

Concluding Remarks.

We feel that the main value of the present study lies in the method, i.e. multifield ^2H NMR relaxation, developed for describing dynamics in isotropic surfactant systems. The method is easily implemented on most NMR systems with an iron core magnet. Since many isotropic surfactant systems are expected to have dynamics on the nanosecond time scale the method should prove very useful for characterizing dynamics in less well characterized systems, e.g. microemulsions.

The results obtained in the present study strongly suggest that the slow motion in an ordinary micellar system is well described by an exponential correlation function whose time constant is given by the micellar rotational tumbling and monomer diffusion over the micellar surface. There is no need to invoke other motions, e.g. order-director fluctuations to interpret micellar NMR relaxation data. For the cubic phase (I_1) the data show unequivocally that, apart from the fast local motion, there are (at least) two slow processes, giving support for a recently suggested structure for this system consisting of anisometric aggregates.

ACKNOWLEDGMENTS.

We would like to thank Prof. Daniel Canet, Nancy, for the use of his 4.7 T NMR system. Thanks are due to Prof. Håkan Wennerström, Dr. Bertil Halle, Dr. Krister Fontell and Dr. Eva Hansson for valuable discussions. Merle Horne is thanked for her linguistic aid. This work was not sponsored by any military agency.

NOTES AND REFERENCES

1 Abbreviations used:
NMR: Nuclear Magnetic Resonance
n.O.e.: nuclear Overhauser effect
DOTAC: Dodecyltrimethylammonium chloride
DPPC: Dipalmitoylphosphatidylcholine
c.m.c.: critical micelle concentration
OTAB: Octyltrimethylammonium bromide

2 G. Tiddy in "Nuclear Magnetic Resonance", ed. G.A. Webb (Specialist Periodical Reports), Royal Society of Chemistry, London, 1981, 10, p.267

3 O. Söderman, B. Lindman and P. Stilbs in "Nuclear Magnetic Resonance", ed. G.A. Webb (Specialist Periodical Reports), Royal Society of Chemistry, London, 1983, 12, p.302

4 O. Söderman in "Nuclear Magnetic Resonance", ed. G.A. Webb (Specialist Periodical Reports), Royal Society of Chemistry, London, in press.

5 D. Canet, J.P. Marchal, H. Nery and B. Robin-Lherbier, J. Coll. Interface Sci., 93, 241 (1983)

6 J.P. Marchal, D. Canet, H. Nery, B. Robin-Lherbier and J.M. Cases, J. Coll. Interface Sci., 99, 349 (1984)

7 H. Walderhaug, O. Söderman and P. Stilbs, J. Phys. Chem., 88, 1655 (1984)

8 Y. Tricot, J. Kiwi, W. Niederberger and M. Gratzel, J. Phys. Chem., 85, 862 (1981)

9 B. Lindman, T. Ahlnäs, O. Söderman, H. Walderhaug, K. Rapacki and P. Stilbs, Faraday Discuss. Chem. Soc., 76, 317 (1983)

10 H. Wennerström, B. Lindman, O. Söderman, T. Drakenberg and J.B. Rosenholm, J. Am. Chem. Soc., 101, 6860 (1979)

11 B. Halle and H. Wennerström, J. Chem. Phys., 75, 1928 (1981)

12 R.R. Balmbra, J.S. Clunie and J.F. Goodman, Nature 222, 1159 (1969)

13 K. Fontell, K.K. Fox and E. Hansson, submitted.

14 A. Abragam, "The Principles of Nuclear Magnetism", Clarendon, Oxford, 1961

15 D. Dodrell, V. Glushko and A. Allerhand, J. Chem. Phys., 56, 3683 (1972)

16 J.R. Hoyland, J. Am. Chem. Soc., 90, 2227 (1968)

17 J.H. Davis and K.R. Jeffrey, Chem. Phys. Lipids, 20, 87 (1977)

18 B. Halle, personal communication.

19 J.H. Davis, K.R. Jeffrey and M. Bloom, J. Mag. Reson., 29, 191 (1978)

20 B. Halle, H. Wennerström and L. Piculell, J. Phys. Chem., 88, 2482 (1984)

21 M.F. Brown, J. Chem. Phys., 80, 2808 (1984)

22 D.J. Siminovitch, M. Rance and K.R Jeffrey, FEBS Lett., 112, 79 (1980)

23 M.T. Rothgeb and E. Oldfield, J. Biol. Chem., 256, 6004 (1981)

24 J.M. Lehn and M. Franck-Neumann, J. Chem. Phys., 43, 1421 (1965)

25 T.K. Pratum and M.P. Klein, J. Mag. Reson., 53, 473 (1983)

26 U. Henriksson, L. Ödberg, J.C. Eriksson and L. Westman, J. Phys. Chem., 81, 76 (1977)

27 E. Williams, B. Sears, A. Allerhand and E.H. Cordes, J. Am. Chem. Soc., 95, 4871 (1973)

28 M.F. Brown, A.A. Ribeiro and G.D. Williams, Proc. Natl. Acad. Sci. USA, 80, 4325 (1983)

29 P.O. Eriksson, A. Khan and G. Lindblom, J. Phys. Chem., 86, 387, (1982)

30 J. Charvolin and P. Rigny, J. Chem. Phys., 58, 3999 (1973)

31 M. Schara, F. Pusnic and M. Sentjurc, Croat. Chem. Acta, 48, 147 (1976)

32 J. Ulmius and H. Wennerström, J. Magn. Reson., 28, 309 (1977)

33 D. Canet, J. Brondeau, H. Nery and J.P. Marchal, Chem. Phys. Lett., 72, 184, (1980)

34 G. Lindblom and H. Wennerström, Biophys. Chem., 6, 167 (1977)

35 G. Lindblom, K. Larsson, L.B.A. Johansson, K. Fontell and S. Forsén, J. Am. Chem. Soc., 101, 5465 (1979)

36 B. Jönsson, personal communication.

37 C.J. Tanford, J. Phys. Chem., 76, 3020 (1972)

38 J.B. Hayter and J. Penfold, Colloid and Polymer Sci., 261, 1022 (1983)

39 T. Ahlnäs, O. Söderman, H. Walderhaug and B. Lindman in "Surfactants in Solution", eds. K. Mittal and B. Lindman, Plenum, N.Y. 1982, p. 107

40 a) G. Lipari and A. Szabo, J. Am. Chem. Soc., 104, 4546 (1982), b) ibid, p. 4559

41 H. Wennerström and J. Ulmius, J. Mag. Reson., 23, 431 (1976)

42 T. Bull and B. Lindman, Mol. Cryst. Liq. Cryst., 28, 155 (1973)

43 V. Mlynewik, Org. Magn. Reson., 17, 178 (1981)

44 B. Lindman and H. Wennerström in "Topics in Current Chemistry", 87, (1980)

45 T. Yoshikazo and H. Yamakawa, J. Chem. Phys., 72, 57 (1980)

46 P.O. Eriksson, G. Lindblom and G. Arvidson, accepted for publication in J. Phys. Chem.

47 H. Hoffmann, R. Nagel, G. Platz and W. Ulbricht, Colloid Polymer Sci., 254, 812 (1976)

48 K. Fontell, unpublished data.

49a K. Kogo and Y. Kamazawa, Biochemistry, 19, 2779 (1980)

49b Y. Kamazawa and K. Kogo, Biochem. Biophys. Res. Commun., 95, 269 (1980)

50 Y.I. Parmar, S.R. Wassall and R.J. Cushley, J. Am. Chem. Soc., 106, 2434 (1984)

FIGURE CAPTIONS.

Fig 1. Phase diagram for the DOTAC/water system. L_1 denotes isotropic (micellar) solution phase. From ref. 12.

Fig 2a-b. ^2H NMR relaxation data at two magnetic field strengths as a function of DOTAC concentration.

Fig 2c. ^{13}C spin-lattice relaxation rates for the α-carbon at three magnetic field strengths as a function of DOTAC concentration.

Fig 3. Spin-lattice and spin-spin relaxation data for ^2H ($O = R_1$, $\Delta = R_2$) and ^{14}N ($\Delta = R_1$, $\square = R_2$) for a micellar sample of DOTAC (30 wt %). The solid lines are fits of the two-step model to the data (for details, see text). The insert shows ^2H R_1 plotted versus the inverse of the square root of the magnetic field strength.

Fig 4a. The order parameter S determined from ^{13}C and ^2H relaxation data as a function of chain position in DOTAC."N-Me" denotes the methyl groups of the ammonium head group.

Fig 4b. The fast correlation time, τ_c^f, as a function of chain position for the same system as in fig 4a.

Fig 5. The reduced spectral density function for the slow motion assuming a single exponential correlation function and a correlation time of 3.9 ns. The vertical lines represent points on the curve sampled by a ^{13}C spin-lattice relaxation experiment. The height of the lines are proportional to the weight each value of $\tilde{J}(\omega)$ has in the equation for R_1 (cf. eq.(3)).

Fig 6. A ^{13}C NMR spectrum of the cubic phase I_1 at a magnetic field strength of 8.45 T. No exponential weighting of the fid was employed.

Fig 7. ^1H NMR spectra of a 30 % micellar solution (lower trace) and a cubic (I_1) phase (upper trace). The temperature was 28^oC and the magnetic field strength used was 2.35 T.

Fig 8. Spin-lattice and spin-spin relaxation data for ^{2}H (O= R_1, Δ = R_2) and ^{14}N (Δ = R_1, $\square$ = R_2) for a cubic (I_1) sample. The solid lines are fits of the three-step model to the data. Note that in order to obtain the experimental spin-spin relaxation rates, a constant amount (see Table 3) has to be added to the R_2 values in the figure. For further details, see text. The insert shows ^{2}H R_1 values plotted versus the inverse of the square root of the magnetic field strength.

Fig 9. The structure of the cubic phase I_1 as suggested by Fontell et al.(13). Hemisphere capped cylinders with an axial ratio of 2:1 are centered at position 6d (+ 1/4, 1/2, 0; 0, 1/2, + 1/4; 1/2, + 1/4, 0) and form cages around position 2a (0,0,0;1/2, 1/2, 1/2). The cylinders at 2a are omitted for clarity.

Fig 10a. The order parameter as a function of chain position in DOTAC for the cubic phase I_1. "N-Me" denotes the methyl groups of the ammonium head group.

Fig 10b. The fast correlation time as a function of chain position for the the same system as in Fig. 10a.

TABLE 1

Parameters obtained from the fits to the ^{2}H and ^{14}N relaxation data in Figure 3 (for details, see under Results and Discussion, The Micellar Phase).

	τ_c^f (ps)	S	τ_c^s (ns)
^{2}H	37±3	0.17±0.01	3.9±0.4
^{14}N	52±15	0.23±0.01	

TABLE 2

^{2}H and ^{14}N quadrupolar splittings in the hexagonal phase of DOTAC/water at 28°C.

	composition (w/w % DOTAC)	Δ (kHz)	S(+)
^{2}H	64.3	12.3±0.1	0.196±0.003
^{14}N	65.7	12.1 *	0.28

(*) Data from Ref. 29.

(+) Obtained from the relation $S=(4/3)(\Delta/X)\cdot 2$ (see text for details).

TABLE 3

Parameters obtained from data in Figure 8 (for details see under Results and Discussion, The Cubic Phase).

	τ_c^f (ps)	S	τ_c^r (ns)	δ^x (s^{-1})
^2H	35.1±1.1	0.2322±0.0027	5.21±0.08	95
^{14}N	22±13	0.32±0.01		120

(x)Constant subtracted from each experimental R_2 value.

Figure 1

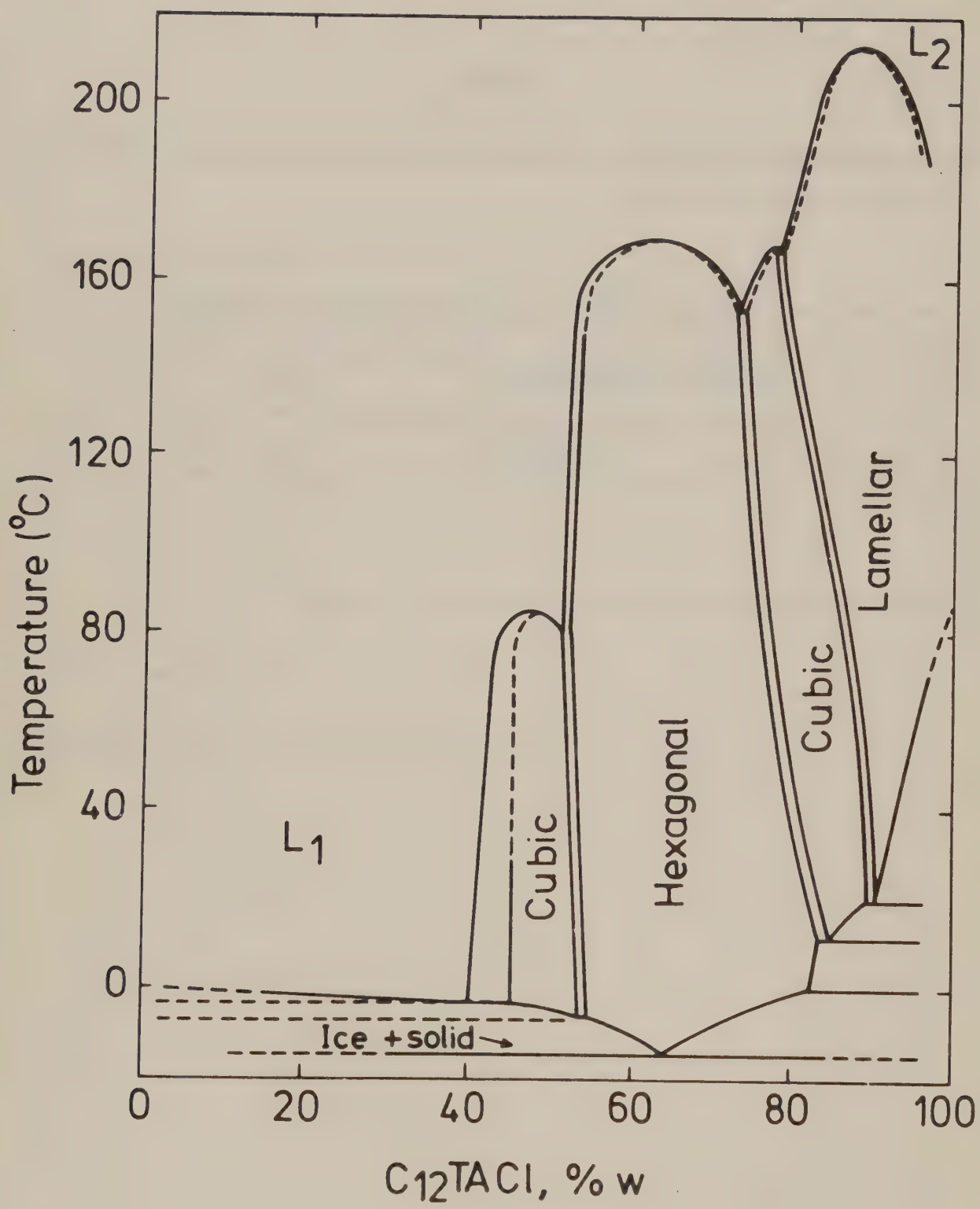
L2
200
160
120
80
40
0
Temperature (°C)
L1
Cubic
Hexagonal
Cubic
Lamellar
Ice + solid
0
20
40
60
80
100
C12TACl, % w

Figure 2

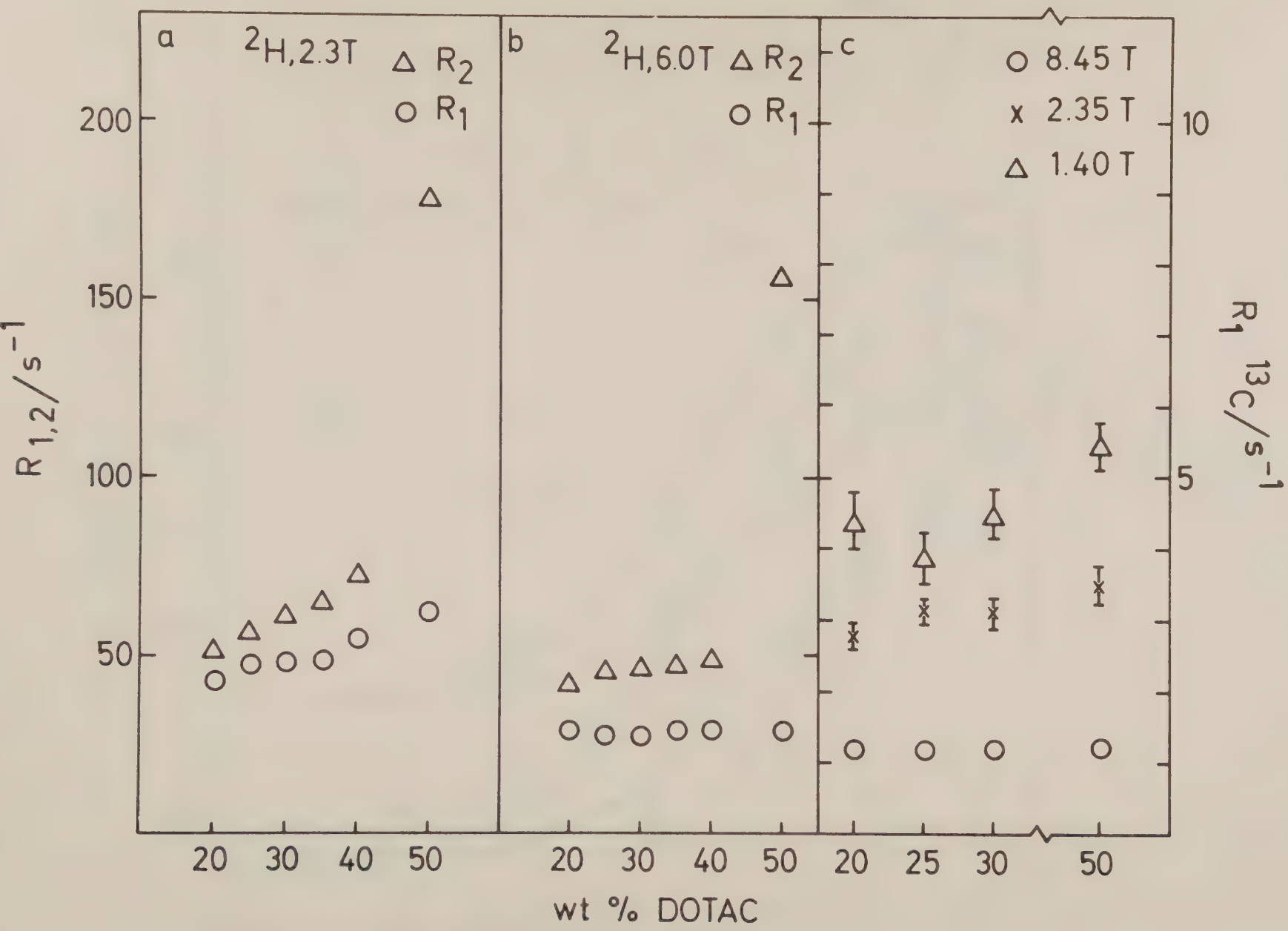
a
^{2}H, 2.3T
△ R_2
○ R_1
b
^{2}H, 6.0T
△ R_2
○ R_1
c
○ 8.45 T
x 2.35 T
△ 1.40 T
$R_{1,2}/s^{-1}$
200
150
100
50
R_1 $^{13}C/s^{-1}$
10
5
20 30 40 50
20 30 40 50
20 25 30 50
wt % DOTAC

Figure 3

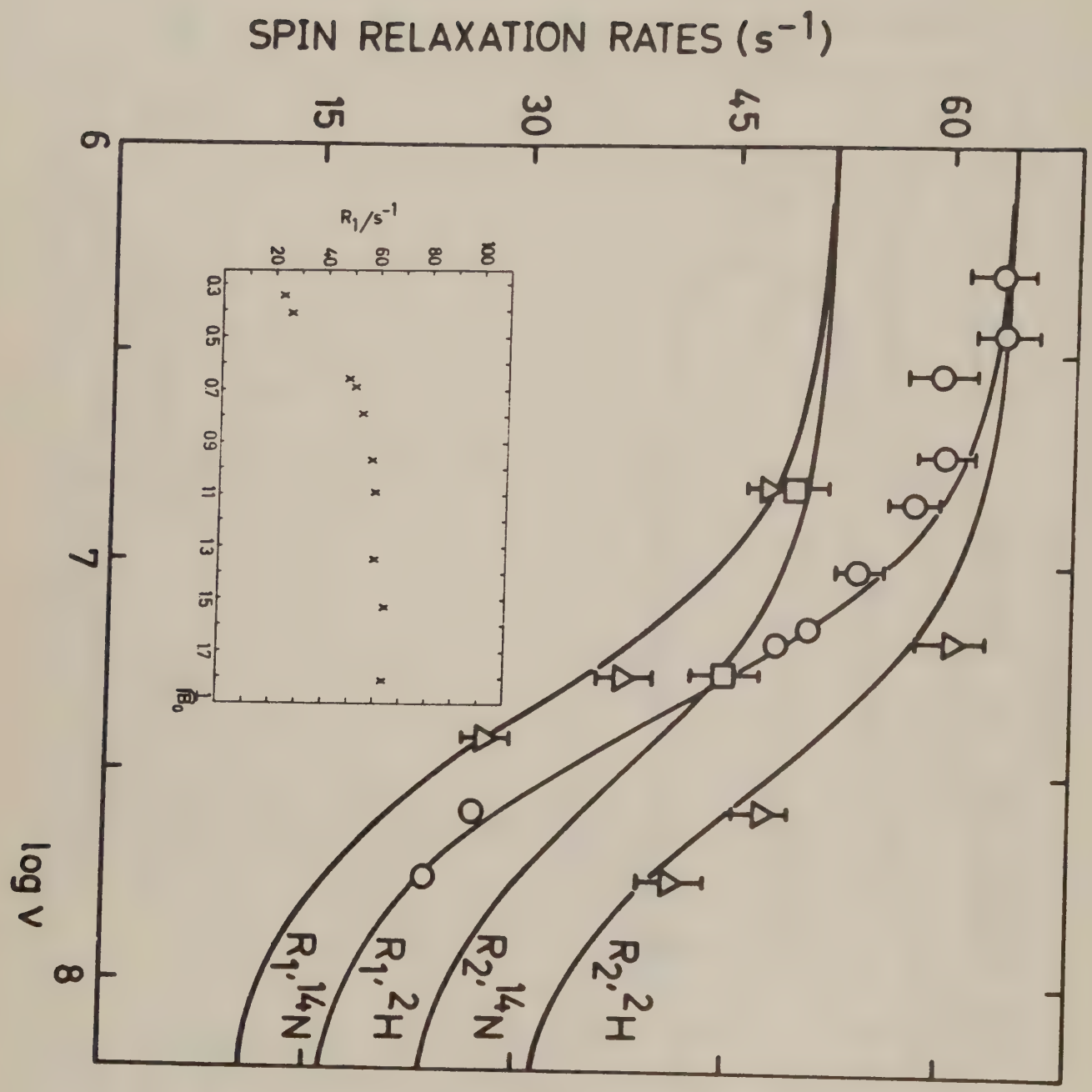
SPIN RELAXATION RATES (s^{-1})
60
45
30
15
6
7
8
log ν
$R_2, {}^2H$
$R_2, {}^{14}N$
$R_1, {}^2H$
$R_1, {}^{14}N$
R_1/s^{-1}
100
80
60
40
20
0.3
0.5
0.7
0.9
1.1
1.3
1.5
1.7
$\frac{1}{\sqrt{B_0}}$

Figure 4

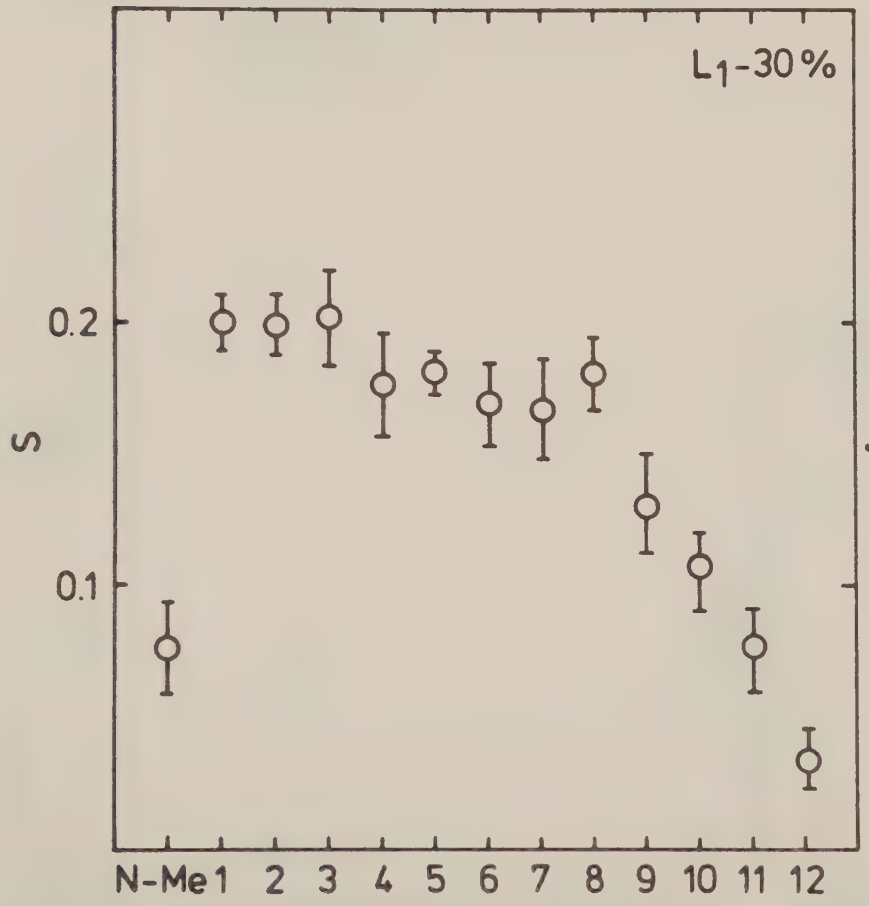
L1-30%
S
0.2
0.1
N-Me 1 2 3 4 5 6 7 8 9 10 11 12

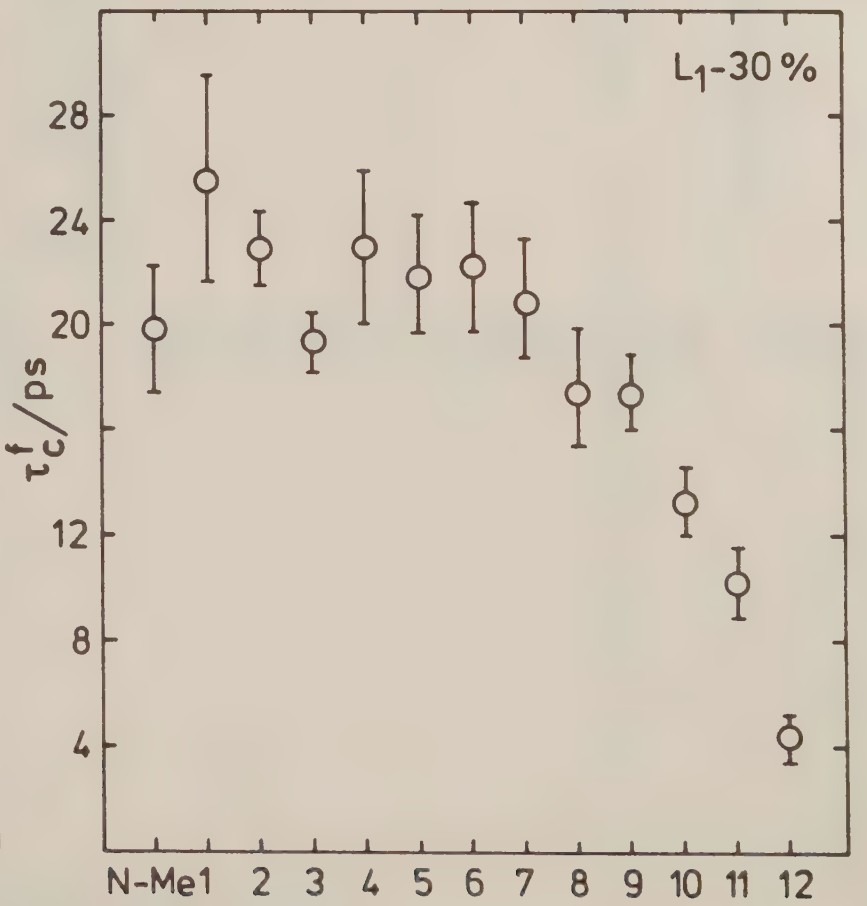
L1-30%
τc f/ps
28
24
20
12
8
4
N-Me 1 2 3 4 5 6 7 8 9 10 11 12

Figure 5

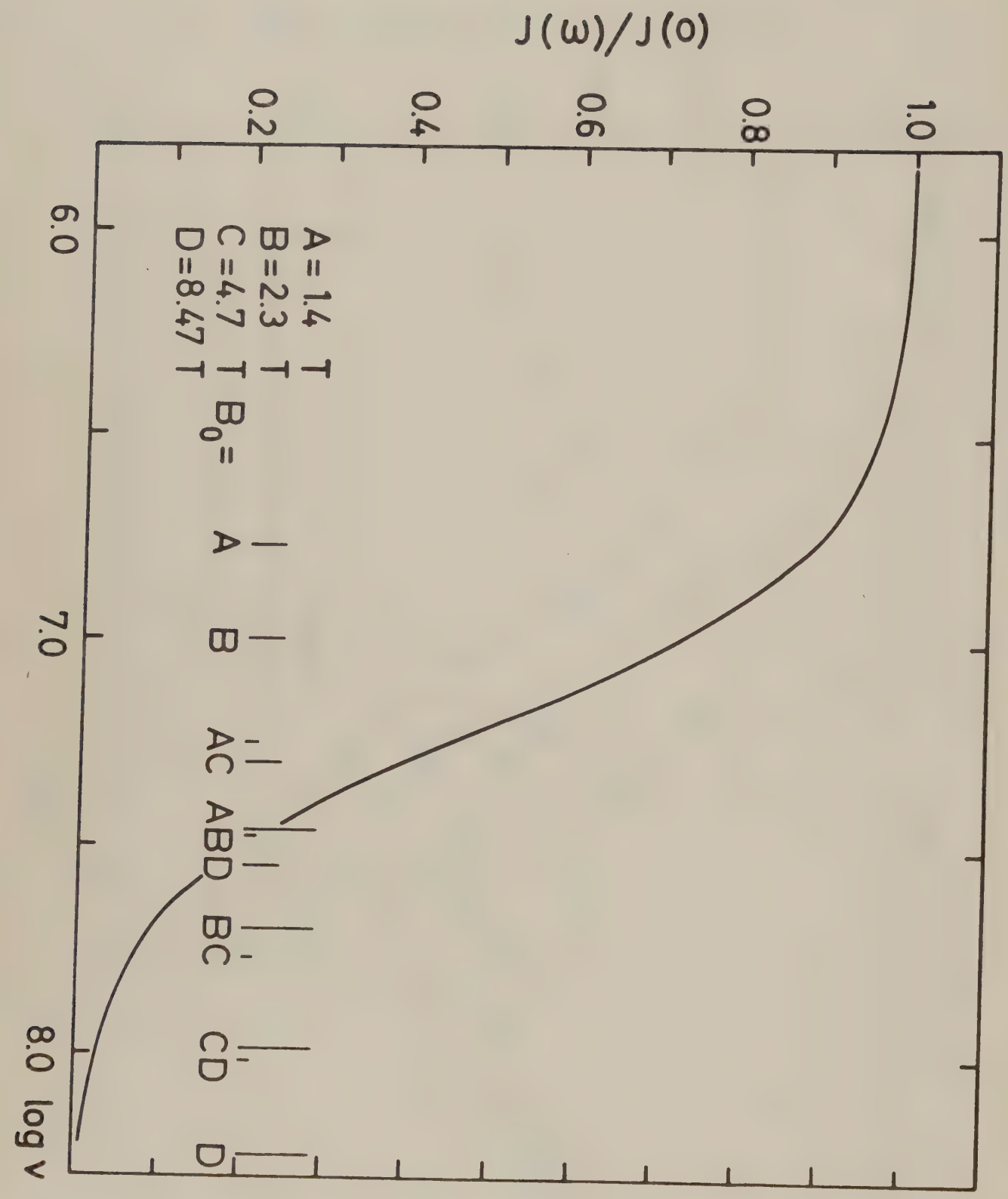
J(ω)/J(0)
1.0
0.8
0.6
0.4
0.2
6.0
7.0
8.0
log ν
A = 1.4 T
B = 2.3 T
C = 4.7 T
D = 8.47 T
B0 =
A
B
AC
ABD
BC
CD
D

Figure 6

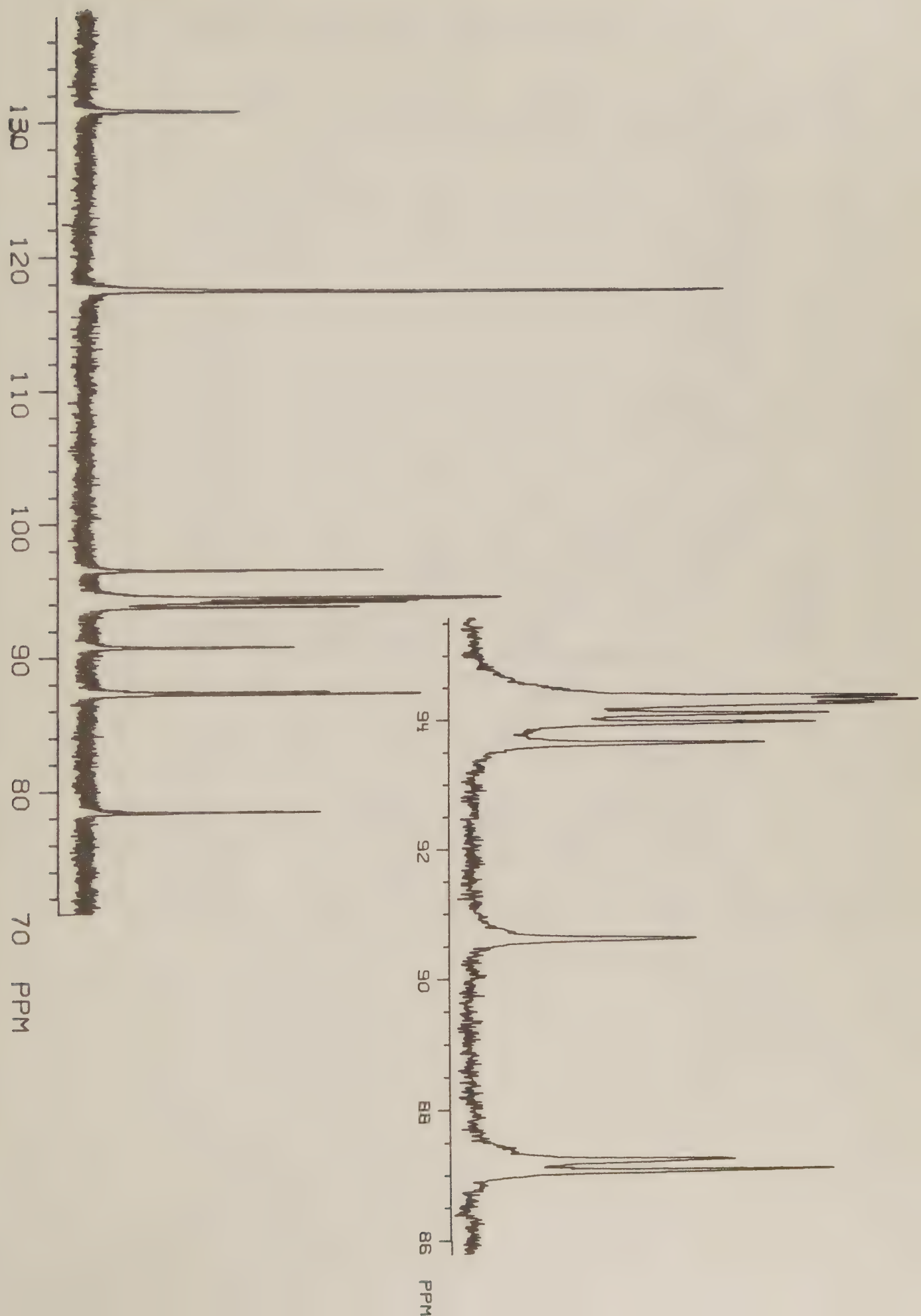

Figure 7

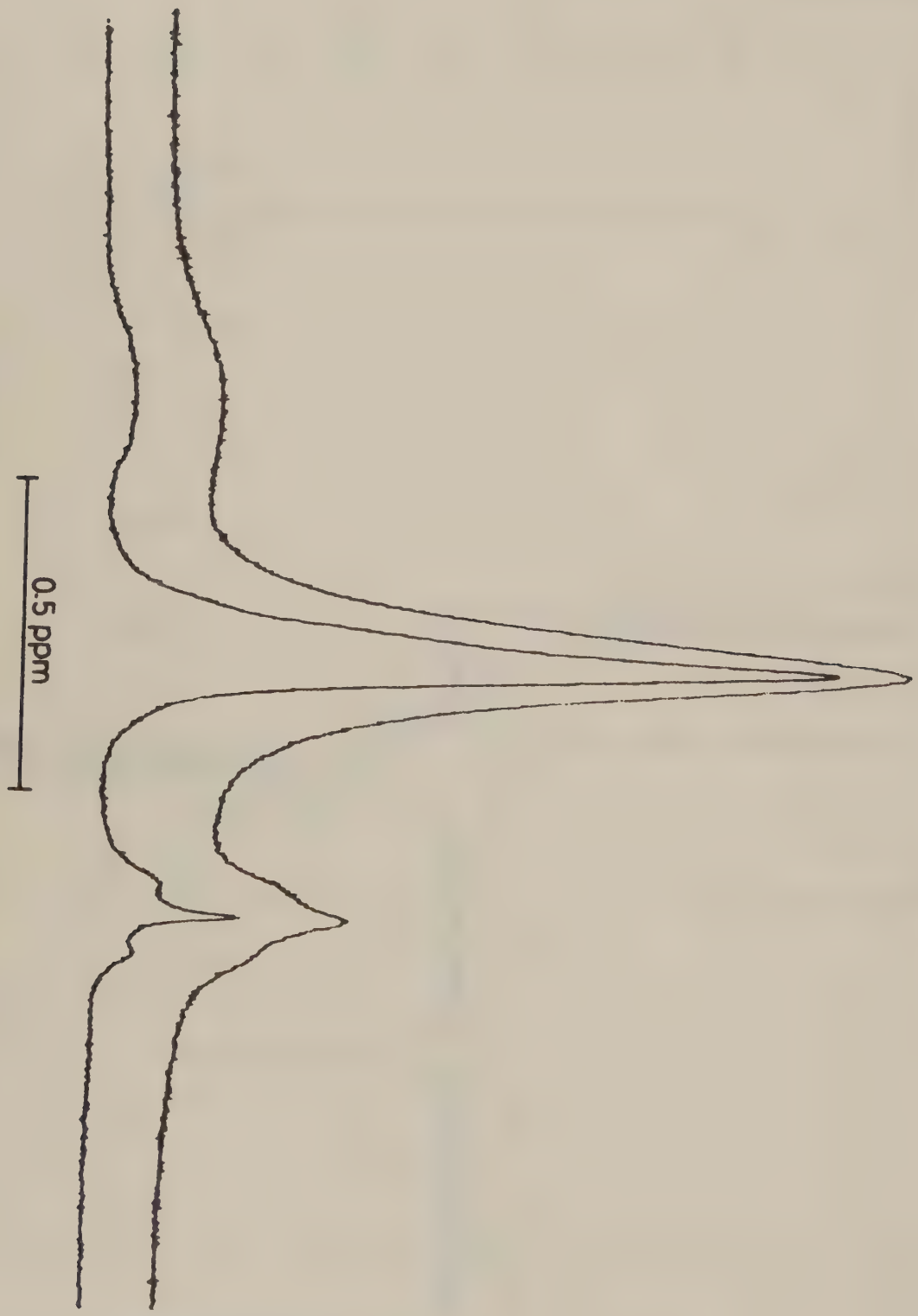

Figure 8

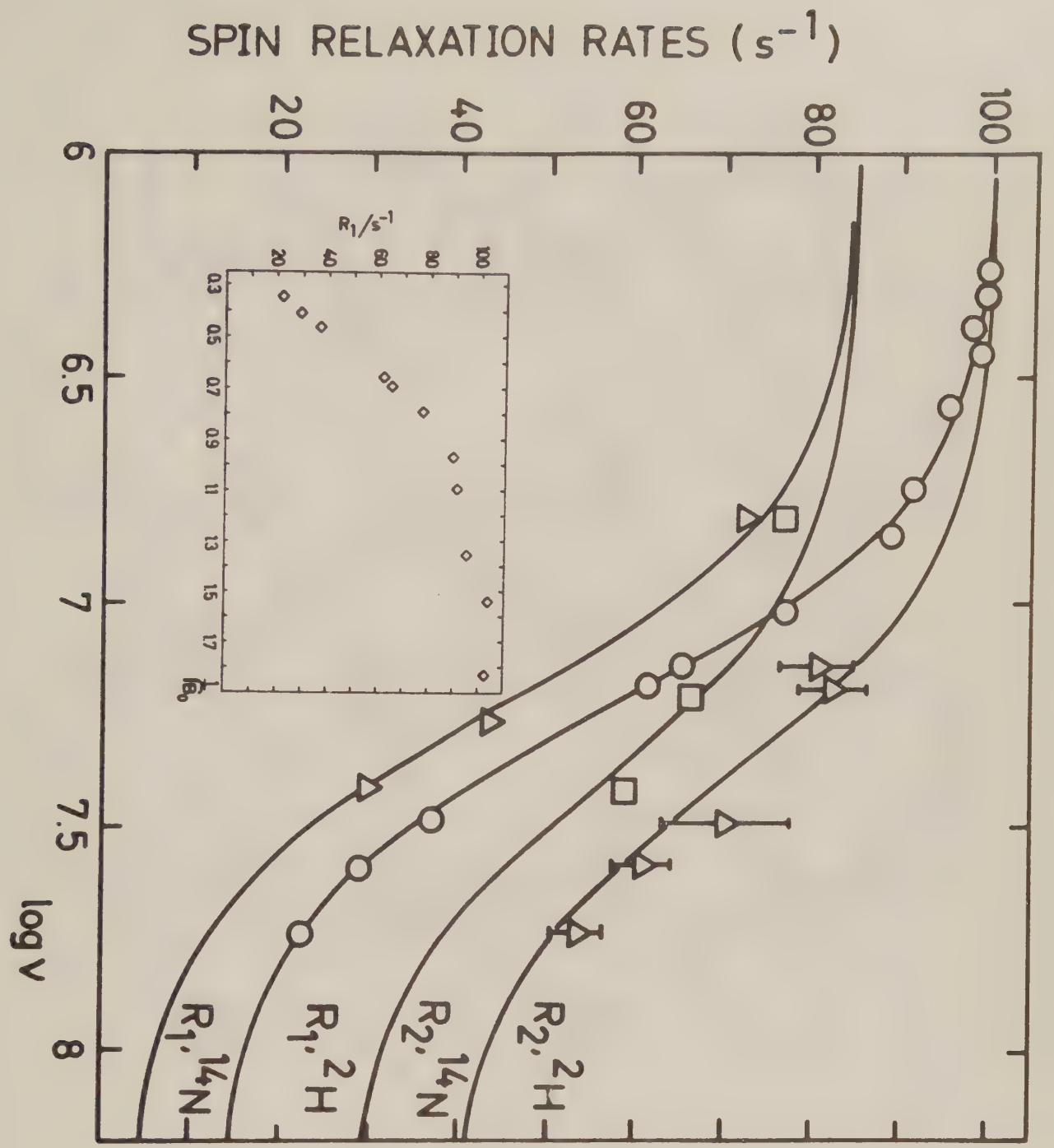
SPIN RELAXATION RATES (s^{-1})
100
80
60
40
20
6
6.5
7
7.5
8
log ν
R_1, ^{14}N
R_1, ^2H
R_2, ^{14}N
R_2, ^2H
R_1/s^{-1}
20
40
60
80
100
0.3
0.5
0.7
0.9
1.1
1.3
1.5
1.7
$\frac{1}{\sqrt{B_0}}$

Figure 9

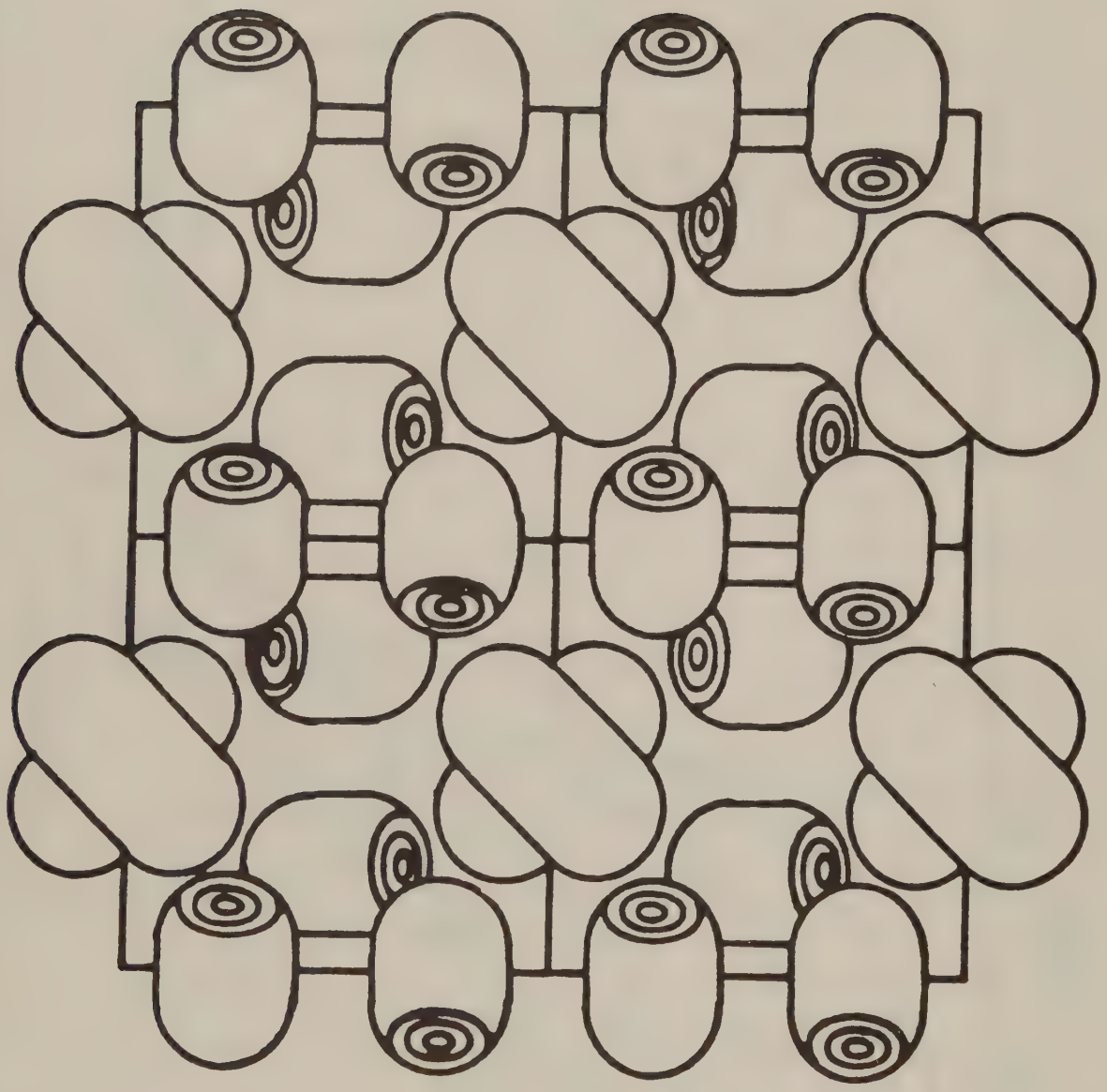

Figure 10

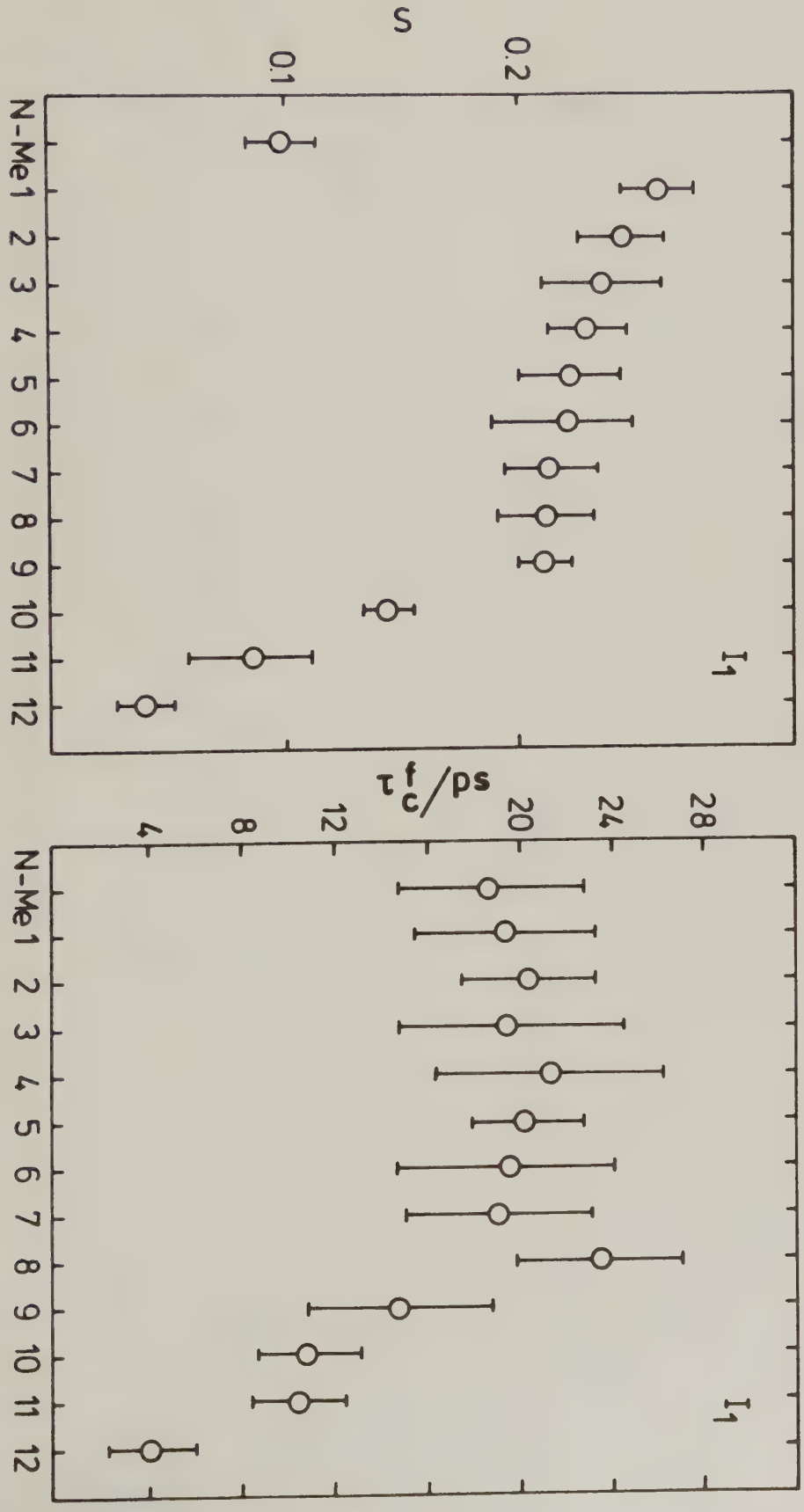
S
0.2
0.1
I_1
N-Me 1 2 3 4 5 6 7 8 9 10 11 12
τ_c^f/ps
28
24
20
12
8
4
I_1
N-Me 1 2 3 4 5 6 7 8 9 10 11 12

IV

A ^{13}C and ^{2}H Nuclear Magnetic Resonance Study of Hydrocarbon Chain Order in Isotropic and Anisotropic Phases Formed in the Sodium p-Octylbenzenesulphonate-Short-Chain Alcohol-Water System.

Olle Söderman,* Harald Walderhaug and Björn Lindman, Division of Physical Chemistry 1, Lund University, Chemical Center, P.O.B. 740, S-220 07 Lund, Sweden

*To whom correspondence should be addressed.

Abstract

The order of the hydrocarbon chain and the phenyl ring of sodium p-octylbenzenesulphonate (SOBS) in some anisotropic phases consisting of SOBS, pentan-1-ol and water is investigated with deuterium NMR and compared with the order in some two-, three- and four-component isotropic solutions consisting of SOBS, water, butan-1-ol and toluene, as extracted from ^{13}C relaxation measurements. These latter measurements also give information on the dynamic state of the SOBS molecules in these "microemulsion" systems. It is found that a short-chain alcohol has the effect of compressing the bilayers of the lamellar phase below the maximum thickness. The odd-even effect clearly seen in the order parameter profile for the lamellar phase is interpreted as a result of the C_2-axis of the phenyl ring not being parallel to the symmetry axis of the hydrocarbon chain. The order parameter profile for a "rectangular" liquid crystalline phase together with X-ray findings are claimed to be a result of the rods constituting the mesophase having a biaxial cross section. From the present relaxation results and earlier NMR self-diffusion measurements the following structural and dynamic picture of microemulsions of the present type of systems emerges: The hydrophobic-hydrophilic interface imposes a local anisotropy which is similar in magnitude to the one in the lamellar phase but has a very short life-time. Ill-defined and highly flexible aggregates with rather large radii of curvature are present.

Introduction

There has recently been an increased interest in surfactant systems that at the same time contain water and oil in a single isotropic phase[1-3]. Such systems are usually termed "microemulsions", and interest has been focussed on four-component systems composed of surfactant, short chain alcohol, such as butan-1-ol or pentan-1-ol, oil and water[3,4]. For a fundamental understanding of these systems it is important to characterize the state (packing, dynamics etc.) of the hydrocarbon chains. Here, nuclear magnetic resonance (NMR) has shown to be a very fruitful approach. Hydrocarbon chain order is conveniently determined in anisotropic surfactant systems by means of the effect partially averaged interactions have on the NMR spectrum, inter alia the quadrupole splittings for deuterated chains[5]. For isotropic systems, such as microemulsions, these static interactions are completely averaged out, and one has to resort to indirect ways of determining the molecular ordering. Fortunately, the NMR relaxation for nuclei in hydrocarbon chains in isotropic surfactant systems depends on both the molecular order and the rates of motions for the chains[6,7]. Thus, with a relevant relaxation model one can obtain information about molecular order in isotropic phases. This way of determining molecular order has one added advantage in that information is also obtained about the dynamic state of the hydrocarbon chains.

We have previously reported on such an analysis for some microemulsions formed by the sodium-p-octylbenzenesulphonate (SOBS)-butan-1-ol-toluene-water system[4b] as well as presented some initial ^{13}C relaxation data. In this context it is very interesting to compare results

for microemulsions with results found for anisotropic phases formed by the same system. Such a comparison makes it possible to assess whether the local organization in the microemulsions differs from that of other phases. Furthermore, it may be possible to make statements about the structure of microemulsions. This follows since the molecular ordering depends on the geometry of the aggregates making up the phases. Therefore, we have performed a deuterium NMR study of two anisotropic phases formed by the SOBS-pentan-1-ol-water system. The results of such a study have an inherent interest especially concerning the possibility of assessing the influence of the aromatic head group on the hydrocarbon chain order. Pentan-1-ol was chosen as third component since the phase diagram (see fig 1) for the three-component system with pentan-1-ol has recently been published[8]. Special interest is focussed on the orientation of the phenyl ring. Some isotropic phases in the SOBS-water, SOBS-butan-1-ol-water and SOBS-butan-1-ol-water-toluene systems have also been investigated with ^{13}C NMR relaxation measurements.

Experimental Section

Two differently deuterated SOBS-samples were used. The first had the octyl chain deuterated while the second had the phenyl ring deuterated. Both were a kind gift from Prof. Jacques Rouvière, U.S.T.L., Montpellier, France. P.A. grade butan-1-ol and pentan-1-ol were obtained from B.D.H. and were used without further purification. $^{2}H_2O$, 99% isotopic enrichment, was from Norsk Hydro.

The samples were weighed into glass ampoules that were flame-sealed. They were left for at least 14 days at 25°C to ensure equilibrium. All experiments, unless stated otherwise, were performed at 27 ± 1°C. Deuterium NMR measurements were performed at 6 Tesla on a homebuilt spectrometer. For the quadrupolar splittings, single pulses (pulsewidth 10 μs) were used. Although the single pulse technique causes distortions of the NMR bandshape, it is possible to accurately determine the quadrupolar splittings.

The ^2H relaxation measurements were performed at 6 and 2.1 Tesla. The spin-lattice relaxation times (T_1) were measured with the inversion recovery technique and the spin-spin relaxation times (T_2) with the Carr-Purcell-Meiboom-Gill technique or deduced from the line widths In all calculations we have set the quadrupolar coupling constants (vide infra) to 167 kHz for a C^2H_2-group[9] and 181 kHz for the deuterons in the phenyl ring[10]. The assignments of the quadrupolar spectra have been made assuming that the order decreases monotonically from the polar head towards the terminal methyl group. ^{13}C T_1 and nuclear Overhauser enhancements were measured as described in ref. 6.

Review of Theory

For a non-oriented (powder) sample which applies to the present investigation, the deuterium quadrupolar splitting is given by[5]:

$$\Delta = \frac{3}{4} \cdot \chi \cdot |S| \qquad (1)$$

where χ is the quadrupolar coupling constant and S is the order parameter given by

$$S \equiv \frac{1}{2} \cdot \langle 3\cos^2\theta_{MD} - 1 \rangle \tag{2}$$

Here, θ_{MD} is the angle between the symmetry axis of the electric field gradient and the director, i.e. the local symmetry axis. The average in eq. 2 is taken over motions that are fast compared with the quadrupolar interaction. The definition implied in eq. 2 assumes that the asymmetry parameter is zero, which is the case for a C^2H_2 group[11,12] and for benzene[10]. If there are motions present that are isotropic on a time that is shorter than the inverse of the quadrupolar interaction, then S = 0 and, according to eq. 1, there are no static effects in the deuterium spectra. This is the case for inter alia a micellar solution.

The interpretation of NMR relaxation data from amphiphilic systems is complicated. There exist in the literature several relaxation models that consider this complication[13,14,15]. In the present work we will use the so called "two-step model" developed by H. Wennerström et al.[16,17]. This model has the advantage of providing data on molecular properties in isotropic systems that can be directly compared with the properties in anisotropic systems.

The relevant relaxation equations for isotropic systems are given below. For deuterium we have[18]:

$$(T_1)^{-1} = (3\pi^2/40)\cdot\chi^2\cdot(2\tilde{J}(\omega_D) + 8\tilde{J}(2\omega_D)) \tag{3}$$

$$(T_2)^{-1} = (3\pi^2/40)\cdot\chi^2\cdot(3\tilde{J}(0) + 5\tilde{J}(\omega_D) + 2\tilde{J}(2\omega_D)) \tag{4}$$

while for carbon "i" along the hydrocarbon chain the ^{13}C spin-lattice relaxation rate and nuclear Overhauser enhancement are given by[19]:

$$(T_{1i})^{-1} = (N_i/20)\cdot[\frac{\mu_o\cdot\gamma_H\cdot\gamma_C\cdot\hbar}{4\pi\cdot r^3_{C-H}}]^2 \cdot (\tilde{J}(\omega_H-\omega_C) + 3\tilde{J}(\omega_C) + 6\tilde{J}(\omega_H+\omega_C)) \quad (5)$$

$$\eta_i = (1/20)\cdot\gamma^3_H\cdot\gamma_C\cdot [\frac{\mu_o\cdot\hbar}{4\pi\cdot r^3_{C-H}}]^2\cdot(N_i T_{1i})\cdot(6\tilde{J}(\omega_H+\omega_C) - \tilde{J}(\omega_H-\omega_C)) \quad (6)$$

Here, μ_o is the permeability of vacuum, γ_H and γ_C represent the magnetogyric ratios of proton and carbon and r_{C-H} denotes the C-H bond length. The $\tilde{J}(\omega)$'s are the various reduced spectral densities, ω_D, ω_C and ω_H are the Larmor frequencies of deuterium, carbon and proton at the actual magnetic field and $\hbar$ is the reduced Planck's constant. N_i is the number of protons directly bonded to carbon "i".

The key point in the two-step model is the expression for the various reduced spectral densities:

$$\tilde{J}(\omega) = (1-S^2)2\tau^f_c + S^2\cdot[\frac{2\tau^s_c}{1 + (\omega\tau^s_c)^2}] \quad (7)$$

Here, τ^f_c is the correlation time for the (fast) local motion, assumed to be sufficiently fast to fall within the extreme narrowing range (i.e. $\omega\tau^f_c \ll 1$), and τ^s_c is the correlation time for the slow motion that averages the local anisotropy to zero. Finally, S is defined analogously to eq. 2, i.e. $S \equiv 1/2\cdot\langle 3\cos^2\theta_{MD} - 1\rangle$. The quantity within the brackets is averaged over a time that is long compared to τ^f_c but short compared to τ^s_c. For deuterium, θ_{MD} is the angle between the symmetry axis of the electric field gradient at the deuterium nucleus and the local director, while for carbon it is the angle between the C-H bond vector and the local director. If the symmetry axis of the electric field gradient is along the C-^{2}H bond then the two

angles are identical and one can directly compare order parameters evaluated from ^{13}C relaxation experiments with those from ^{2}H NMR (quadrupole splitting or relaxation) experiments.

Results and Discussion

Order Parameter Profiles for the Hydrocarbon Chains in the Lamellar Phase.

Presented in fig 2 a-d are the order parameter profiles for the hydrocarbon chains for four samples in the lamellar phase (see fig 1). In all cases the order parameter decreases rapidly when going from the polar head towards the terminal methyl group. In many surfactant-water and surfactant-alcohol-water lamellar systems one observes an order parameter plateau in that the order parameters[12,20] are essentially constant for all carbons except for the two or three closest to the methyl group.

One crucial parameter determining the molecular conformations and thus the order along the chain is the cross sectional area available for the chains. Simple geometrical considerations show that the larger this area the more disordered is the chain, the largest effect being at the nonpolar end. The existence of a plateau thus indicates that the chains are close to a minimal cross sectional area situation or, equivalently, that the bilayer has maximum thickness[12]. In the present case the rapidly changing order along the chain indicates that the SOBS molecules are compressed. The two main factors determining the area per polar head group are the tendency to decrease the hydrocarbon-water contact striving to minimize the area, and the electrostatic repulsion

between the charged head groups which tends to maximize the area. The electrostatic effect will decrease in importance as the content of alcohol increases, since the alcohol molecules will shield the electrostatic interactions between the charged head groups and decrease the charge density. In fact, for a molar ratio of alcohol to surfactant in excess of one to one, the electrostatic effects start to become negligible[21] and the bilayer thickness is then simply determined by geometrical factors, i.e. the difference in length between the surfactant and the alcohol molecules. Since the pentan-1-ol molecule is shorter than the SOBS molecule it follows that the SOBS chains should be compressed with a high degree of disorder. When the ratio of pentan-1-ol to SOBS decreases the order parameter profile is moved towards higher S-values without changing shape (see fig 2) except for the lowest alcohol-surfactant ratio, where electrostatic effects presumably are important.

These observations are supported by X-ray measurements. The bilayer thickness for a lamellar sample with the same composition as in fig 2c is 19.3 Å. As the ratio of pentanol to SOBS increases, the bilayer thickness decreases; at the composition given in fig 2a it is 17.5 Å[22]. This value can be compared with the result for a decan-1-ol-SOBS-water sample with a molar ratio of alcohol to soap of roughly 2, where the thickness is 27 Å[23]. Given in fig 2f is the order parameter profile for this latter sample. As is evident the order parameters, in particular for the first five carbons, are displaced to higher values and although the shape of the profile is not the typical plateau shape, it certainly resembles this shape more than do the profiles in fig 2a-d. Thus, for these high alcohol contents it is the length of the alcohol molecule that determines the bilayer thickness which in turn determines the order parameters.

Finally, we note that there is an odd-even effect in the order parameter profiles shown in fig 2. Such a behavior has been predicted for

thermotropic liquid crystals composed of molecules having a rigid section[24]. This effect has also been observed in a binary surfactant-water mixture by Davis and Jeffrey[12]. These authors suggest that the effect is caused by the first C-C bond having an average orientation different from that of the bilayer normal. Every second segment in the chain will then get an increased alignment parallel to the bilayer normal while, for the others, this alignment is reduced when the chain is in an all-trans configuration, thus causing the observed effect. For SOBS the C_2 axis of the substituted phenyl ring will not be parallel to the symmetry axis of the hydrocarbon chain in its all-trans configuration, suggesting that the mechanism proposed by Davis and Jeffrey is applicable also in the present case.

Hydrocarbon Chains in the "Rectangular Phase".

Presented in fig 2 e is the order parameter profile for one sample in the phase marked R in fig 1. In reporting these order parameters we have multiplied the observed S by a factor of 2 (vide infra) in order to obtain values that can be directly compared with the lamellar ones[25]. In ref 8 it is suggested that the area marked "R" in the phase diagram is not a hexagonal phase which is normally encountered in surfactant systems. Instead, the X-ray data were discussed in terms of a centered rectangular lattice. As can be inferred from fig 2 e, the order parameter profile for this phase is very similar to the ones for the lamellar phase although the absolute values of the order parameters are displaced to higher values. This is contrary to what is observed for the alkali alkanoate -

alcohol-water systems[20] where the shape of the order parameter profile differs between the hexagonal and the lamellar phases and the values are lower for the hexagonal phase. To account for this observation we propose that the rods constituting the mesophase have a biaxial cross section. Thus, the local molecular packing in the phase resembles the packing in the lamellar phase, explaining the similarity in order parameter profiles between the phases. One should note that the deuterium lineshape shows that, within experimental error, the asymmetry parameter is zero. Thus, on a time that is long compared to the time scale of the fast local motion but short compared to the inverse of the quadrupolar splitting, the rods are uniaxial. One possible mechanism causing this effect is a rotation of either part of or the complete rods making up the mesophase around their long axis. It is the effect of this additional motion that justifies the above mentioned multiplication of the order parameters with a factor of 2 for comparison with the lamellar case.

A similar situation has been found for the hexagonal phases of 1-palmitoyl-2-oleoylphosphatidylcholine-sodium cholate-water system[26] and for the sodium decyl sulphate-decanol-water system[27]. In the latter system the position of the rectangular phase in the phase diagram is roughly the same as in the present system, i.e. close to the lamellar phase.

Hydrocarbon Chain Order in Isotropic Solutions.

In fig 3 a-c we present order parameter profiles for three isotropic solution samples as evaluated from ^{13}C relaxation data. The samples are one micellar solution at a slightly elevated temperature ($42^{o}C$), one three-component SOBS-butan-1-ol-water system and, finally, one four-component system SOBS-butanol-water-toluene (ref 4b). The compositions of the samples are given in Table 1. As can be seen in fig 3 the order parameter profiles are not very different for the isotropic phases when compared with the anisotropic phases, perhaps with the exception of the micellar phase. For the two-component system this finding presumably reflects the absence of pentanol and the packing restrictions imposed by the spherical shape of the micelle. For the two microemulsions presented in fig 3 b-c, the similarity between the curves implies that the local environment for the hydrocarbon chains is not drastically changed as toluene is added to the SOBS-butan-1-ol-water system. Furthermore, the resemblance between the microemulsions and the lamellar samples implies that the local packing of hydrocarbon chains is similar in these two cases. Thus, the hydrophobic-hydrophilic interfaces cannot have very small radii of curvature. On the other hand, the narrow ^{13}C NMR absorption lines imply that the isotropic motion that averages the residual anisotropy to zero must be rather fast. Thus, within the framework of the two-step model the following picture of microemulsions in the present system emerges: The hydrophobic-hydrophilic interface imposes a local anisotropy on the surfactant molecules which is similar to the one that is observed in the lamellar phase. This anisotropy is short-lived, i.e. the interface changes shape rather rapidly.

A picture of ill-defined aggregates with low energy barriers for structural deformations emerges, in agreement with recent self-diffusion studies of microemulsions[4, 28, 29].

The Order Parameter of the Phenyl Ring in Anisotropic Phases.

As can be inferred from Table 2 the order parameters for the phenyl ring in the lamellar and rectangular phases are very low. There are two possible explanations for this observation. First, the phenyl ring may be moving almost isotropically. Secondly, it may be oriented in such a way that θ_{MD} in eq. 2 is close to the "magic angle", 54.74^{o}, for which S = 0. There are two observations that are in favour of the second of these possibilities. First, the general observation that there is a local order in amphiphilic systems and, secondly, the fact that the order parameter for the methylene adjacent to the phenyl ring is rather large. If the phenyl ring was moving about almost isotropically this carbon would be much less ordered. For a case where the orientation of the phenyl ring is as described above, a very small change of the angle θ_{MD} would cause a large change in S since the function $3\cos^2\theta_{MD} - 1$ varies rapidly around the magic angle. Thus, it is not surprising that the order parameter for the rectangular phase is about a factor of 4 and not, as expected, a factor of 2 smaller than in the lamellar phase. As regards the absolute values of the order parameters in the lamellar phase, they follow the same trend as for the hydrocarbon chains.

^{13}C and ^{2}H Relaxation in the Phenyl Ring.

Presented in Table 3 are ^{13}C T_1's and η's and ^{2}H T_1's and T_2's for the micellar and three-component SOBS-pentanol-water systems. Looking first at the micellar case, it is clear that, within the experimental accuracy, there is no frquency dependence for the ^{13}C T_1 and that $T_1=T_2$ for ^{2}H in the deuterated phenyl ring. This result implies a very low order parameter (eq. 7), a result in agreement with what was found for the anisotropic phases. Also given in Table 3 are the correlation times computed by letting S=0 in eq. 7. Due to the length of duration of a ^{13}C T_1 experiment it has not been possible to measure ^{13}C relaxation at 27°C for the micellar case. This is a result of the fact that the Krafft point is higher than 27°C, causing the surfactant to eventually precipitate at this temperature. The higher experimental temperature is the main cause of the shorter correlation times from the micellar ^{13}C data.

When pentanol is added to the micellar SOBS-water system a somewhat unexpected relaxation behaviour is observed. The ^{13}C T_1's do now in fact depend on the frequency and the ^{13}C n.O.e. is reduced from its maximum value, while for deuterium there is no difference in T_1 at 2.1 T and 6 T and $T_1=T_2$ at 6 T within the experimental accuracy. From the ^{13}C data alone it is possible to predict the outcome of a deuterium relaxation experiment. Given in Table 4 are the parameters τ_c^s,τ_c^f and S together with predicted deuterium T_1 and T_2 for the phenyl ring deuterons of sample 7. Since the α-carbon in the hydrocarbon chain has the largest dependence in the ^{13}C T_1, and thus shows the largest dependence on τ_c^s, this parameter was deduced from ^{13}C data for that carbon. By comparing Table 3 and Table 4 it is clear that the difference between experimental and predicted deuterium relaxation times is larger than what can be explained as experimental uncertainty.

The origin of this "descrepancy" is not fully understood at present. One should note that predicted ^{2}H results are obtained using an exponential correlation function for the slow motion (see eq. 7). While this is probably true for spherical micelles[30] it may not be the case for microemulsions. Thus, one could imagine correlation functions that would produce the obtained result, since our ^{13}C measurements at 8.5 T sample higher frequencies on the spectral density curve than does our deuterium measurements. It is, however, not possible from our limited data set to evaluate the form of the spectral density in detail and thus to be more specific on this point. Another explanation is as follows. The two order parameters,S, that enter into eq. 7 are only equivalent as long as the symmetry axis of the electric field gradient for deuterium exactly corresponds to the C-H bond vector. It is clear, from symmetry arguments, that this is the case for pure benzene. However, for a substituted phenyl ring this may not longer be true. Since the function $S^2=(1/4)(3\cos^2\theta_{MD}-1)^2$ varies rapidly around the magic angle, a difference by only a few degrees between the electric field gradient symmetry axis and the C-H bond vector will cause a marked difference in the relaxation behaviour between ^{13}C and ^{2}H. We are presently investigating this possibility by means of quantum mechanical calculations.

Finally, the correlation times for the deuterated phenyl ring are shortened as pentanol is added to the pure SOBS-water system. Thus, the decreased interaction between the charged head groups, induced by the alcohol, manifests itself in an increased mobility for the phenyl ring.

Acknowledgements.

We would like to thank Dr. Ulf Henriksson for performing the deuterium relaxation measurements at 2.1 T and Dr. Krister Fontell for performing the X-ray measurement on the SOBS-decan-1-ol-water system. Sincere thanks also go to Dr. Peter Stilbs who wrote the computer programs used in this work and to Dr. Håkan Wennerström for enlightening discussions. This work was supported by the Swedish Natural Sciences Research Council and the Swedish Board of Technical Development.

References

1. "Microemulsions", ed. L.M. Prince (Academic Press, New York, 1977).

2. "Microemulsions", ed. I. Robb (Plenum Press, New York, 1982).

3. "Surfactants in Solution", vol.3, eds. K.L. Mittal and B. Lindman (Plenum Press, New York, 1982).

4a. B. Lindman and H. Wennerström in "Solution Behaviour of Surfactants", vol.1, p.3, eds. K.L. Mittal and E.J. Fendler (Plenum Press, New York, 1982).

4b. B. Lindman, T. Ahlnäs, O. Söderman, H. Walderhaug, K. Rapacki and P. Stilbs, Faraday Discuss. Chem. Soc., 1983, 76.

5. J. H. Davis, Biochim. Biophys. Acta, 1983, 737, 117-171.

6. H. Walderhaug, O. Söderman and P. Stilbs, J. Phys. Chem.,1984, 88, 1655.

7. M.F. Brown, J. Chem. Phys.,1982, 77, 1576.

8. F.C. Larchè, J. Marginau, J.L. Dussossoy and J. Rouvière, J. Colloid Interface Sci., 1983, 94, 564.

9. L.J. Burnett and B.H. Muller, J. Chem. Phys.,1971, 55, 5829.

10. R.G. Barnes and J.W. Bloom, J. Chem. Phys., 1972, 57, 3082.

11. J.R. Hoyland, J. Am. Chem. Soc., 1968, 90, 2227.

12. J.H. Davis and K.R. Jeffrey, Chem. Phys. Lipids, 1977, 20, 87-104.

13. R.E. London and J. Avitabile, J. Am. Chem. Soc., 1977, 99, 7765.

14. D. Canet, J. Brondeau, H. Nery and J.P. Marchal, Chem. Phys. Lett., 1980, 72, 184.

15. Y.K. Levine, N.J.M. Birdsall, A.G. Lee, J.C. Metcalfe, P. Partington and G.C.K. Roberts, J. Chem. Phys., 1974, 60, 2890.

References (continued)

16. H. Wennerström, B. Lindman, O. Söderman, T. Drakenberg and J.B. Rosenholm, J. Am. Chem. Soc., 1979, 101, 6860.

17. B. Halle and H. Wennerström, J. Chem. Phys., 1981, 75, 1928-1943.

18. A. Abragam,"The Principles of Nuclear Magnetism", Oxford University Press, London, 1961.

19. D. Dodrell, V. Glusco and A. Allerhand, J. Chem. Phys., 1972, 56, 3683.

20. T. Klason and U. Henriksson in "Solution Behaviour of Surfactants", vol. 1, p. 417, Eds. K.L. Mittal and E.J. Fendler, Plenum Publishing Corp., New York, 1982.

21. B. Jönsson, personal communication.

22. B. Faucompré, Thesis, U.S.T.L., Montpellier, 1982.

23. K. Fontell, personal communication.

24. S. Marčelja, J. Chem. Phys., 1974, 60, 3599.

25. J. Charvolin and P. Rigny, J. Chem. Phys., 1973, 58, 3999.

26. J. Ulmius, G. Lindblom, H. Wennerström, L.B.Å. Johansson, K. Fontell, O. Söderman and G. Arvidson, Biochemistry, 1982, 21, 1553.

27. Y. Hendrikx and J. Charvolin, J. Phys., 1981, 42, 1427.

References (continued)

28. B. Lindman, P. Stilbs and M. Moseley, J. Colloid Interface Sci., 1981, 83, 569.

29. P. Stilbs, J. Colloid Interface Sci., 1982, 89, 547.

30. H. Walderhaug, O. Söderman, P. Stilbs and U. Henriksson, manuscript in preparation.

Table 1. Compositions in w/w % for the Isotropic Samples Studied.

Sample	SOBS	butanol	toluene	water
6	5.0	-	-	95.0
7	6.9	13.9	-	79.2
8	14.4	25.5	45.0	15.1

Table 2. Order Parameters for the Phenyl Ring in SOBS.

Sample[§]	S
1 (Lamellar phase)	0.045 *
2 "	0.051
3 "	0.059
4 "	0.046
5 (Rectangular phase)	0.010

*: Error limits ± 3%

§: Compositions can be obtained from fig 1.

Table 3. Table of Experimental ^{13}C and ^{2}H Relaxation Data and Calculated Fast Correlation Times for the Phenyl Ring of SOBS for a Micellar and a Microemulsion System.

Sample §	^{13}C ortho			^{13}C meta			^{2}H ortho			^{2}H meta		
	T_1(s) 8.5 T	η 8.5 T	T_1(s) 1.4 T	T_1(s) 8.5 T	η 8.5 T	T_1(s) 1.4 T	T_1(ms) 6 T	T_2(ms) 6 T	T_1(ms) 2.1 T	T_1(ms) 6 T	T_2(ms) 6 T	T_1(ms) 2.1 T
6	* 1.13 ± 0.02 [o]	- -	* 1.03 ± 0.04	* 1.12 ± 0.002	- -	* 1.07 ± 0.03	30.4 ± 0.9	27.8 ± 1.5	-	27.2 ± 1.2	27.8 ± 1.5	-
7	1.51 ± 0.07	1.47 ± 0.05	0.80 ± 0.10	1.25 ± 0.03	1.69 ± 0.16	0.88 ± 0.06	48.7 ± 0.5	51.0 ± 1.0	49.5 ± 0.2	48.5 ± 0.5	49.0 ± 1.0	47.2 ± 0.1

τ_c [+] (ps)

6	37 *	40 *	37 *	39 *	68	74	76	74
7					42	41	43	42

§: Sample compositions are given in Table 1.

[o]: Error limits correspond to one standard deviation, random errors only.

*: At 42°C. [+]: Evaluated by setting S=0 in eq. 7.

Table 4. τ_c^s, τ_c^f and S from ^{13}C Data and Predicted ^2H T_1 and T_2 for the Phenyl Ring in Sample 7.

Carbon	τ_c^s (ns)	τ_c^f (ps)	S	T_1 (6 T) *	T_2 (6 T) *	T_1 (2.1 T) *
ortho	2.9	24 ± 4	0.15 ± 0.01	42	29	26
meta		33 ± 4	0.12 ± 0.02	44	35	32

*: Relaxation times for deuterium in milliseconds.

Figure Captions

Fig. 1. Partial schematic phase diagram for the sodium p-octylbenzene-sulfonate (SOBS)-pentan-1-ol-water system at 25°C. The diagram has been redrawn from ref.8. The compositions of the samples studied are marked with an x. L_1 and L_2 denote isotropic solution phases while D and R denote lamellar and rectangular phases, respectively.

Fig. 2. The order parameter profile for the hydrocarbon chain of SOBS for four samples in the lamellar phase (a-d) and one in the rectangular phase (e) formed by the system SOBS - pentan-1-ol - water. The compositions of the samples are given in fig 1 (the numbers in the upper left hand corner correspond to the numbers in fig 1). The order parameter profile for SOBS in the lamellar phase formed by the system SOBS - decan-1-ol - water is shown in (f) (see text).

Fig. 3. The order parameter profiles for three isotropic solutions as deduced from ^{13}C relaxation data. The composition of the samples are given in Table 1. The error bars correspond to an 80% confidence level.

Figure 1

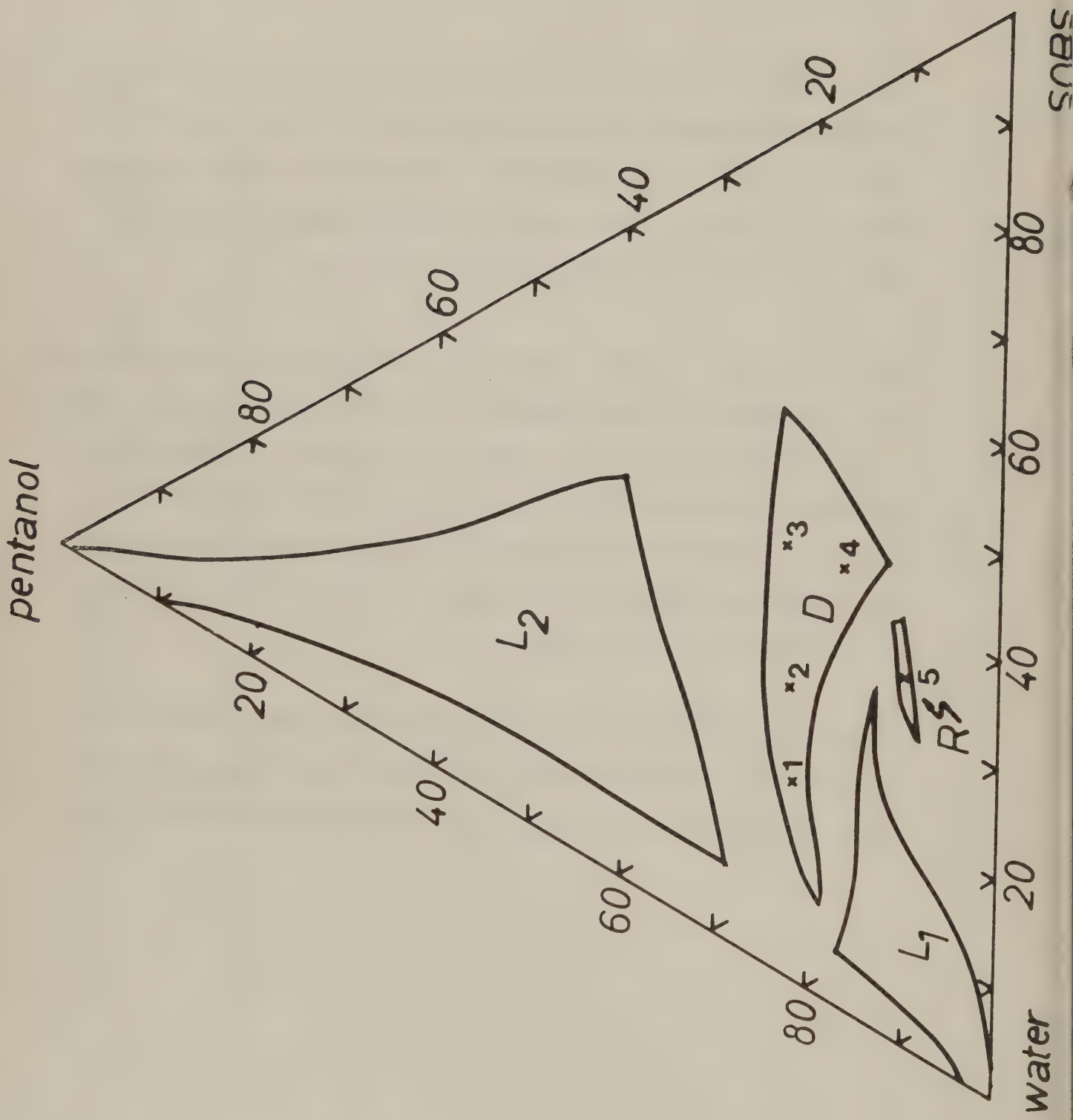
pentanol
water
SDBS
20
40
60
80
20
40
60
80
20
40
60
80
L2
L1
D
R
×1
×2
×3
×4
5

Figure 2

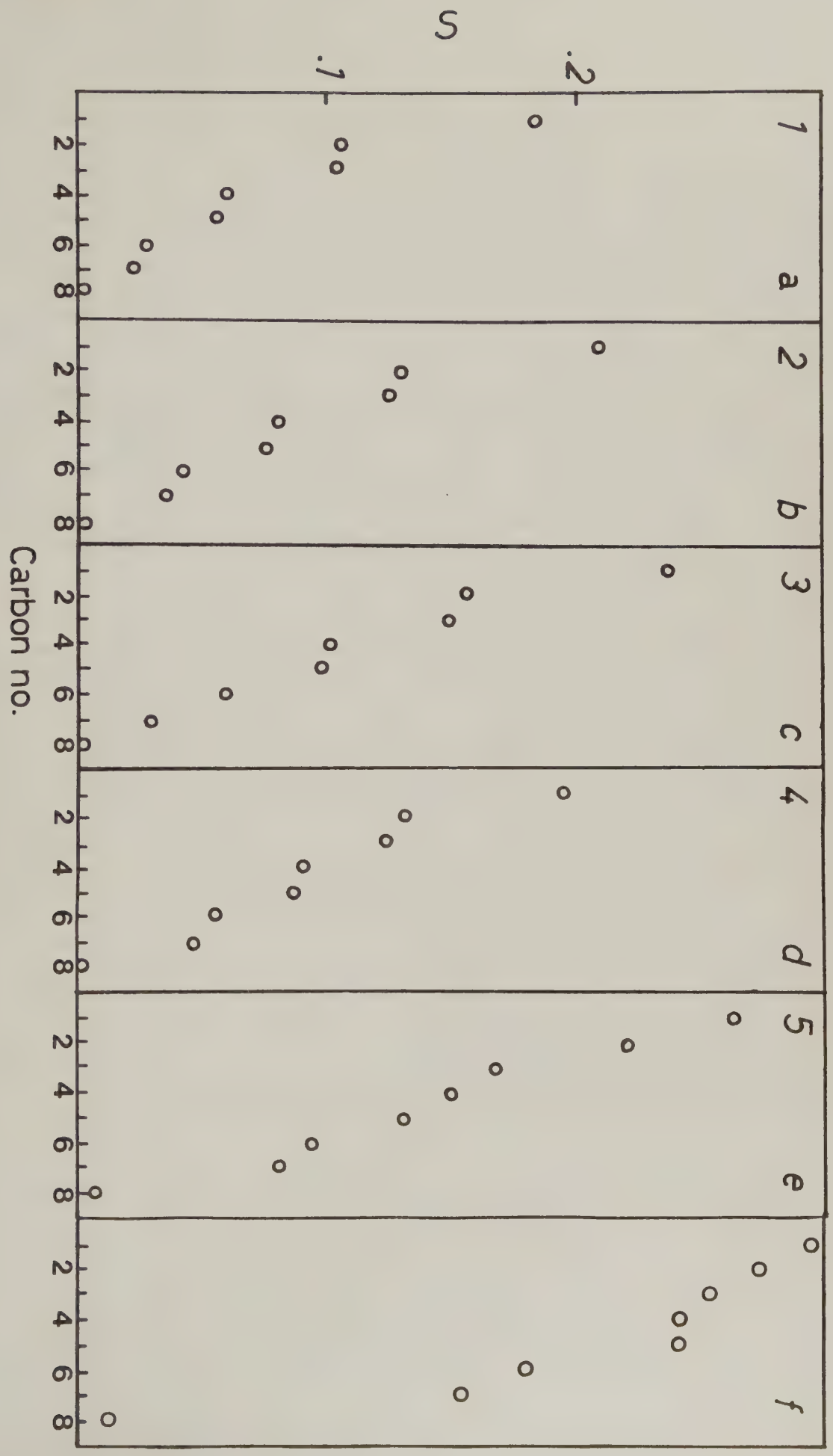

Figure 3

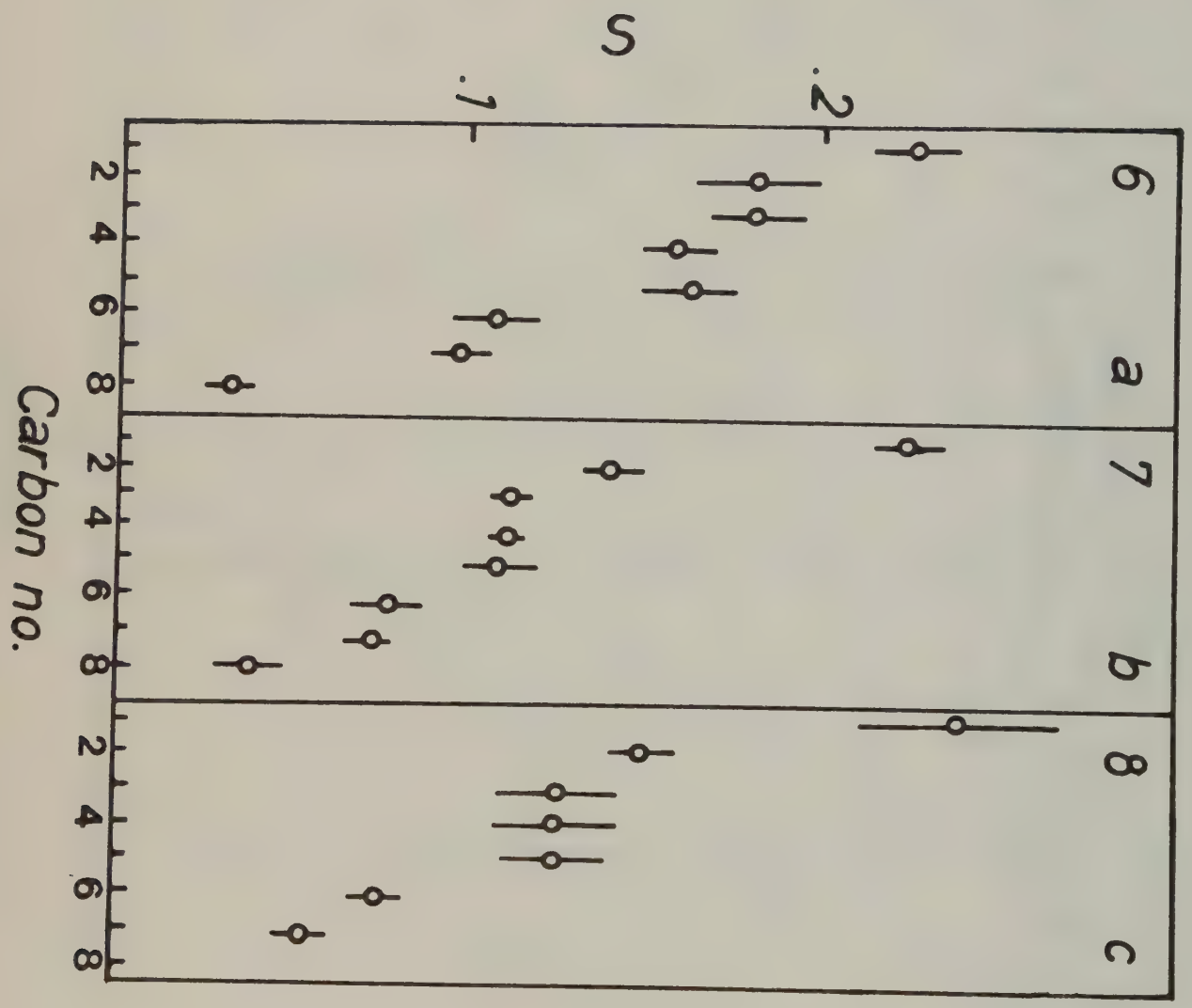

V

ORDER AND DYNAMICS OF THE HYDROPHOBIC/HYDROPHILIC INTERFACE IN MICROEMULSIONS OF THE COSURFACTANT TYPE. A ^{13}C NMR RELAXATION STUDY.

Olle Söderman and Harald Walderhaug

Division of Physical Chemistry 1

Lund University, Chemical Center,

P.O.B. 124, S-221 00 Lund, Sweden

ABSTRACT

^{13}C NMR spin-lattice relaxation times and $\{^{1}H\}$ - ^{13}C nuclear Overhauser enhancements have been measured for the alkyl chain carbons of sodium p-octylbenzenesulfonate (SOBS) in the four-component microemulsions formed by SOBS, butan-1-ol, water and toluene. It is found that the spin relaxation depends on the magnetic field strength. The relaxation is interpreted by means of a two-step model providing correlation times for two independent processes occuring on the picosecond and nanosecond time scales, respectively, and order parameters. The magnitude of the order parameters so extracted are similar to those found in other surfactant systems like micellar solutions and lamellar liquid crystalline phases. The fast correlation times indicate that the segmental motions of the surfactant alkyl chains are rapid. The slow correlation times are around 1-2 nanoseconds and are discussed in terms of a hydrophobic-hydrophilic interface that is highly flexible on a time scale of a few nanoseconds. This interpretation is in line with a recent neutron scattering study on microemulsions indicating zero mean curvature for these interfaces.

Introduction

According to a recent definition, microemulsions are "thermodynamically stable isotropic solutions of surfactant, oil (where "oil" is to be understood in a broad sense) and water" [1]. Microemulsions have attracted a lot of attention, not the least due to the possible technical applications of these systems [2-4], but also from a desire to gain an increased knowledge of fundamental characteristics of microemulsions, such as solution structure and dynamics.

Much of the interest has been focussed on four-component microemulsions consisting of surfactant, a cosurfactant (usually an alcohol of medium chain length, such as butan-1-ol, pentan-1-ol or hexan-1-ol), oil and water. With these medium chain length alcohols it is possible to form microemulsions over a very wide range of water to oil mole ratios (see fig. 1). Diffusion studies have shown conclusively for a large number of such systems that, except for the water- and oil-rich regions where one has swollen micelles of ordinary and reversed types, microemulsions are continuous in both water and oil [5-8] over large concentration ranges. It is safe to state that the solution structure of these bicontinuous cosurfactant-type microemulsions still remains unknown. Some recent light scattering studies have, however, contributed to our knowledge in this regard [9-10]. These studies emphasize the presence of bicontinuous structures over a wide range of compositions, in agreement with the above cited diffusion studies. Furthermore, X-ray and neutron scattering indicate the existence of a well-defined surfactant film with zero mean curvature in

microemulsions [11]. Thus, a picture of ill-defined (as regards the shape) and flexible aggregates emerges. These observations suggest that the structure and dynamics of the interface are fundamental properties needed to gain a deeper insight into important characteristics of these systems.

De Gennes and Taupin [12] stress the role of the flexibility of the interface and, on the basis of Electron Spin Resonance (EPR) work, state that the order of the surfactants in the interface is lower than in ordered systems like lamellar phases. However, few direct methods exist for extraction of such information from microemulsions. Bellocq et al. [13] used proton NMR spin-lattice relaxation data to study the systems sodium dodecylsulfate/butan-1-ol/toluene/water. From the regular trends in the data as the concentrations of all compounds are changed they conclude that there is a continuous transition between different types of aggregates in these microemulsions. From ^{1}H NMR data alone it is, however, difficult to extract information on the state of the surfactant in the surfactant film, since both intra- and intermolecular interactions contribute to the NMR relaxation. For this reason one has to use data from nuclei such as ^{13}C or ^{2}H whose relaxation is dominated by intramolecular interactions. In previous work we have shown that relaxation data from ^{13}C and ^{2}H interpreted with a model based on some physically reasonable ideas about the molecular dynamics in surfactant systems [14-17] provides such information. In particular, the approach gives information that is directly comparable with data for anisotropic phases, inter alia order parameters deduced from deuterium quadrupolar splittings for the hydrocarbon chains in lamellar phases [17].

One problem when dealing with four-component systems is the rather large number of different possible sample compositions that can be studied. The present work presents a systematic study on the sodium p-octylbenzene-sulfonate (SOBS)/ butan-1-ol/ water/ toluene system where we have chosen a fixed weight ratio of cosurfactant to surfactant, equal to 2:1. Six samples have been studied, the compositions of which have been chosen to cover a wide concentration range; from one sample without toluene up to 60 % toluene by weight. (See fig. 1 where the compositions of the samples are indicated). ^{13}C T_1's have been measured at two different field strengths and the ^{13}C - $\{^1H\}$ nuclear Overhauser enhancement (n.O.e.) at one field strength. Order parameters and correlation times for the fast local molecular motion for the SOBS chain together with the lifetime of the anisotropy of the surfactant molecules, induced by the hydrophobic/hydrophilic interface, are presented. A comparison is also made with order parameters in the lamellar phase formed by SOBS, pentan-1-ol and water.

Materials and Methods

The SOBS was from a special batch prepared for "The Lund Project" (see ref. 16) by Professor Bothorel's group in Bordeaux. Heavy water (Norsk Hydro, Norway, 99 % enrichment) was needed to provide an internal field-frequency lock for the spectrometers. The butan-1-ol and toluene were purchased from BDH (99 % purity) and were used without further purification. The samples were prepared by weighing into glass ampoules the appropriate amounts of each component. After temporary sealing with rubber

stoppers and cooling, the ampoules were flame-sealed and the samples equilibrated at 25°C until they were isotropic phases as judged by viewing the samples between crossed polarizers. The samples were subsequently transferred to NMR tubes.

The fast inversion recovery technique was used to determine the ^{13}C spin-lattice relaxation times. These were measured at 8.45 T on a Nicolet NM 360 spectrometer and at 1.40 T on a Jeol FX-60 spectrometer. At the high field strength so-called bilevel decoupling was employed to prevent heating the samples because of the high effect needed for the proton decoupling field. n.O.e. measurements were performed at 8.45 T on the Nicolet spectrometer using the dynamic n.O.e. technique. This is a combined T_1 and n.O.e. measurement, and for all n.O.e.'s used in the calculations the T_1's thus determined and the T_1's determined by the fast inversion recovery method agree to within ±10 %. The experimental uncertainties for the T_1's are about ±5 % at the high field strength and about ±10 % at the low field strength. The uncertainties in the n.O.e.'s are about ±10 %. The procedure for extracting the T_1's and the n.O.e.'s from the experimental raw data, assignments of the spectra as well as the procedure for the fits of the two-step model to the relaxation data are described in ref. 15. The uncertainties given in the experimental relaxation data and evaluated parameters correspond to an approximately 80 % level of confidence, taking only random errors into consideration. The experimental temperature was, unless stated otherwise, 25°C.

Theoretical Considerations

All six microemulsion samples investigated in the present study show the following features as regards their NMR relaxation behaviour: the ^{13}C T_1's are rather long and depend on the magnetic field strength, while the ^{13}C linewidths are narrow. This behaviour is by no means restricted to the present system; rather it has been found in a number of isotropic solutions of surfactants. These include micellar systems [15,17-19] and other microemulsion systems [14,20]. These observations immediately suggest that more than one motion cause the relaxation and that at least one of these motions occur at a rate causing the observed magnetic field strength dependence, i.e. its correlation time (assuming a single exponential correlation function for this motion, vide infra) has to be of the same order of magnitude as the inverse Larmor frequency. Furthermore, the narrow linewidths (in the present case the ^{13}C linewidths are dominated by the magnetic field inhomogeneties) exclude significant contributions to the NMR relaxation from slower motions. This does of course not mean that such motions are not present. It simply means that most of the dipolar interaction is averaged by the fast motions for which the correlation times are much smaller than the inverse Larmor frequency, and that the fastest isotropic motion averaging the residual interaction to zero is so rapid that it does not cause any appreciable line broadening (see also under "Results and Discussion" below).

In order to proceed further and analyze the ^{13}C NMR relaxation data one needs a relaxation model, compatible with the observations stated above. Such a model, termed the "two-step" model, has been presented by

Wennerström et al. [21,22]. Detailed discussions on the model as well as applications to a number of different surfactant systems can be found elsewhere [14-16]. Its main feature is a division of the motions causing NMR relaxation into two parts; one fast local motion that is slightly anisotropic and averages the interaction to a level which is averaged out by slow motions that are isotropic. The part of the total interaction being left over to the slow motion is described by an order parameter. With the usual assumption that the relaxation of the ^{13}C nucleus is given solely by the dipole-dipole interaction with directly bonded protons the expressions for ^{13}C R_1 (= $1/T_1$) and n.O.e., η, are given by (broad-band decoupling conditions) [23]:

$$R_1 = (N_i/20)\,[\mu_o \gamma_H \gamma_C\, \hbar/4\pi\, r_{C-H}^3]^2\, (\tilde{J}(\omega_H-\omega_C) + 3\tilde{J}(\omega_C) + 6\tilde{J}(\omega_H+\omega_C)] \qquad (1)$$

$$\eta = (1/20)(\gamma_H{}^3\gamma_C)\,[\mu_o\, \hbar/4\pi\, r_{C-H}^3]^2\, (N_i\, T_1)\{6\tilde{J}(\omega_H+\omega_C) - \tilde{J}(\omega_H-\omega_C)\} \qquad (2)$$

Here N_i is the number of protons directly bonded to the carbon atom, r_{C-H} is the carbon-proton bond length (taken to be 1.09 Å) and the other symbols have their usual meaning.

The key point in the "two-step" model is the expression for the various reduced spectral densities, $\tilde{J}(\omega)$, which are given by:

$$\tilde{J}(\omega) = (1-S^2)\tilde{J}^f(\omega) + S^2\tilde{J}^s(\omega) \qquad (3)$$

where $\tilde{J}^f(\omega)$ and $\tilde{J}^s(\omega)$ are the reduced spectral densities for the fast and slow motions, respectively. S is the (local) order parameter defined as:

$$S = (1/2) < 3\cos^2\theta_{MD} - 1 >_f \tag{4}$$

where θ_{MD} is the angle between the C-H bond vector and the local director which is taken to be perpendicular to the hydrophobic/hydrophilic interface. The symbol $< >_f$ means an average of the quantity inside the brackets over the fast local motions. S is analogous to the order parameter measured by deuterium quadrupolar splittings in anisotropic phases.

If one assumes a functional form for the spectral densities in eq. (3) it is possible to extract the order parameter as well as information on the dynamics of the two kinds of motion from ^{13}C relaxation measurements. In the present work we will assume that the correlation functions for the two types of motion are single exponentials, an assumption further discussed under Results and Discussion. For such a case eq. (3) becomes (assuming extreme narrowing conditions for the fast motion):

$$\tilde{J}(\omega) = (1-S^2)\cdot 2\tau_c^f + S^2\cdot 2\tau_c^s/(1+(\omega\tau_c^s)^2) \tag{5}$$

Here τ_c^f and τ_c^s are the correlation times for the fast and slow motions, respectively.

One interesting feature of eq. (3) is that it is possible to determine quantities which are proportional to the order parameters of the hydrocarbon chain only by assuming that the fast motions give rise to a field independent part of the relaxation. We can therefore extract the order parameter profile, but not absolute values of S, since the proportionality constant will be the same for all carbons along the chain. This follows since the motion contributes equally to all carbons. Thus the difference between the ^{13}C spin-lattice relaxation rates determined at two different magnetic field strengths produces a quantity proportional to S^2. This is perhaps most readily seen if we evaluate $\tilde{J}(\omega)$ in eq. (3) at two frequencies, ω and ω', and take the difference:

$$\tilde{J}(\omega) - \tilde{J}(\omega') = S^2\{\tilde{J}^S(\omega) - \tilde{J}^S(\omega')\} \tag{6}$$

Inserting eq. (6) in eq. (1) we obtain

$$R_1(\omega) - R_1(\omega') = (N_i/20)\,[\mu_o\gamma_H\gamma_C\,\hbar/4\pi\, r^3_{C-H}]^2\, A\, S^2 \tag{7}$$

$$A = \{\tilde{J}^S(\omega_H-\omega_C) - \tilde{J}^S(\omega'_H-\omega'_C) + 3(\tilde{J}^S(\omega_C) - \tilde{J}^S(\omega'_C) + $$
$$+ 6(\tilde{J}^S(\omega_H+\omega_C) - \tilde{J}^S(\omega'_H+\omega'_C)\} \tag{8}$$

In eq. (7) the constant A is the same for all carbons along the chain since the slow motion, as stated above, contributes equally to all carbons. It then follows from eq. (7) that the square root of the difference in R_1 for all carbons along the chain measured at two field strengths gives the shape of the order parameter profile.

We end this section by noting that several other ways of interpreting NMR relaxation data from isotropic surfactant systems have been presented. Canet and coworkers [24] employ a formalism which is based on the Woessner equations and which can be shown to be equivalent to our two-step model [25]. Tricot et al. [20] use a distribution of correlation times. Although formally correct, we believe that such an approach is unnecessarily complex and gives little physical insight into the system under study. Finally, Martin and Magid [26] define an effective correlation time for the fast and slow motions as:

$$1/\tau_c = 1/\tau_c^f + 1/\tau_c^s \qquad (9)$$

In order to write the relation between an effective correlation time and correlation times for two (or more) motions as is done in eq. (9), two criteria have to be fulfilled. First, the two motions have to be independent, and secondly, they have to average the same part of the interaction. While the first criteria is fulfilled, it should be clear from what is said above that the second condition is not met for aggregated surfactant systems. Thus, eq. (9) is not correct. It also follows that single field relaxation studies on associated surfactant systems are of little value.

Results and Discussion

Presented in fig. 1 is a coarse trial-and-error phase diagram for the SOBS/butan-1-ol/water/toluene system. The composition of the six samples studied in the present investigation can be found in fig.1. As is evident

from this figure it is possible to go from water rich solutions without oil to oil rich solutions, poor in water, without ever leaving the one-phase area. This feature is by no means restricted to the present system but appears to be a rather general property for four-component micro-emulsions with medium chain alcohols as cosurfactants. In fig. 2 we present ^{13}C R_1's measured at two different magnetic field strengths for carbons no. one and six in the alkyl chain of SOBS, the numbering starting at the polar head group. In addition, the corresponding values at a slightly elevated temperature (42°C) for ordinary micelles (SOBS in water) are also given (data from ref. 15). As is evident there is a clear magnetic field dependence for carbon no. one in all samples. There is also a field dependence for carbon no. six, although less marked. As pointed out above this field dependence demonstrates the contribution of slow motions to the relaxation. Thus, it strongly suggests that the surfactant is aggregated and, therefore, gives support for the view that an interfacial surfactant film exists in all samples studied here. The lifetime of the interfacial film is not shorter than the correlation time for the slow process, i.e. a few nanoseconds. Thus, the data in fig. 2 give further support for the observation [11], cited above, that an interfacial film does indeed exist in these kinds of systems. In order to go further in the interpretation of the relaxation data one needs a model for the dynamics. As stated under Theoretical Considerations we will employ the "two-step" model mentioned there. It provides the three parameters τ_c^f, S and τ_c^s.

Before discussing the extracted values of these parameters we will, as a point of reference, present in fig. 3 some self-diffusion data (data from refs. 8a and 27) for the samples studied in the present investigation.

In a number of reports the usefulness of such data when obtaining information regarding solution structure in microheterogeneous systems has been pointed out [5-8]. This follows since a molecular species that is confined to an aggregate necessarily will diffuse with the aggregates and thus diffuses much more slowly than a corresponding molecule in a continuous medium under comparable physical conditions. Three features in fig. 3 are immediately apparent. First, the surfactant diffusion is slow in all samples (the diffusion coefficient of monomeric SOBS at $33^{o}C$ in water is approximately $6 \times 10^{-10}\ m^2s^{-1}$ [28]). Secondly, there is a continuous change in the diffusion coefficient for water and oil as the composition is varied. The diffusion of water is fast in the oil-poor sample and slow in the oil-rich one, while the opposite holds for the toluene (oil) diffusion. Finally, the diffusion coefficients of oil and water have approximately the same value in sample 3. These observations strongly suggest that the surfactant is aggregated in all samples, that the water-rich sample contains swollen micelles and, finally, that the oil-rich sample consists of reversed micelles (note that the diffusion rates of surfactant and water are the same in sample 6). Furthermore, any suggestion for a structure of microemulsions which are rich in both water and oil must not be at variance with the observed rough equality of diffusion rate for these two components.

The Order Parameter Profile

The order parameter, S, is a measure of the degree of ordering imposed on the surfactant molecules by the presence of the hydrophobic/hydrophilic interface. In order to extract the value of S for the various methylene

groups in the alkyl chain of SOBS from the relaxation data one needs to assume a form for the spectral density function for the slow motion. While the slow motion is well described by a single exponential correlation function for ordinary micelles [18], this may not be the case for the present systems (vide supra). However, as discussed under Theoretical Considerations, it is possible to determine relative order parameters along the hydrocarbon chain - the so called "order parameter profile". In fig. 4 we present such profiles for all samples studied. The profiles have arbitrarily been normalized so that the value of S for carbon no. 1 is set at 0.25. Also given are the profiles obtained when a single exponential correlation function for the slow process is assumed. The uncertainties in the order parameters when extracted from the relaxation rates at two field strengths are somewhat larger than for those obtained from a fit to all relaxation data, including the n.O.e.'s. This effect is seen especially for the carbons close to the end of the hydrocarbon chain where the differences in relaxation rates are rather small. Still it is clear that the profiles are very similar in the two cases. Thus it appears that the single exponential correlation function approximation for the slow process is not too critical. Note also that the parameters extracted from the full fit are rather well determined. The exception is sample 3 where the uncertainties are rather large, although the accuracy of the experimental data is about the same for all samples. A possible explanation for this observation is that the above mentioned approximation may not be so good for this sample.

Finally, for comparison, we show the order parameter profiles for ordinary micelles (at 42°C) and for two compositions in the lamellar phase formed

by the SOBS/pentan-1-ol/water system (data from ref. 17) in fig. 4. In the latter case the profiles have been determined from ^{2}H quadrupole splittings of the perdeuterated surfactant. As regards the shape of the profile there is a definite change when going from sample 1 to sample 6. In sample 1 the order drops significantly from carbon no. 1 to carbon no. 2, then stays fairly constant until carbon no. 5 where it starts to decrease again. For sample 6 there is an almost exponential decrease of the order along the chain. It is also worth noting that in the samples 2-5 there is a gradual change from the shape of sample 1 to the shape of sample 6. These findings reflect a change in the packing situation as the composition of the microemulsions is varied. For sample 1 the profile resembles that found for ordinary micelles although the order in the microemulsion is lower. This suggests that the structure in this sample is that of swollen micelles where the solubilization of the alcohol reduces the order as compared to the two-component system. The shapes of the order parameter profile for sample 6 suggests a structure of reversed aggregates. For such a structure, where the chains point out from a sphere, the order decreases in a more continuous fashion since the packing restrictions are less severe compared to an ordinary micelle. Both these findings are in good agreement with the interpretation of the diffusion data in fig. 3 given above.

The same features for the order parameter when going from a normal to a reversed structure have also been found by Klason and Henriksson [29] for hexagonal liquid crystalline phases of the system sodium octanoate/decan-1-ol/water.

As regards the shape of the order parameter profile of samples 2-5 it is clear that there are no abrupt changes from the shape of the profile for sample 1 to that for sample 6. This finding suggests that there is no composition where an interconversion between swollen and reversed micelles occurs. Rather, it gives further evidence for the existence of a bicontinuous microemulsion structure where the curvature of the interface between the hydrophilic and hydrophobic components is close to zero on the time-scale of the fast process [11].

Turning to the absolute magnitudes of corresponding order parameters, it is clear that they do not differ significantly between the various samples. Furthermore, they have roughly the same values as in the ordinary micellar and lamellar phases (see fig. 4). In ref. 12 De Gennes and Taupin state that the order parameter as measured by an EPR probe is approximately a factor of two less in microemulsions as compared to that for a lamellar phase, a result that is clearly at variance with the present study. However, when obtaining order parameters from EPR data the further averaging due to diffusion of the EPR probe over the curved interface was included in the quoted value [30]. Thus, the order parameters given in ref. 12 are not directly comparable with the ones presented in this work. As a general remark, one has to be careful with order parameters determined from EPR measurements since the bulky probe may perturb the system [31].

In conclusion, the present study indicates that there is no significant difference in the surfactant ordering in microemulsions and in other systems, both isotropic and anisotropic. This conclusion is in line with a number of other studies [18,19,32,33].

The Fast Correlation Time, τ_c^f

Presented in fig. 5 are the fast correlation times as a function of chain position for the 6 microemulsion samples together with the corresponding data for ordinary micelles at 42°C of the system SOBS/water. As for the order parameters the uncertainties in the τ_c^f's for sample 3 are quite large. As is evident from fig. 5 the change in the fast correlation time along the chain is almost the same for the 6 samples, within the uncertainties of the extracted parameters. There is a difference between sample 1 and sample 6 in that the fast correlation time profile shows a more linear decrease in sample 6, but the difference is slight. As regards the magnitude of the fast correlation times they are short, of the order of 10 - 20 ps, and roughly equal to those found for ordinary micelles at a slightly elevated temperature. They are also similar to the values of the correlation times extracted from ^{13}C NMR relaxation data for n-alkanes of comparable chain lengths [34,35]. Thus, the dynamic state of the hydrocarbon chains in the interfacial film resembles that for the corresponding n-alkanes.

As regards the nature of the fast local motion it is presumably complex. There will be rotations around carbon-carbon bonds (gauche-trans isomerizations), torsions, diffusion etc. The extracted fast correlation times are then effective correlation times for all these fast processes.

The Slow Correlation Time, τ_c^s

In Table 1 are given the slow correlation times for the six samples. Within the uncertainty of the fits of eqs. (1), (2) and (5) to the relaxation data there are no significant variations in τ_c^s between the various samples. We have previously shown [15,18] that ^{13}C relaxation data may under certain conditions be rather insensitive to the slow process(es). This occurs when the slow correlation time is longer than about 4 ns. In that case the relaxation, particularly at the higher field strengths, is almost exclusively determined by the fast process. In order to investigate the influence of the values of τ_c^s on the fit of the two-step model to the relaxation data in the present study we have assigned various values to τ_c^s for samples 4 and 6 and made a two parameter fit to the data. As is evident from fig. 6 there is a clear minimum in the error square sum, indicating that the value of the slow correlation times are rather well determined.

The short τ_c^s values imply that the local ordering of the surfactant molecules, imposed by the hydrophobic/hydrophilic interface, is short-lived in comparison with that of liquid crystalline systems where the order prevails much longer. The slow motion correlation times presented in Table 1 are in fact one or two nanoseconds less than what would be expected for ordinary SOBS micelles if τ_c^s were determined by aggregate rotation and surfactant lateral diffusion over the (curved) aggregate surface. Thus, the short τ_c^s's found in this work could be explained by the presence of predominantly small aggregates with a radius not larger than the

extended surfactant chain. But they are also compatible with the presence of larger aggregates if the hydrophobic/hydrophilic interfaces are highly flexible so that the local director (normal to the interface) changes direction extensively in a few nanoseconds. This implies that over a time span longer than 10^{-9} s, the aggregate structure in microemulsions is highly dynamic. Not only do the aggregates change shape continuously, but presumably they also break and reform easily. Such a situation would give little resistance to flow, accounting for the low viscosities in these systems. In this case it is conceivable that the motion of the interface may not be completely isotropic. In such a case there would be a fraction of the interaction left which eventually will be averaged by even slower motions. In fact, these motions could well be of such a nature that they do not contribute to R_1 but cause line broadening.

As was pointed out above both diffusion data and the order parameter profile suggest a structure of the reversed micellar type for sample 6. Using the diffusion coefficient for the surfactant and the Debye-Stokes-Einstein equation a hydrodynamic radius, r_h, can be calculated for these micelles if they are assumed to be spherical. Taking the viscosity of the intermicellar medium to be that of pure toluene a value of 50 Å for the radius is estimated from the data in fig. 3. The correlation time for the aggregate rotational tumbling and surfactant diffusion over the (curved) aggregate surface can then be estimated from the Debye-Stokes-Einstein and diffusion equations to be 40 ns (these equations together with relevant parameters can be found in ref. 15). This correlation time is so long that these motions will only contribute to the ^{13}C linewidth. Providing that all the interaction left over by the fast segmental motion is averaged by these

slow processes the natural linewidth for carbon no. 1 is predicted to be 5 Hz at 1.40 T. The experimental linewidth is certainly smaller than this; the line is in fact so narrow that it is difficult to measure the linewidth exactly, and this is the reason why we have not tried to estimate T_2. This indicates that most, if not all, of the interaction left over by the fast process is averaged by the flexing motion of the hydrophobic/hydrophilic interface alluded to above. One should note that in the case where the flexing motion is not fully isotropic eq. (3) is not strictly valid. However, as pointed out in ref. 18 the two-step model can be generalized into a three-step model to account for this complication. Of the parameters presented in figures 4 and 5 only S would be changed and by the same fraction for all carbons along the chain. Thus, the shape of the order parameter profiles would not be changed.

As pointed out above a recent X-ray and neutron scattering study shows the existence of interfaces with a zero mean curvature for Winsor type microemulsions with equal volume fractions of water and oil [11]. This is not compatible with the presence of small aggregates with an extension equal to or smaller than the extended surfactant molecule, but it supports a view of larger interfaces that are highly flexible. In ref. 12 De Gennes and Taupin discuss the role of the fluidity of the interface and state that for a microemulsion to be stable, the interface has to be highly fluid. Furthermore, based on EPR work, they claim that the cosurfactant does indeed decrease the order in the film as compared to the situation in ordered phases.

The present work gives an alternative picture. On a short time-scale ($\sim 10^{-11}$s) there are only slight differences in the amplitude of the motions that the surfactant molecules undergo in microemulsions and ordered phases. On a longer time-scale, on the other hand, there are marked differences, with the interface in the ordered phases being rigid and not very mobile while the contrary holds for microemulsions where there is little resistance to deformations of the interface.

It is conceivable that these deformations, including many surfactant molecules and thus being collective in nature, would give rise to non-exponential correlation functions. However, as pointed out above, we find no evidence for this - the only possible exception being sample 3. This is perhaps not to be expected either, since we are then trying to determine a form for the spectral density function from only a few points on the curve describing this function. We have previously shown that a multifield deuterium NMR relaxation study is a very useful method to obtain more reliable information regarding this problem. Such a study on microemulsions is under-way.

Finally, we would like to add a few words about the possibility that surfactant exchange between aggregates is the slow process. It has been argued that the interaction between aggregates in microemulsions may under certain conditions become increasingly attractive, thus causing rapid exchange of surfactant molecules between the aggregates. Although such exchange is definitely present, we feel that it is unlikely to be so

rapid as to contribute significantly to the slow process seen by NMR spin-lattice relaxation. A surfactant molecule travels a mean distance, $\langle r \rangle$, during a time t, given by

$$\langle r \rangle = (6Dt)^{\frac{1}{2}}$$

where D is the lateral diffusion coefficient of the surfactant. In one nanosecond and with a value for D of 6×10^{-10} m^2 s^{-1}, $\langle r \rangle$ = 19 Å, which is roughly the length of the extended surfactant molecule. It seems conceivable that surfactants would have to travel at least two molecular lengths to reach a new aggregate. Thus, the time-scale for the exchange would be longer than the reported slow correlation times in Table 1.

Conclusions

The frequency dependent ^{13}C relaxation data presented in this work strongly indicate that the surfactant molecules are aggregated, i.e. some sort of surfactant interface is present in the systems under study. When the relaxation data are interpreted with the "two-step" model for relaxation the following picture regarding the properties of this film emerges. The amplitude of the motions that the surfactant molecules undergo in the interfacial film is roughly equal to that found for ordered systems like lamellar phases. The motions are rapid. In fact, the rates are comparable to those of the corresponding n-alkanes. On a longer time-scale the interfacial film is in a highly dynamic state, changing shape as well as size extensively within a few nanoseconds.

REFERENCES

1. I. Danielsson and B. Lindman, Colloids and Surfaces, 3, 393, 1981.

2. "Microemulsions", ed. L.M. Prince (Academic Press, New York, 1977).

3. "Microemulsions", ed. I. Robb (Plenum Press, New York, 1982).

4. "Surfactants in Solution", vol. 3, eds. K.L. Mittal and B. Lindman (Plenum Press, New York, 1984).

5. B. Lindman, N. Kamenka, T.M. Kathopoulis, B. Brun and P.G. Nilsson, J. Phys. Chem., 84, 2485 (1980).

6. B. Lindman, P. Stilbs and M. Moseley, J. Colloid Interface Sci., 83, 569 (1981).

7. B. Lindman and P. Stilbs in "Surfactants in Solution", eds. K.L. Mittal and B. Lindman (Plenum Press, New York, 1984, vol. 3, p. 1651).

8a. P. Stilbs and B. Lindman, Progr. Colloid and Polymer Sci., 69, 39 (1984).

8b. P. Stilbs and B. Lindman, to appear in "Microemulsions", eds. S. Friberg and P. Bothorel (CRS Press).

9. E.W. Kaler, K.E. Bennet, H.T. Davis and L.E. Scriven, J. Chem. Phys. 79, 5673 (1983).

10. E.W. Kaler, H .T. Davis and L.E. Scriven, J.Chem. Phys., 79, 5685 (1983).

11. L. Auvray, J.P. Cotton, R. Ober and C. Taupin, J. Phys. Chem., 88, 4586 (1984).

12. P.G. De Gennes and C. Taupin, J. Phys. Chem., 86, 2294 (1982).

13. A.M. Bellocq, J. Biais, B. Clin, P. Lalanne and B. Lemanceau, J. Colloid Interface Sci., 70, 524 (1979).

14. T. Ahlnäs, O. Söderman, C. Hjelm and B. Lindman, J. Phys. Chem. 87, 822 (1983).

15. H. Walderhaug, O. Söderman and P. Stilbs, J. Phys. Chem. 88, 1655 (1984).

16. B. Lindman, T. Ahlnäs, O. Söderman, H. Walderhaug, K. Rapacki and P. Stilbs, Chem. Soc. Faraday Disc., 76, 317 (1983).

17. O. Söderman, H. Walderhaug and B. Lindman, J. Phys. Chem., accepted for publication.

18. O. Söderman, H. Walderhaug, U. Henriksson and P. Stilbs, J. Phys. Chem., submitted.

19. D. Canet, J.P. Marchal, H. Nery and B. Rhobin-Lherbier, J. Colloid Interface Sci., 93, 241 (1983).

20. Y. Tricot, J. Kiwi, W. Niederberger and M. Grätzel, J. Phys. Chem., 85, 862 (1981).

21. H. Wennerström, B. Lindman, O. Söderman, T. Drakenberg and J.B. Rosenholm, J. Am. Chem. Soc., 101, 6860 (1979).

22. B. Halle and H. Wennerström, J. Chem. Phys., 75, 1928 (1981).

23. D. Dodrell, V. Glushko and A. Allerhand, J. Chem. Phys., 56, 3683 (1972).

24. D. Canet, J. Brondeau, H. Nery and J.P. Marchal, Chem. Phys. Letters, 72, 184 (1980).

25. H. Nery, O. Söderman, H. Walderhaug, D. Canet and B. Lindman, to be published.

26. C.A. Martin and L.J. Magid, J. Phys. Chem., 85, 3938 (1981).

27. P. Stilbs, unpublished data.

28. B. Lindman, M.C. Pyual, N. Kamenka, B. Brun and G. Gunnarsson, J. Phys. Chem., 86, 1702 (1982).

29a. T. Klason and U. Henriksson in "Solution Behaviour of Surfactants", vol. 1, p. 417, eds. K.L. Mittal and E.J. Fendler, Plenum Publishing Corp., New York, 1982.

29b. T. Klason and U. Henriksson, T. Klason Thesis, Stockholm 1983.

30. C. Taupin, personal communication.

31. M.G. Taylor and I.C.P. Smith, Biochim. Biophys, Acta, 599, 140 (1980).

32. M. Schara, F. Pusnic and M. Sentjurc, Croat. Chem. Acta, 48, 147 (1976).

33. J. Ulmius and H. Wennerström, J. Magn. Reson., 28, 309 (1977).

34. Y.K. Levine, N.J.M. Birdsall, A.G. Lee, J.C. Metcalfe, D. Partington and G.C.K. Roberts, J. Chem. Phys., 60, 2890 (1974).

35. J.R. Lyerla, H.M. McIntyre and D.A. Torchia, Macromolecules, 7, 11 (1974).

Figure Captions

Figure 1. A coarse trial-and-error phase diagram for the system SOBS/ butan-1-ol/ water/ toluene at 25°C. The weight ratio C_4OH/SOBS = 2. The dashed lines indicate the composition boundaries for the microemulsion phase and the circles indicate the compositions of the samples studied. The numbering of the samples is the one referred to in the text and figures.

Figure 2. Observed ^{13}C spin-lattice relaxation rates as a function of sample number (see fig. 1) for carbons no. 1 and 6 in the alkyl chain of SOBS at two different magnetic field strengths. Also shown are the corresponding data for a micellar solution consisting of 10 % SOBS in water at a temperature of 42°C. The error bars correspond to an approximately 80 % level of confidence (see "Materials and Methods").

Figure 3. Self-diffusion data at 25°C for the six microemulsion samples. The symbols △ ,□,● and X denote self-diffusion coefficients for water, toluene, butanol and SOBS, respectively.

Figure 4. Order parameters as a function of chain position for the alkyl chain of SOBS for the six microemulsion samples (see fig. 1). Also shown are the corresponding order parameters for the micellar solution for which relaxation data are shown in fig. 2. The error bars correspond to an approximately 80 % level of confidence. Corresponding order parameters for the alkyl chain of SOBS for two lamellar liquid crystalline samples consisting of SOBS, pentan-1-ol and water extracted from ^{2}H quadrupolar splittings of deuterated surfactant are also shown. The composition in weight per cent

of the components are given at the top of each figure (S = surfactant, Cs = cosurfactant, W = water.

Figure 5. Fast correlation times as a function of chain position for the alkyl chain of SOBS for the six microemulsion samples (fig. 1) and the same micellar solution as in figures 2 and 4. The error bars correspond to an approximately 80 % level of confidence.

Figure 6. The function CHISQ = $\Sigma\{[R_1(obs) - R_1(calc)]/R_1(obs)\}^2 + \Sigma\{[\eta(obs) - \eta(calc)]\eta\ (obs)\}^2$ plotted versus the slow correlation time for two of the six microemulsion samples (fig. 1). $R_1(obs)$ is the experimental relaxation rate, $\eta(obs)$ the experimental n.O.e. and $R_1(calc)$ and $\eta(calc)$ are given by eqs. (1), (2) and (5). The slow correlation time was fixed at the indicated values and two-parameter fits (to τ_c^f and S) for all carbons in the chain were performed.

Table 1. The Slow Correlation Time, τ_c^s.

Sample	τ_c^s (ns)
1	2.6 ± 0.5
2	2.2 ± 0.6
3	1.8 ± 1.1
4	1.9 ± 0.6
5	1.8 ± 0.6
6	1.5 ± 0.3

Figure 1

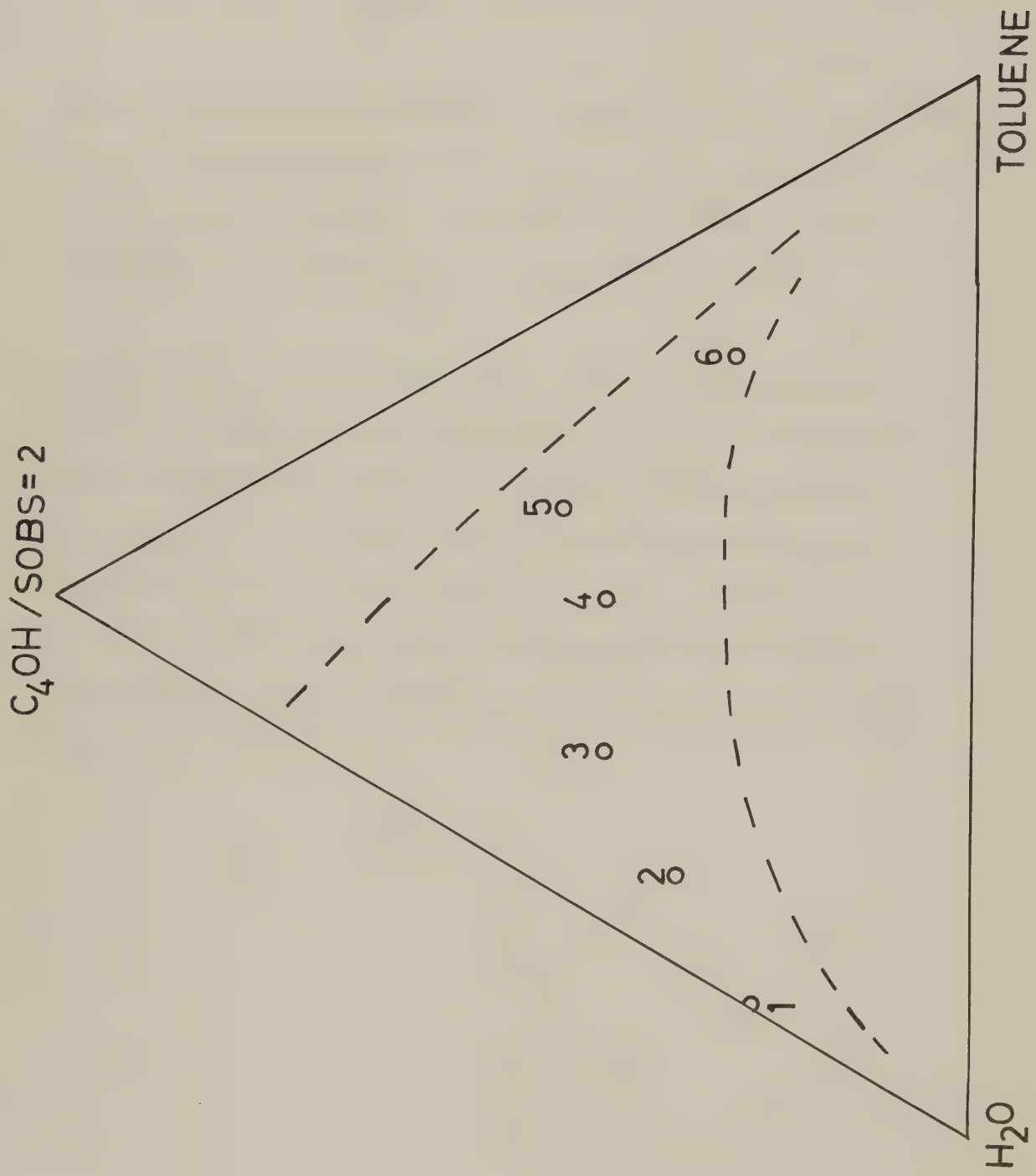

Figure 2

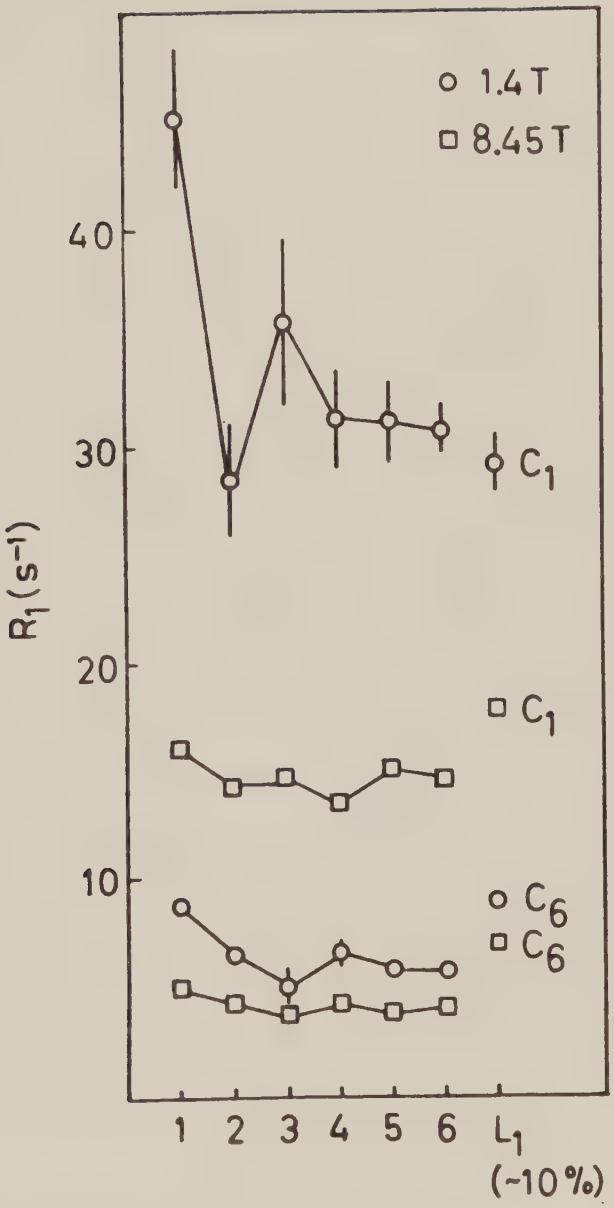

Figure 3

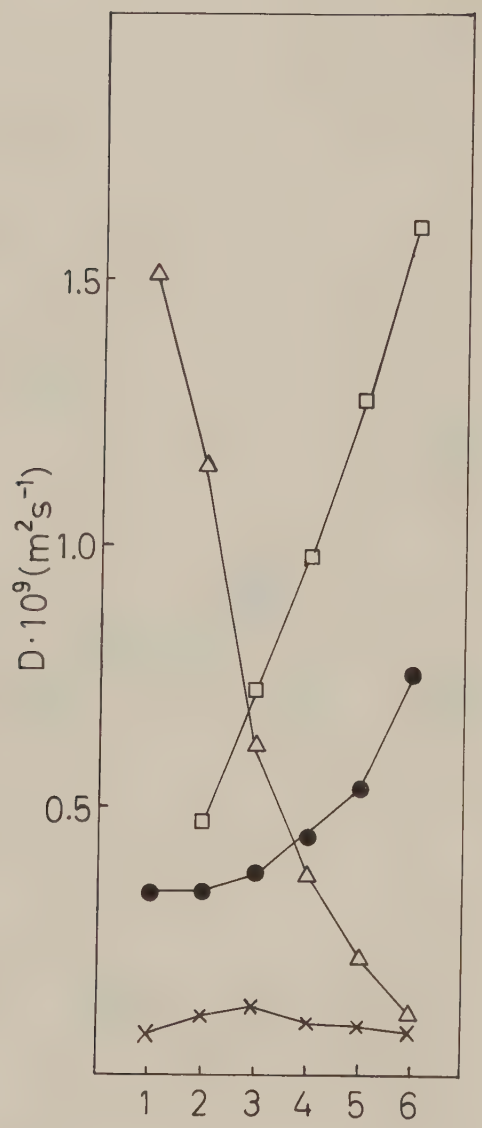

Figure 4

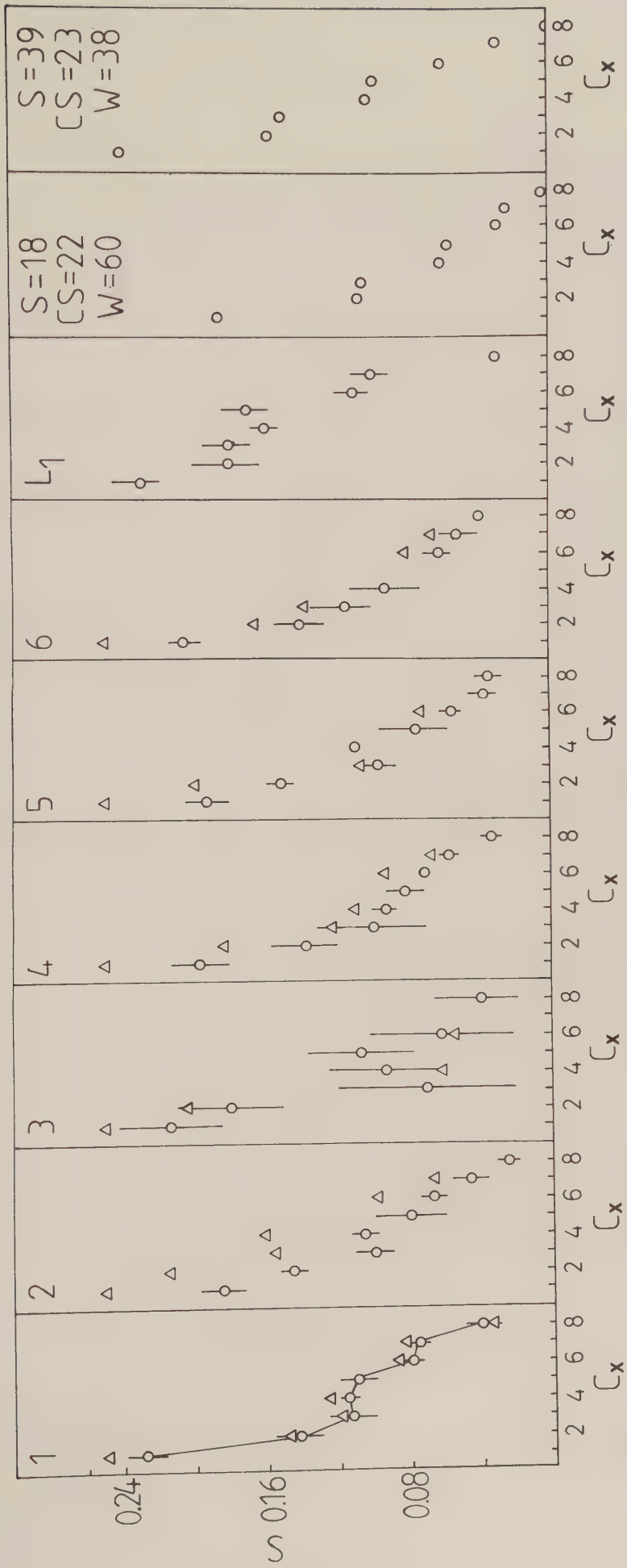

Figure 5

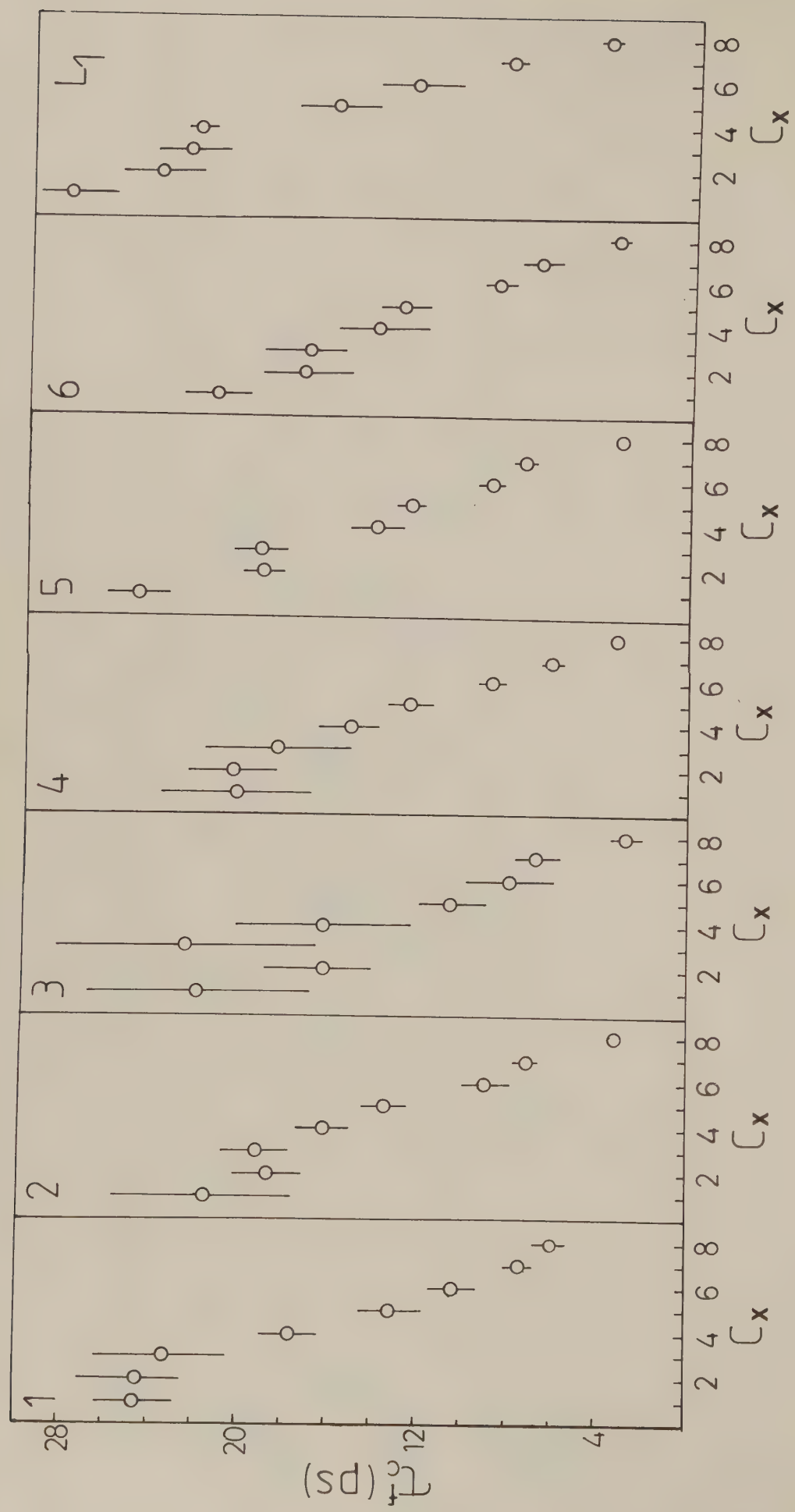

Figure 6

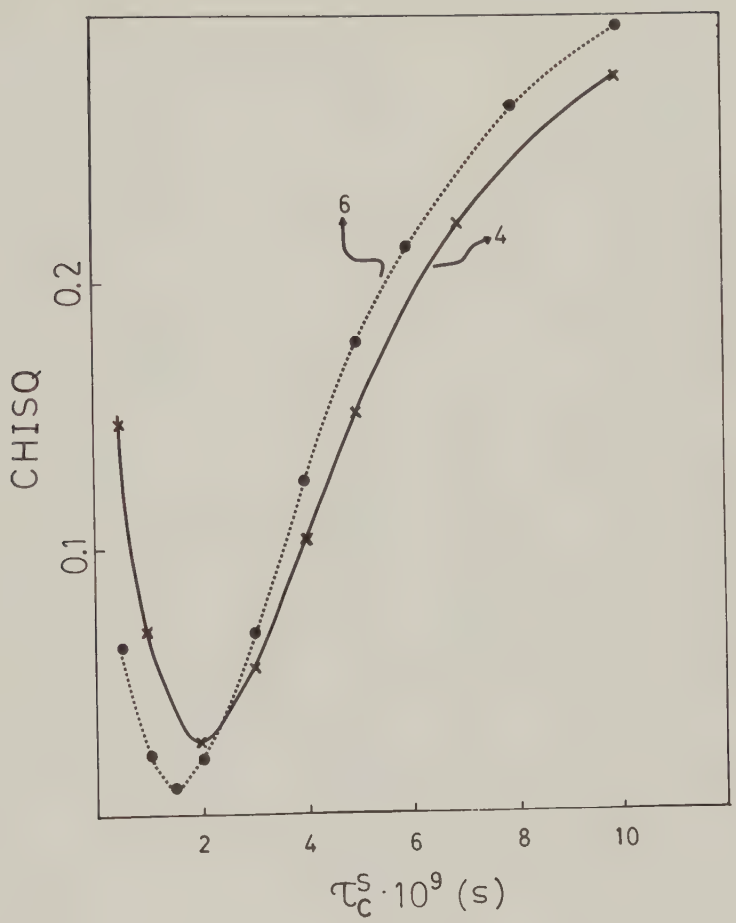

VI

A Study of the ^{13}C NMR Relaxation of AOT in Water-in-Oil Microemulsions

Joseph Carnali, Björn Lindman, Olle Söderman and Harald Walderhaug

Physical Chemistry 1, Chemical Center, University of Lund, P.O.B. 124, S-221 00 Lund, Sweden

ABSTRACT

The motions of the alkyl chains of AOT have been studied for samples within the L_2 phase of the system water - AOT - p-xylene. The water content of the samples was varied from 10 to 50 wt.% at a constant AOT/p-xylene wt. ratio of 73:27. The ^{13}C NMR T_1 relaxation times of the carbons in the chains were determined at 1.4 and 8.5 T and the nuclear Overhauser enhancements were determined at 8.5 T. The results were interpreted using a two-step model for the spectral densities. Parameters characterizing the rate, τ_c^f, and amplitude, S, of the hydrocarbon chain segmental motion were extracted for each carbon along the chains. The segmental motions were characteristic of liquid alkanes ($\tau_c^f \sim 20$ ps) and the chain order decreased on going from the head group to the terminal methyl group. A parameter characterizing the overall motions of the surfactant chain, τ_c^s, was found to be on the order of a ns. This time scale is too fast to include the rotational diffusion of the inverse micelle and the lateral diffusion of AOT. ^{13}C and ^1H NMR line widths suggest that these slow motions affect T_2 but not T_1. Therefore, an as yet unexplained process must be responsible for the nanosecond motion which gives a field dependence to T_1 measurements. It is also demonstrated that the chain order profile can be extracted directly from T_1 measurements at only two different fields.

INTRODUCTION

Sodium di-2-ethylhexylsulfosuccinate (AOT) is an anionic surfactant with two, branched hydrocarbon tails (see Figure 1). Its structure imparts a well balanced hydrophile-lipophile property to the surfactant which is evident in its ability to solubilize large amounts of water in oil or of oil in water, depending upon the temperature [1]. In particular, the phase diagram of the three component system water, AOT and oil shows a large reversed micellar (L_2) region at room temperature. For the case of p-xylene as the oil component, Ekwall et al. [2] have determined the phase diagram given in Figure 2 which shows the L_2 phase extending up to almost 60 weight percent water.

The structure of these L_2 solutions has been investigated quite thoroughly by a variety of techniques. Eicke et al. have demonstrated using elastic light scattering [3], ultracentrifugation [3] and quasi-elastic light scattering [4] that the phase in the absence of water consists of globular aggregates of 15-20 AOT molecules. As the water/AOT molar ratio increases, these aggregates first swell as their polar groups are hydrated and then they begin to coalesce to form water droplets surrounded by a monolayer of AOT molecules. This coalescence takes place at a water/AOT molar ratio of 6 [5] to 10 [3,4] and the resulting systems are termed microemulsions. These findings have been corroborated in a variety of organic solvents using quasi-elastic light scattering [6,7], neutron scattering [8] and self-diffusion measurements [9]. The water/AOT aggregates are approximately spherical and their size increases with the water/AOT mole ratio. It has also been noted that the aggregate size depends upon the organic solvent, indicating that these solvents penetrate

the AOT monolayer to varying degrees [7]. The picture is further complicated at limiting water/AOT mole ratios as the system approaches phase separation [10] and, in particular, a critical point [8,11]. In this case a large polydispersity is found. The situation at high water/AOT ratios is not totally understood. Self-diffusion measurements still find closed water droplets [9] but conductivity measurements suggest that droplet aggregation into conductive channels can occur [12]. The transition between the L_2 phase and the lamellar liquid crystalline phase has been studied in this regard [13,14].

On the molecular level, the configurational structure and dynamics of AOT molecules within the L_2 phase have been studied by NMR. Ueno et al. [15] studied the ^1H NMR spectra of AOT in chloroform in the absence of water. These authors found that the chemical shifts of the protons associated with carbons 1, 1', 3 and 3' of AOT moved downfield as aggregates began to form. This change can be attributed to the fact that aggregation occurs through the polar headgroup, thereby providing a more polar environment towards the polar end of the AOT molecule. Studies of the spin-spin coupling constants [16,17] of the protons on carbons 1 and 1' have shown that in chloroform and isooctane the headgroup conformation of AOT has the carbonyl 2' gauche to the SO_3 group and to the carbonyl 2. This arrangement provides a maximum water/polar group interaction and the corresponding gauche orientation of the hydrocarbon chains is favorable from packing considerations in micelles. Thus a conformation is favored which enhances the amphiphilic character of AOT. As the water/AOT mole ratio increases, other conformations of the headgroup become less unfavorable. This observation has also been made in an infared spectroscopy analysis [18].

The dynamics of the hydrocarbon chains in AOT have been the subject of several ^{13}C NMR studies. Ueno et al. [19] found that the spin-lattice relaxation time (T_1) increased on moving down the chains away from the headgroup for the case of AOT dissolved in chloroform or benzene [20]. They found also that T_1 for carbons 7 and 8 were longer than those for the corresponding carbons 9 and 10 of the side chain. These authors interpreted their data in terms of an effective correlation time containing contributions from the rotational correlation time of the micellar aggregates and from the correlation time of internal motion for each carbon. Their results indicate that segmental motion increases on moving away from the headgroup with carbons 1 and 1' being particularly restricted. The side chains (carbons 9,9' and 10,10') were found to have lower mobilities than the main chain.

Upon increasing the water/AOT mole ratio from zero up to 5-10, a rapid decrease in the effective correlation time is observed, the more so the closer the carbon to the headgroup [21]. This observation was interpreted as an increased mobility of the chain with water content. This result, found with isooctane as the solvent, was also observed with cyclohexane, benzene and carbon tetrachloride [18] . As the water/AOT mole ratio is increased still further, the effective correlation times decrease more slowly. The mobility of the hydrocarbon chains was thus found to be approximately constant throughout the microemulsion region.

In the latter study [18], the authors found that the measured T_1's showed a dependence upon the magnetic field strength. The presence of such a dependence implies the presence of molecular motions whose correlation times are approximately equal to the inverse resonance

frequency. At the magnetic field strengths employed, these motions are too slow to be the segmental motion of the surfactant chains. It must be then that a second kind of motion is contributing to the spin-lattice relaxation on a time scale different from that of the segmental motion. Further, the contribution from the segmental motion is not isotropic since the nature of the aggregates in the L_2 phase is such as to order the head groups. This ordering imparts an anisotropy, restricting the motion of the surfactant chain normal to the aggregate interface. The slower motion must reduce this anisotropy by allowing reorientation of the chain. Because the two motions modulate different parts of the relaxation interaction, the use of an effective correlation time to describe both motions is incorrect [18,22]. In this paper we report the results of a ^{13}C NMR spin-lattice relaxation study on the system water, AOT and p-xylene. We have made our study at two different magnetic field strengths and have interpreted our data using the formalism of Wennerström et al. [23]. In this approach, the different symmetries of the two motions are taken into account explicitly.

EXPERIMENTAL SECTION.

Materials

AOT, 444.57 g/mole from Fluka AG, Switzerland, was purified according to the procedure recommended by Shinoda [1]. The p-xylene (BDH Chemicals Ltd., England) was of reagent quality and the heavy water was of 99.8% ^2H_2O from Norsk Hydro, Rjukan, Norway.

Sample Preparation

The samples studied were from within the L_2 phase of the system water, AOT and p-xylene (see Figure 2). The AOT/p-xylene weight ratio was held constant at 73/27 and samples were made up at overall water contents of 10, 20, 30, 40 and 50% by weight. In the NMR experiments, heavy water (D_2O) was used in place of H_2O and care was taken to keep the number of moles of water constant upon substitution. Samples were prepared by weight in glass vials which were then flame sealed and stored until they had reached equilibrium before any measurements were performed.

^{13}C NMR Measurements

The ^{13}C T_1 relaxation measurements were performed at magnetic field strengths of 8.5 T and 1.4 T on a Nicolet NM 360 spectrometer and a Jeol FX-60 spectrometer, respectively. An internal field-frequency lock on the solubilized D_2O was used in all cases. The spin-lattice relaxation times were determined using the fast inversion recovery technique. T_1 was extracted from the raw relaxation data by fitting to a three parameter equation [24]. The $\{^1H\}$-^{13}C nuclear Overhauser enhancements (n.O.e) were determined on the 8.5 T spectrometer by the dynamic n.O.e technique [24,25]. For both types of measurements, the experimental temperature was $(27 \pm 1)^oC$ as determined by a calibrated copper/constantan thermocouple. Our assignment of the ^{13}C spectrum of AOT was based on the work of Ueno et al. [19]. With reference to Figure 1, we were able to resolve separately the 1,1', 2,2', 3 and 3' carbons. The peaks of the remaining carbons were resolved only as the pairs (4,4'), (5,5'), etc.

THEORY

For a ^{13}C nucleus whose relaxation is dominated by ^{13}C-^{1}H dipolar interactions, the appropriate expressions for T_1 and the nuclear Overhauser enhancement are [26]

$$1/T_1 = \frac{N}{20}\left[\frac{\mu_o \gamma_H \gamma_C \hbar}{4\pi r^3_{C-H}}\right]^2 (\tilde{J}(\omega_H - \omega_C) + 3\tilde{J}(\omega_C) + 6\tilde{J}(\omega_H + \omega_C)) \qquad (1)$$

and

$$\eta = \left[\frac{\gamma_H^3 \gamma_C}{20}\right]\left[\frac{\mu_o \hbar}{4\pi r^3_{C-H}}\right]^2 (NT_1)\ (6\tilde{J}(\omega_H + \omega_C) - \tilde{J}(\omega_H - \omega_C)) \qquad (2)$$

respectively. N is the number of protons directly bonded to the carbon of interest, μ_o is the permeability of free space, γ_H and γ_C are the magnetogyric ratios of proton and carbon respectively, $\hbar$ is Planck's constant divided by 2π and r_{C-H} is the C-H bond length which was taken as 1.09 Å. The functions $\tilde{J}(\omega)$ represent the spectral densities in terms of the angular Larmor frequencies of protons (ω_H) and carbons (ω_C) at a given magnetic field.

The form chosen for these spectral densities is that of Wennerström et al. [22,23]:

$$\tilde{J}(\omega) = (1-S^2)\frac{2\tau_c^f}{1+(\omega\tau_c^f)^2} + S^2\frac{2\tau_c^s}{1+(\omega\tau_c^s)^2} \qquad (3)$$

The motivation behind this choice is related to our view of the structure in these systems. Multicomponent systems involving oil, water and surfactant likely possess an oil/water interface at which the surfactant can be adsorbed. In the adsorbed state, the motions of the surfactant chain can be conceptually divided into two types. On one hand there are the segmental motions of the chain which differ from those of long chain hydrocarbons in isotropic solution because they become progressively more anisotropic on going from the terminal methyl group to the adsorbed headgroup. On the other hand there are the motions of the surfactant molecule as a whole, comprising the motion of the interface as well as diffusion of the surfactant along the interface.

The conceptual division of the surfactant motions is quantified by assigning characteristic correlation times to each type of motion. Thus, τ_c^f describes the segmental motion while τ_c^s describes the motion of the surfactant molecule as a whole. The time scales represented by τ_c^f and τ_c^s are expected to be much different. The segmental motions are rapid, with τ_c^f on the order of 10^{-11} s, but as mentioned above, they are not isotropic. The C-H bond vector for a particular carbon atom does not sample all directions with equal probability. The residual anisotropy is characterized by an order parameter S defined for each carbon as

$$S = (\tfrac{1}{2}) < 3 \cos^2 \theta_{LD} - 1 >_f \qquad (4)$$

where θ_{LD} is the angle between the C-H bond vector and the local director which is perpendicular to the oil/water interface. This parameter is

defined for times long enough to have averaged over the segmental motions, as is indicated by the symbol $\langle\ \rangle_f$.

The residual anisotropy indicated by a non-zero value of S should manifest itself in terms of quadrupole splittings of the deuteron signal of deuterated surfactants [27]. In L_1 or L_2 phase systems, however, these splittings are not observed. It is reasonable to assume that the slower motions characterized by τ_c^s are themselves isotropic and serve to randomize the C-H bond direction on a longer time scale. In Figure 3 we have plotted the function $\tilde{J}(\omega)/\tilde{J}(0)$ versus the logarithm of ω for $S = 0.2$, $\tau_c^f = 1 \times 10^{-11}$ s and $\tau_c^s = 1 \times 10^{-9}$ s. For the spectral frequencies employed in this work (9×10^7 to 3×10^9 rad/s) it can be seen that $(\omega\tau_c^f)^2 \ll 1$. In this extreme narrowing range, Equation 3 can be simplified by putting $1 + (\omega\tau_c^f)^2 \sim 1$. From Equations 1 and 2 it is apparent that the experimentally determined T_1 and η depend on ω and hence on the external magnetic field strength if the time scale, τ_c^s, of the overall surfactant motion is near the reciprocal of the angular Larmor frequency.

Advantage may be taken of this field dependence to determine the order parameter profile along the surfactant hydrocarbon chain. In the extreme narrowing limit of Equation 3 ($(\omega\tau_c^f)^2 \ll 1$), the difference between the relaxation rates obtained for a particular carbon at two different field strengths should be independent of the first term on the left-hand side of Equation 3. The field/frequency dependence should be present only in the second term giving

$$(1/T_1)_L - (1/T_1)_H = NAS^2\tau_c^s\ (\Delta(\omega)) \tag{5}$$

where A is a product of constants and $\Delta(\omega)$ is simply the sum of differences involving terms in $(1 + (\omega\tau_c^s)^2)^{-1}$. Because the overall motion characterized by τ_c^s is assumed to be the same for any carbon in the surfactant chain, the field dependence for any one carbon is directly proportional to NS^2. This allows a quantity proportional to S to be determined for all resolvable carbons in a hydrocarbon chain directly from T_1 measurements at two different field strengths.

DATA TREATMENT

For the present case, the experimental data consisted of eleven T_1 and η values obtained at 8.5 T and eleven T_1 values obtained at 1.4 T for each system examined. As unknowns we have the eleven τ_c^f and S values, a set for each carbon in the chain, and a single τ_c^s. To determine these unknown parameters, the entire data set for a given system was subjectedto a least-squares analysis as has been described previously [28]. We reiterate that although 23 parameters are involved in the present fit, they are only weakly covariant and the individual (τ_c^f, S) estimates for a given carbon are almost independent of those for the other carbons since they only couple weakly through τ_c^s [24].

RESULTS

That the experimentally determined T_1 values are field dependent is shown in Table I where the data for systems with 10 and 50 weight percent water are listed. We note that the relaxation time is always longer at the higher field. Further, T_1 increases at fixed magnetic field strength with increasing water content and increases also on going down the hydrocarbon chain from the headgroup to the terminal methyl group. Also shown in Table 1 are the nuclear Overhauser enhancements (η) which were determined at 8.5 T. The η values of carbons near the AOT headgroup are seen to be considerably below the value of 1.988 valid if $(\omega\tau_c^f)^2$ and $(\omega\tau_c^s)^2 \ll 1$ in Equation 3 [26]. Such reduced values can be accounted for with the present model for $\tilde{J}(\omega)$ if $(\omega\tau_c^s)^2 \sim 1$. This condition immediately implies that τ_c^s must be near the range 1×10^{-9} to 3×10^{-10} s.

A quantity proportional to the order parameter, S, as extracted from Equation 5, is shown in Figure 4 plotted versus the carbon number (as defined in Figure 1). In this same figure a comparison is made with the S parameter extracted from the least-squares fit to each data set. The proportionality constant of Equation 5 is scaled so that both order parameter profiles are identical at carbon numbers 4 and 4'. The agreement between the two sets of values indicates that the least-squares fitted parameters faithfully describe the experimental data. The near zero S value found for the terminal methyl carbons combined with the extreme narrowing limit for $\omega\tau_c^f$ explains the nearly full n.O.e. values of Table I.

The correlation time for segmental motion, τ_c^f, is shown in Figure 5 plotted versus the carbon number. The error bars in this figure represent 80 % confidence levels determined using the Monte Carlo technique outlined in ref. [29]. In all cases the fast correlation time, τ_c^f, decreases on going down the hydrocarbon chain from carbon 4,4' to the terminal methyl group, carbon 8,8'. The side chain (9,9' and 10,10') shows a similar trend. With increasing water content, τ_c^f for the carbons near the headgroup shows an increasing trend. Lastly the slow correlation time, τ_c^s, for each system is reported in Table II. It will be observed that these values are all near the longer limit for τ_c^s which was observed from the n.O.e. data.

DISCUSSION

Inspection of Figures 4 and 5 gives a picture of the local motions occurring within the hydrocarbon chain of AOT. An important caveat with regards to this data is that Equation 3 becomes inaccurate if the amount of anisotropy in the fast motion becomes too large [22]. This anisotropy, as indicated by the magnitude of the order parameter, is quite large for carbons 1,1' through 4,4'. For this reason, the values of S and τ_c^f for these carbons are not trustworthy. Nevertheless, the strong field dependence found for these carbons allows a qualitative discussion about their order. A large field dependence implies that the slow motion must make a very large contribution to the spin-lattice relaxation. This means that the fast motion is rather inefficient in giving rise to relaxation, with the plausible explanation being that they are very anisotropic.

The high order implied by the above anisotropy is not surprising since both carbonyl groups (2,2') are probably coordinated with the sulfonate group as a compound headgroup [16]. Thus a high order for carbons 1 and 1' and for 3 and 3' is expected. The methine carbons (4,4') are the site of the branching of the chain and they likely suffer steric hindrance, especially since the branching occurs fairly close to the headgroup where steric effects would be high due to the curvature of the aggregate.

The carbons located further from the headgroup (5,5' - 10,10') show a behaviour characteristic of alkyl chains. The correlation time for the fast local motions is on the order of 20 ps which is a value similar to what is observed in simple alkanes [30,31]. The consistent decrease of τ_c^f on going away from the headgroup indicates that carbon 5 is more motionally restricted than carbon 8, for example. Such a restriction must presumably come as a result of the headgroup being spacially confined in the aggregate. This effect is seen with carbon 9 versus 10 as well. There is little change in the segmental motion with increasing water content. In all cases the motion is that of liquid-like chains with residual restriction toward the polar headgroup.

The order parameters for these same carbons show that the anisotropy in the segmental motion decreases on moving down the chain toward the terminal methyl group. The magnitude of S for carbon 5 is quite large indicating that the amplitude of these motions is severely restricted. Again, this restriction is related to the anchoring of the headgroup in the aggregate. The amplitude of the segmental motion increases on moving

out either the main (5,5' - 8,8') or the side (9-9' - 10,10') chains. The side chain appears to be more restricted than the corresponding portion (carbons 7,7' and 8,8') of the main chain. This is a reflection of the fact that the side chain is closer in sequence to the polar head-group. Thus its order follows that of the middle of the main chain (compare carbons 5,5' and 9,9'). Our results are then in agreement with the earlier ^{13}C NMR studies [20] in these regards. The sensitivity of the order profile to the water content appears to be slight. This finding comes as little surprise since the order profile of the surfactant shows a similar constancy in the L_2 phase of the system sodium octanoate, octanoic acid and water [28]. In fact, the order profile is found to be relatively insensitive to the geometry of the aggregate in isotropic or in anisotropic phases [32].

In summary then, the local picture of the AOT chains is consistent with what would be expected of inverse, water swollen micelles. Further, this picture seems to apply even at high water contents.

The slow correlation times of Table II should be a reflection of the size and shape of the aggregates. To extract such information, however, it is necessary to postulate a mechanism for the contribution to relaxation on this time scale. For spherical surfactant aggregates, we have previously suggested a mechanism consisting of the overall rotation of the aggregate combined with the diffusion of the surfactant species around the curved surface of the aggregate [24,28]. The theoretical slow correlation time for this mechanism can be written as (both contributions are isotropic)

$$(\tau_c^s)^{-1} = \frac{3kT}{4\pi r_A^3 \eta} + \frac{6D}{r_c^2} \qquad (6)$$

where η is the viscosity of the medium, k is Boltzmann's constant and T is the absolute temperature. The radius of the water core in these aggregates is r_c and that of the entire aggregate, consisting of r_c plus the length of the surfactant shell, is r_A. The surfactant can be pictured as diffusing around the water core with a lateral diffusion coefficient D.

Using Equation 6, we have estimated τ_c^s for the systems studied. In our calculations we used a water core radius obtained from the expression [11]

$$r_c = \frac{3v_w}{a_o} X \qquad (7)$$

Here v_w is the specific volume of a water molecule and X is the appropriate mole ratio of water to AOT. For the area per AOT molecule at the water core surface (a_o) the value 55 $Å^2$ was used [3]. r_A was obtained by adding the length of the AOT molecule (11 Å [18]) to r_c. The viscosity used was that of p-xylene and the lateral diffusion coefficient was taken as 2.7×10^{-11} m^2/s as determined in lamellar systems [33].

The calculated values for τ_c^s appear in Table II where they may be compared with those found experimentally. At 10 % water, the values are comparable but at higher water contents τ_c^s increases, reflecting the

theor

growing water core, while $\tau^s_{c_{exp}}$ is approximately constant. Thus the experimental results suggest that the aggregates remain small over the whole region studied, a suggestion contrary to the other experimental studies on these systems. Such a discrepancy between calculated and determined slow correlation times has been found previously [24]. In this instance it was noted that rotational diffusion and surfactant diffusion will always be present but the extent to which they contribute to the spin-lattice relaxation dependes upon their time scale.

To consider the above point more closely, we expand the spectral density proposed in Equation 3 to include motions on three different time scales [34,35]. If the intermediate motion (characterized by τ^i_c) is not completely isotropic, then there will remain a residual order to be averaged by the slower motion. If the order left on time scales slower than the fast motion is S_1 and that left after the intermediate motion is S_2, then we may rewrite Equation 3 as ($\omega\tau^f_c \ll 1$)

$$\tilde{J}(\omega) = (1-S_1^2)\ 2\tau^f_c + (S_1^2-S_2^2)\ \frac{2\tau^i_c}{1+(\omega\tau^i_c)^2} + S_2^2\ \frac{2\tau^s_c}{1+(\omega\tau^s_c)^2} \qquad (8)$$

This equation could be expanded to include even more terms. In fact, consecutively slower τ_c's should be considered but once an isotropic motion is reached, S goes to zero and the sum is terminated. From the field dependence on T_1 observed experimentally, it is obvious that a major contribution to the spin-lattice relaxation occurs on a time scale of about one nanosecond. Motions much slower than this, such as $\tau^s_{c_{theor}}$ at high water contents, will not make an appreciable contribution

to the measured T_1. This is readily seen in Equation 8 by considering the denominator of the third term. Thus these slow motions may be present but a ^{13}C T_1 experiment is not an appropriate way to observe them. Further, the experimental results indicate an intermediate relaxation mode on the time scale of 1 - 2 ns which is independent of the water content.

We note in passsing that since the motion characterized by τ_c^i involves the AOT molecule as a whole, it lowers the order S_1 by a fraction which is constant for all carbons along the chain. Thus the factor $(S_1^2 - S_2^2)$ is still proportional to S_1^2 and is still a reflection of the chain order after the averaging due to segmental motion. The previous interpretation of the order profile is then not invalidated if a three time-scale spectral density is employed.

A step toward solidifying the arguments given above would be to find evidence for the long correlation times due to rotational diffusion and surfactant monomer diffusion. A measurement of the spin-spin relaxation time (T_2) is more sensitive to slow motions as is evident from its appropriate expression [26]

$$(1/T_2) = \frac{N}{40} K^2 \left[\frac{20}{T_1 K^2 N} + 4\,\tilde{J}(0) + 6\,\tilde{J}(\omega_H) \right] \tag{9}$$

where K is the term

$$\frac{\mu_o \gamma_H \gamma_C \hbar}{4\pi\, r_{C-H}^3}$$

from Equation 1. The zero frequency term $\tilde{J}(0)$ weighs the longest

τ_c very strongly as is obvious from Equation 8. Thus if the intermediate motion is anisotropic so that $S_2 \neq 0$, then the slower motion should make a contribution to T_2. We have determined T_2 from the width of the line corresponding to carbon 1' in the 40 % water system at 1.4 T. The measured line width (17 ± 2 Hz) corrected for the effect of magnetic field inhomogeneity and residual proton couplings is 14 ± 2 Hz. This corresponds to a T_2 of 23 ± 3 ms. We can calculate the difference $(T_2)^{-1} - (T_1)^{-1}$ using Equations 9 and 1 in the two time-scale model of the spectral densities. This difference has the attractive property of being independent of τ_c^f. Thus for a fixed τ_c^s, it depends linearly on S^2. Using $\tau_c^s = 1.3 \times 10^{-9}$ s, there are no possible values which could explain the large difference between T_2 and T_1 (T_1 = 41 ms). The fact that the 1' carbon line is broader than is predicted by the two time-scale model for the spectral densities indicates that a motion slower than the nanosecond intermediate motion is making a contribution to T_2. It is also necessary that this intermediate motion be anisotropic so that the term S_2^2 in Equation 8 be nonzero.

T_2 as measured from ^{13}C NMR line widths is subject to uncertainties from the effects mentioned above. We have made ^1H NMR measurements on these systems and found that the width of the carbon 1' proton line increased appreciably with water content. The line shape in this case depends on the chain order [36] but the likely cause of the broadening with water content is a lengthening rotational correlation time due to aggregate growth.

As an independent test for slow motions we have incorporated sodium octanoate 1,1 ^2H into the 40 % water system and determined the ^2H T_1 and T_2. T_2 was again extracted from the line width and T_1 was obtained by the inversion-recovery technique. The mole ratio of AOT to octanoate was varied between 10 and 20 with no significant differences in the measured values being obtained. The results were T_1 = 44 ms and T_2 = 3 ms. The difference $(T_2)^{-1} - (T_1)^{-1}$ for ^2H can be cast in the two time-scale model for the spectral densities analogously to the ^{13}C case. Again the difference depends only on S^2 and τ_c^s. Since τ_c^s (or τ_c^i) is assumed to involve motion of the surfactant molecule as a whole, we have assumed that both sodium octanoate and AOT will have the same type and time scale of overall motion. Again a slow correlation time of 1.3×10^{-9} s is incompatible with the large value of $(T_2)^{-1} - (T_1)^{-1}$.

The available data thus indicate that the motion with $\tau_c^s \sim 1 \times 10^{-9}$ s cannot be aggregate rotation and surfactant monomer diffusion because the latter motions are isotropic and the former is anisotropic. Large inverse micelles cannot be ruled out although their size cannot be extracted from our data. The question at hand is to identify the nature of this intermediate motion which is slightly anisotropic and does not depend on the water content of the system. We cannot at this time give any real answer to this question. The possibility of deformations in the aggregate shape which would alter the orientation of the local director has been postulated previously [24,37]. However, these deformation modes would have to have short wavelengths, on the order of the length of an AOT molecule, to account for the residual anisotropy and composition independence. Further

the time scale of these modes would have to be on the nanosecond level, again indicating short wavelengths. Motion of the AOT tail as a whole while the position of headgroup in the aggregate remained unchanged might also be a possibility.

In conclusion, our study of these inverse micellar systems has revealed that the two time-scale model for the spectral densities is not sufficient to explain the data. A motion exists on a time scale intermediate between the segmental motion of the AOT chains and the motion of the aggregate as a whole. This motion, occuring near the inverse Larmor frequency, gives a field dependence to T_1 measurements. Slower aggregate motion does not contribute to T_1 but does to T_2, indicating that the intermediate motion is anisotropic. Our values of τ_c^f and S extracted using the two time-scale model are thus in error. But this error, appreciable when S is large, is not so great when $(1 - S^2)$ is near unity. Thus our fast correlation times for the portion of the AOT chain near the terminal methyl groups are valid. Further, we have demonstrated that the parameter S (or $(S_1^2 - S_2^2)^{\frac{1}{2}}$) can be obtained by performing T_1 measurements at only two field strengths.

REFERENCES

1. H. Kunieda and K. Shinoda, J. Colloid Interface Sci., 70, 577 (1979).
2. P. Ekwall, L. Mandell and K. Fontell, J. Colloid Interface Sci., 33, 215 (1970).
3. H.F. Eicke and J. Rehak, Helv. Chim. Acta, 59, 2883 (1976).
4. M. Zulauf and H.F. Eicke, J. Phys. Chem., 83, 480 (1979).
5. M. Wong, J.K. Thomas and T. Nowak, J.A.C.S., 99, 4730 (1977).
6. R.A. Day, B.H. Robinson, J.H.R. Clarke and J.V. Doherty, J. Chem. Soc., Faraday Trans. I, 75, 132 (1979).
7. J.D. Nicholson, J.V. Doherty and J.H.R. Clarke, in "Microemulsions", ed. I.D. Robb, Plenum Press, New York, 1982.
8. C. Toprakcioglu, J.C. Dore, B.H. Robinson, A. Howe and P. Chieux, J. Chem. Soc., Faraday Trans. I, 80, 413 (1984).
9. P. Stilbs and B. Lindman, J. Colloid Interface Sci., 99, 290 (1984).
10. E. Gulari, B. Bedwell and S. Alkhafaji, J. Colloid Interface Sci., 77, 202 (1980).
11. M. Kotlarchyk, S.H. Chen and J.S. Huang, J. Phys. Chem., 86, 3273 (1982).
12. C. Boned, J. Peyrelasse, J. Heil, A. Zradba and M. Clausse, J. Colloid Interface Sci., 88, 602 (1982).
13. B. Tamamushi and N. Watanabe. Colloid Polym. Sci., 258, 174 (1980).
14. H.F. Eicke and Z. Markovic, J. Colloid Interface Sci., 79, 151 (1981).

15. M. Ueno, H. Kishimoto and Y. Kyogoku, Chem. Lett., 1977, 599, 1977.

16. A.N. Maitra and H.F. Eicke, J. Phys. Chem., 85, 2687 (1981).

17. A. Maitra, G. Vasta and H.F. Eicke, J. Colloid Interface Sci., 93, 383 (1983).

18. C.A. Martin and L.J. Magid, J. Phys. Chem., 85, 3938 (1981).

19. M. Ueno, H. Kishimoto and Y. Kyogoku, Bull. Chem. Soc. Japan, 49, 1776 (1976).

20. M. Ueno, H. Kishimoto and Y. Kyogoku, J. Colloid Interface Sci., 63, 113 (1978).

21. H.F. Eicke and P.E. Zinsli, J. Colloid Interface Sci., 65, 131 (1978).

22. B. Halle and H. Wennerström, J. Chem. Phys., 75, 1928 (1981).

23. H. Wennerström, B. Lindman, O. Söderman, T. Drakenberg and J.B. Rosenholm, J.A.C.S., 101, 6860 (1979).

24. H. Walderhaug, O. Söderman and P. Stilbs, J. Phys. Chem., 88, 1655 (1984).

25. R. Freeman, H.D.W. Hill and R. Kaptein, J. Magn. Resonance, 7, 327 (1972).

26. D. Doddrell, V. Glushko and A. Allerhand, J. Chem. Phys., 56, 3683 (1972).

27. T. Klason and U. Henriksson in "Solution Chemistry of Surfactants", eds. K.L. Mittal and E.J. Fendler, Plenum Press, New York, 1982.

28. T. Ahlnäs, O. Söderman, C. Hjelm and B. Lindman, J. Phys. Chem., 87, 822 (1983).

29. P. Stilbs and M.E. Moseley, J. Magn. Resonance, 31, 55 (1978).

30. R.R. Lyerla Jr., H.M. McIntyre and D.A. Torchia, Macromolecules, 7, 11 (1974).

31. Y.K. Levine, N.J.M. Birdsall, A.G. Lee, J.C. Metcalfe. P. Partington and G.C.K. Roberts, J. Chem. Phys., 60, 2890 (1974).

32. O. Söderman, H. Walderhaug and B. Lindman, J. Phys. Chem., in press.

33. G. Lindblom and H. Wennerström, Biophys. Chem., 6, 167 (1977).

34. O. Söderman, H. Walderhaug, U. Henriksson and P. Stilbs, J. Phys. Chem., submitted.

35. J.H. Davis, K.R. Jeffrey and M. Bloom, J. Magn. Resonance, 29, 191 (1978).

36. H. Wennerström and J. Ulmius, J. Magn. Resonance, 23, 431 (1976).

37. M.F. Brown, J. Chem. Phys., 77, 1576 (1982).

Figure Captions

Figure 1. Structural formula of Aerosol OT.

Figure 2. Ternary phase diagram for the system Aerosol OT - p-xylene - water at $20^{o}C$. Compositions in terms of weight percent. L_1 and L_2 are isotropic solution phases, D is a lamellar liquid crystal, F is a reversed hexagonal liquid crystal and I is a cubic liquid crystal. Redrawn from Ref. [11].

Figure 3. $\tilde{J}(\omega)/\tilde{J}(0)$ as a function of log ω for $S = 0.2$, $\tau_c^f = 1 \times 10^{-11}$ s and $\tau_c^s = 1 \times 10^{-9}$ s.

Figure 4. The order parameter profile along the AOT chains (see Figure 1) for different water contents. (O) refers to the order parameter extracted from the least-squares fit to each data set. The error bars represent the range of the order parameter as obtained from the field dependence of T_1 alone (see Equation 5). These ranges are scaled to the fitted values so that both agree at carbon 4,4'.

Figure 5. The fast correlation time, τ_c^f, for segmental motion of a carbon atom as a function of its position along the AOT chains (see Figure 1).

Table I. The spin-lattice relaxation time (T_1)[a] as determined at two different magnetic field strengths and the nuclear Overhauser enhancement (η)[b] for systems containing 10 and 50 weight percent water.

	10 % system			50 % system		
Carbon no.	T_1(1.4T)	T_1(8.5T)	η(8.5T)	T_1(1.4T)	T_1(8.5T)	η(8.5T)
1	0.047	0.230	0.359	0.081	0.257	1.064
1'	0.023	0.137	0.400	0.045	0.124	1.381
3	0.041	0.161	0.664	0.088	0.215	1.021
3'	0.060	0.201	0.687	0.135	0.235	1.319
4,4'	0.100	0.306	0.849	0.208	0.444	1.209
5,5'	0.117	0.284	1.069	0.249	0.415	1.463
6,6'	0.149	0.356	1.280	0.438	0.583	1.188
7,7'	0.360	0.788	1.368	0.727	1.064	1.600
8,8'	1.220	1.800	1.861	1.992	2.197	1.832
9,9'	0.139	0.287	0.992	0.233	0.367	1.348
10,10'	0.670	1.245	1.469	1.232	1.772	1.789

[a] T_1 values quoted in seconds and having a precision of ± 10 %.

[b] η values have a precision of ± 10 %.

Table II. The slow correlation time $\tau^s_{c_{exp}}$ determined from the experimental data compared with that predicted ($\tau^s_{c_{theor}}$) from aggregate rotational diffusion and AOT monomer lateral diffusion.

wt.% water	$\tau^s_{c_{exp}}$ (ns)	$\tau^s_{c_{theor}}$ (ns)
10	2.1±0.25	1.3
20	0.9±0.1	5.2
40	1.3±0.4	37
50	1.4±0.3	88

Figure 1

Figure 2

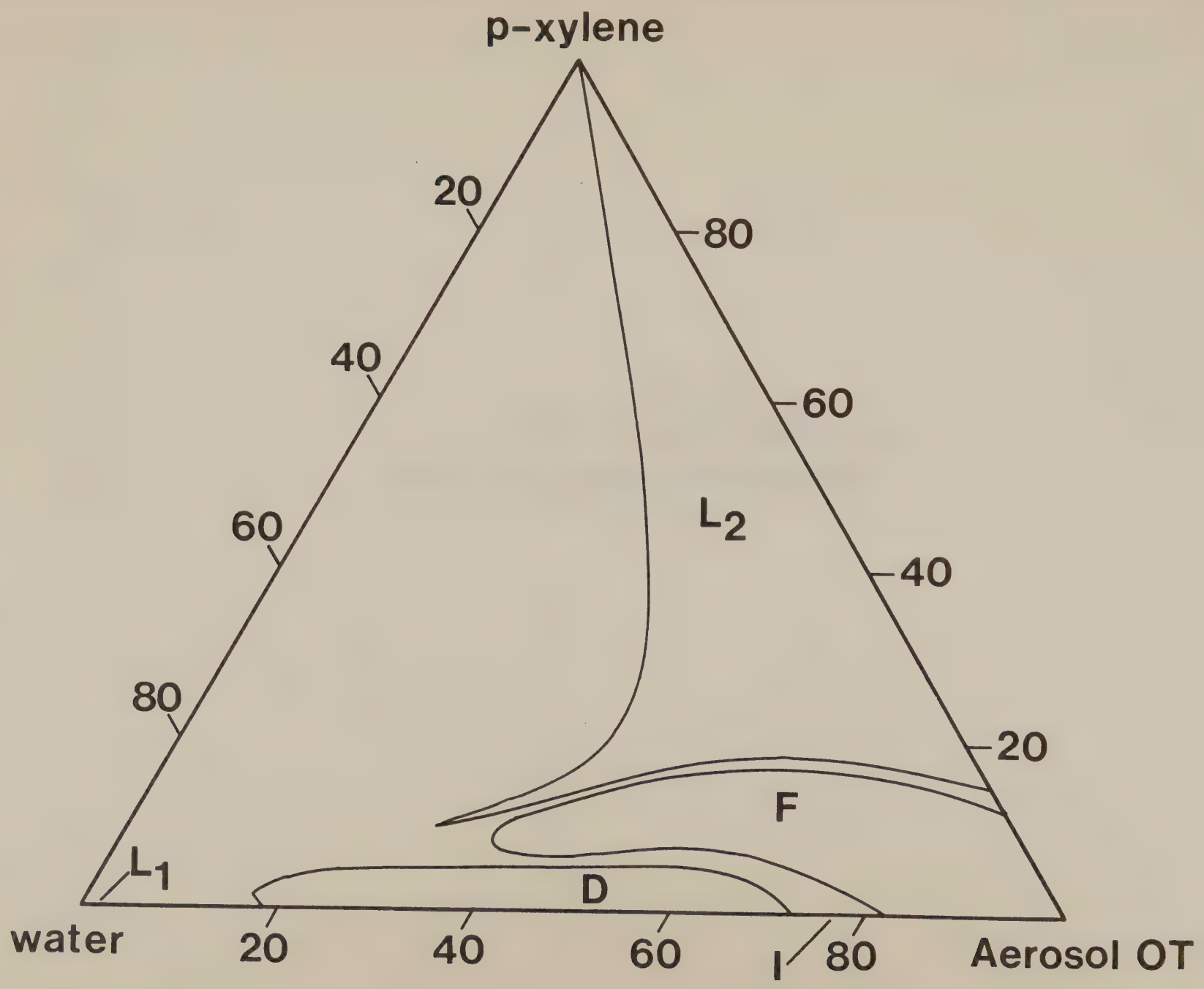
p-xylene
20
40
60
80
80
60
40
20
L2
F
L1
D
water
20
40
60
I
80
Aerosol OT

Figure 3

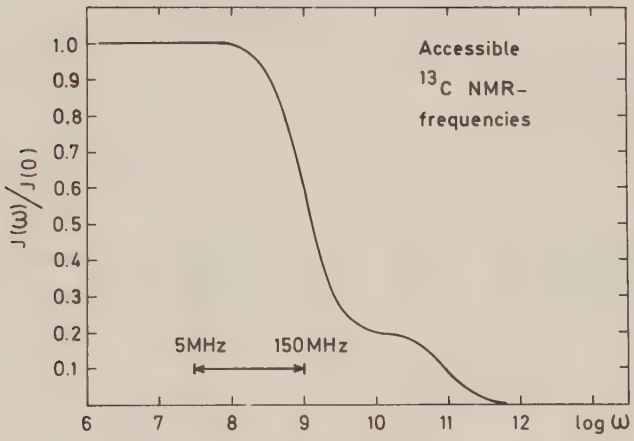
Accessible
^{13}C NMR-
frequencies
5MHz
150MHz
J(ω)/J(0)
1.0
0.9
0.8
0.7
0.6
0.5
0.4
0.3
0.2
0.1
6
7
8
9
10
11
12
log ω

Figure 4

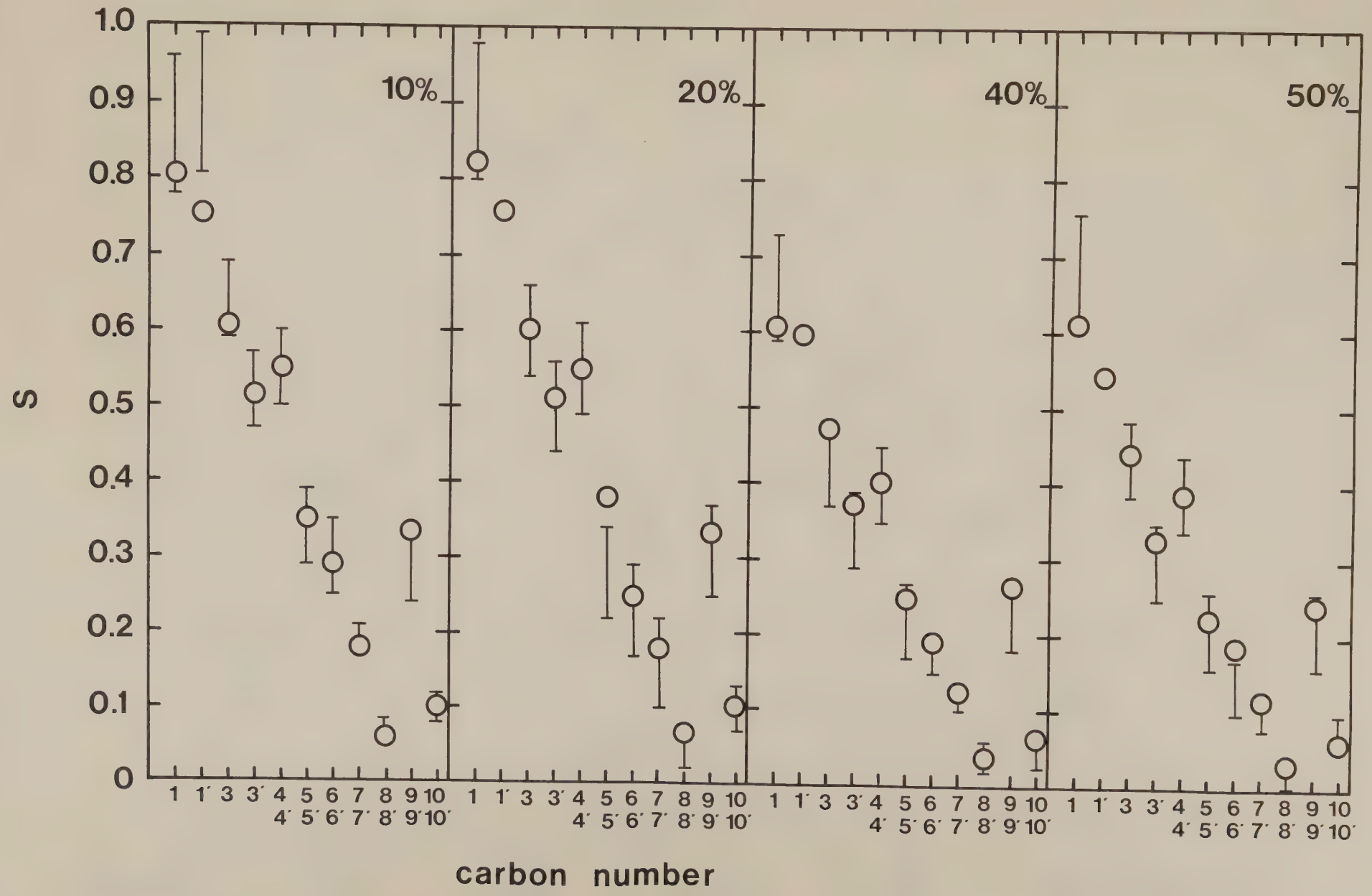
S
1.0
0.9
0.8
0.7
0.6
0.5
0.4
0.3
0.2
0.1
0
10%
20%
40%
50%
1 1′ 3 3′ 4 4′ 5 5′ 6 6′ 7 7′ 8 8′ 9 9′ 10 10′
carbon number

Figure 5

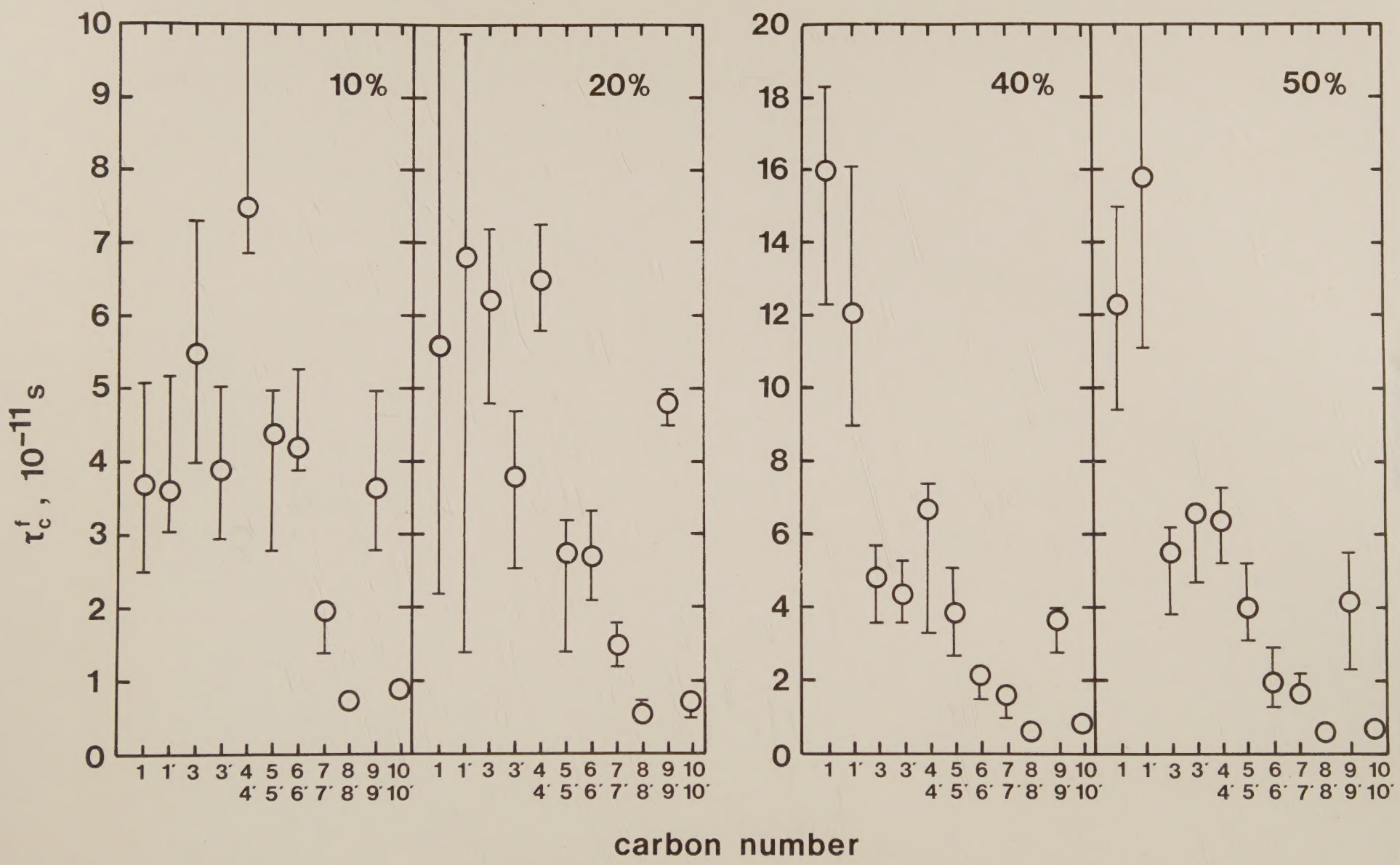
10%
20%
40%
50%
τ_c^f, 10^{-11} s
carbon number
1 1′ 3 3′ 4 4′ 5 5′ 6 6′ 7 7′ 8 8′ 9 9′ 10 10′

Tryckericentralen
AVC Lund 1985